VITAMIN B_{12} AND FOLATE INTERACTIONS IN NUCLEAR ONE-CARBON METABOLISM

A Dissertation

Presented to the Faculty of the Graduate School

of Cornell University

In Partial Fulfillment of the Requirements for the Degree of

Doctor of Philosophy

by

Ashley M. Palmer

January 2017

VITAMIN B_{12} AND FOLATE INTERACTIONS IN NUCLEAR ONE-CARBON METABOLISM

Ashley M. Palmer, Ph.D.

Cornell University 2017

Vitamin B_{12}-associated pathologies are common, but the underlying mechanisms are unclear. In the cytosol, vitamin B_{12} functions as a required cofactor for methionine synthase (MTR) in the remethylation of homocysteine to methionine, which regenerates tetrahydrofolate (THF) for subsequent nucleotide biosyntheses. Impairments in this pathway are most apparent in megaloblastic anemia, which results from the inhibition of DNA synthesis due to the trapping of folate cofactors as 5-methyltetrahydrofolate (5-methylTHF).

The first objective sought to determine the impact of maternal vitamin B_{12} deficiency and *Shmt1* disruption on neural tube defect (NTD) incidence. Vitamin B_{12} deficiency, independently of folate status, caused NTDs in *Shmt1*$^{-/-}$ and *Shmt1*$^{-/+}$ embryos. Folate status and folate-deficiency in vitamin B_{12} deficiency did not affect NTD incidence. Folate, but not vitamin B_{12} deficiency, significantly increased plasma homocysteine in pregnant dams and resulted in decreased embryonic growth. Taken together, these findings suggest that neural tube closure is more sensitive to maternal vitamin B_{12} deficiency than homocysteine remethylation or embryonic growth.

The second objective aimed to determine the impact of a cytosolic vitamin B_{12} deficiency on nuclear *de novo* thymidylate (dTMP) biosynthesis, given the recent discovery of a nuclear, multi-protein complex for *de novo* synthesis of dTMP. Both

human fibroblasts with loss-of-function mutations in *MTR* and HeLa cells treated with nitrous oxide (N_2O) gas demonstrated intracellular accumulation of 5-methylTHF ranging from 1.75-2.5-fold compared to control conditions. In vitamin B_{12} depleted HeLa cells, the nucleus was the most sensitive cellular compartment to 5-methylTHF accumulation, with a greater than 4-fold increase observed at the expense of THF. Vitamin B_{12} depletion in HeLa cells impaired rates of *de novo* dTMP biosynthesis and increased DNA damage; both outcomes were exacerbated by folate depletion. By contrast, MTR loss-of-function depressed rates of *de novo* dTMP biosynthesis, but did not increase DNA damage; this latter observation may be explained by the fact that specific tissues exhibit differential sensitivity to vitamin B_{12} deficiency. Taken together, these findings demonstrate cytosolic vitamin B_{12} depletion traps nuclear folate as 5-methylTHF, decreases rates of *de novo* dTMP biosynthesis, and increases DNA damage, providing a mechanism that can be extended to vitamin B_{12}-associated pathologies.

BIOGRAPHICAL SKETCH

Born in 1982, Ashley Melissa Palmer was raised on both extremes of the east coast (first Maine, and later Florida). Following high school, she traded in her flip flops for snow boots (again!) and enrolled in Wellesley College with the intentions of becoming an English major, but somehow became sidetracked and promptly majored in biology instead. After graduation, she worked at Massachusetts General Hospital as a research technician for several years. She then spent the better part of a year backpacking through New Zealand and the South Pacific, fulfilling a life-long dream. Her experiences farming there, combined with her interests in science, ultimately led her to the Division of Nutritional Sciences at Cornell University.

To my parents, for everything

ACKNOWLEDGMENTS

First and foremost, I would like to thank my advisor, Patrick Stover, for giving me the opportunity to pursue science at the highest level, for challenging me to do the very best work, and for believing in me even when I doubted my own abilities. Patrick has inspired me by his ability to simultaneously see the big picture and zoom into the details without getting “lost in the weeds”. I would also like to thank Martha Field for being a mentor to my work, for her expertise in experimental approaches, and for always being available either by door knocks or text messages. Her ability to collaborate, teach, and nurture a squadron of graduate students and an armada of undergraduates is beyond impressive.

I am grateful to Elena Kamynina for her talent, enthusiasm, and patience with me in the experiments involving γH2AX-based quantification as detailed in Chapter 3. I stand in awe of her ability to connect the literature to the practice of science in the lab.

I would like to thank Julia Finkelstein for her statistical expertise, helpful comments for Chapter 2, and thoughtful insights on future careers.

I would like to thank my committee members Bob Weiss, Dave Lin, and Martha Stipanuk for their time, availability, and helpful comments.

I would like to thank the CSCU, specifically Lynn Johnson and Francoise Vermeylen, for their outstanding statistical advice. I would also like to thank Carol Bayles at the Institute of Biotechnology for her expertise and help with flow cytometry and microscopy, as well as the Weill Barrier Core for their help and support with my animal studies.

I would like to thank the members of the Stover Lab for their camaraderie, support, and for ordering me takeout so many times last summer. I would also like to thank my undergraduates Callie Shubin, Nick Santiago, and “Ashley II” Macomber for their help.

I am thankful for the friendship of many individuals who have kept me sane and balanced outside of the lab, especially: David Keifer, Jeremy Allen, Judith & Francis, Kevin & Brittany, Laura Smith, Suze Colt, Uncle Tom, and Elaine Yu.

I would like to thank the Rosenblatt Lab at McGill University for providing me the human fibroblasts for the experiments detailed in Chapter 3. I would also like to thank the Brosnan and Stabler laboratories for providing the metabolite panel measurements in Chapter 2. My training has been generously funded by the following entities: Cornell University, The Division of Nutritional Sciences, The Cornell Developmental Vertebrate Genomics Training Grant (NIH T32 HD057854), and The National Institutes of Child Health and Human Development (Ruth L. Kirschstein NRSA F31 HD081858-02).

I would like to thank my family, especially my parents, without whose love and support I would not be where I am today. They have always encouraged me to pursue all of my passions and dreams, while giving me every opportunity in life to do so. I am fortunate to have acquired a second set of parents during this journey whose love, contagious Brazilian optimism, and Portuguese sayings have served as a gentle reminder that life should never be taken too seriously.

Finally, I am eternally grateful to my wonderful Marcos for his unconditional love and support, as well as the joy and laughter he brings into my life each and every day, no matter the distance.

TABLE OF CONTENTS

LIST OF FIGURES

LIST OF TABLES

LIST OF ABBREVIATIONS

1C	one-carbon
5-methylTHF	5-methyltetrahydrofolate
AICAR Tfase	aminoimidazolecarboxamide ribonucleotide transformylase
AMT	aminomethyltransferase
ANOVA	analysis of variance
AdoHcy	S-adenosylhomocysteine
AdoMet	S-adenosylmethionine
CD1	methyleneTHF labeled with one deuterium atom
CD2	methyleneTHF labeled with two deuterium atoms
CNS	central nervous system
DHF	dihydrofolate
DHFR	dihydrofolate reductase
DLD	dihydrolipoamide dehydrogenase
DSB	double-strand break
FOCM	folate-mediated one-carbon metabolism
GAR Tfase	glycinamide ribonucleotide tranformylase
GCS	glycine cleavage system
GCSH	glycine cleavage system protein H
GLDC	glycine decarboxylase
MTHFD1	methylenetetrahydrofolate dehydrogenase 1
MTHFD1L	methylenetetrahydrofolate dehydrogenase 1-like
MTHFD2	methylenetetrahydrofolate dehydrogenase 2
MTHFD2L	methylenetetrahydrofolate dehydrogenase 2-like
MTHFR	methylenetetrahydrofolate reductase
MTHFS	methenyltetrahydrofolate synthetase

MTR	methionine synthase
MUT	L-methylmalonyl-coenzyme A mutase
N_2O	nitrous oxide
NADPH	nicotinamide adenine dinucleotide phosphate
NTD	neural tube defect
SHMT	serine hydroxymethyltransferase
SUMO	small ubiquitin-like modifier
THF	tetrahydrofolate
TYMS	thymidylate synthase
cblG	cobalamin metabolism complementation group G
dT	deoxythymidine
dTMP	thymidylate
dU	deoxyuridine
dUMP	deoxyuridine monophosphate
holo-TC	holotranscobalamin
γH2AX	phosphorylated histone H2AX

CHAPTER 1: IN SEARCH OF A COMMON MECHANISM UNDERLYING FOLATE-RESPONSIVE NEURAL TUBE DEFECTS

Introduction

Neural tube defects (NTDs) result from improper neural tube closure, occurring approximately 22-28 days post conception, before a woman is aware she is pregnant (1). The birth prevalence is 6-60/10,000 live births worldwide and varies widely by ethnicity and geographic region (1, 2). Neurulation encompasses a series of highly regulated cellular events including proliferation, migration, and differentiation in the transformation and folding of the neural plate into the neural tube (3, 4). Disruptions to this coordinated sequence of events can result a number of structural defects. Anencephaly, which occurs at anterior sites of closure along the mid-hindbrain region, is almost always incompatible with life, whereas individuals with spina bifida face a spectrum of life-long disabilities with varying degrees of paralysis that incur high social and economic costs (5).

It has been nearly 25 years since two landmark randomized controlled trials (RCTs) demonstrated that maternal folic acid supplementation in the periconceptional period could reduce the risk of recurrence and first occurrence of an NTD by up to 70% (6, 7). These findings led to a series of recommendations from public health officials in the United States (U.S.) urging women of childbearing age to consume 400-4,000 μg folic acid daily to prevent the first occurrence or subsequent recurrence of an NTD-affected pregnancy (8–10). Fortification of enriched cereal grain products in the U.S. with 140 μg of folic acid per 100 grams product was mandated by the

beginning of 1998 (11). The greatest reduction in the birth prevalence of NTDs occurred during the period immediately following the fortification mandate in the U.S. (1999-2000), with the estimated annual number of NTD-affected pregnancies falling from 4,000 to 3,000 in the U.S. during this time (12). The success of this public health initiative has since led to the implementation of mandatory fortification programs in over 50 countries (13). Despite several decades of research, the mechanism by which folic acid prevents NTDs remains unknown; however, it is widely accepted that maternal folate supplementation does not prevent NTDs by correcting for a deficiency of folate as mothers with NTD-affected pregnancies do not present with an overt folate deficiency (14, 15). These findings are supported by the observations that rendering mice folate-deficient alone does not induce NTDs (16).

Family history is another risk factor for NTDs, and the risk of spina bifida and/or anencephaly in siblings of NTD-affected individuals is increased by 3-8% (17). Furthermore, risk for NTDs varies widely by ethnicity and geographical region, suggesting a strong genetic component in disease pathogenesis (2, 17). The initial reports from epidemiological reports prompted investigators to prioritize identifying those variants in genes that metabolize folate; however, the genetic burden has yet to be identified. Therefore, the etiology of folate-responsive NTDs likely involves a complex interaction between genetic and environmental factors that modify disease risk (Figure 1), suggesting there may be a metabolic basis for folate-responsive NTDs. This chapter provides a review of the metabolic evidence that illustrates the known folate-dependent mechanisms of neural tube closure from both relevant human studies and animal models.

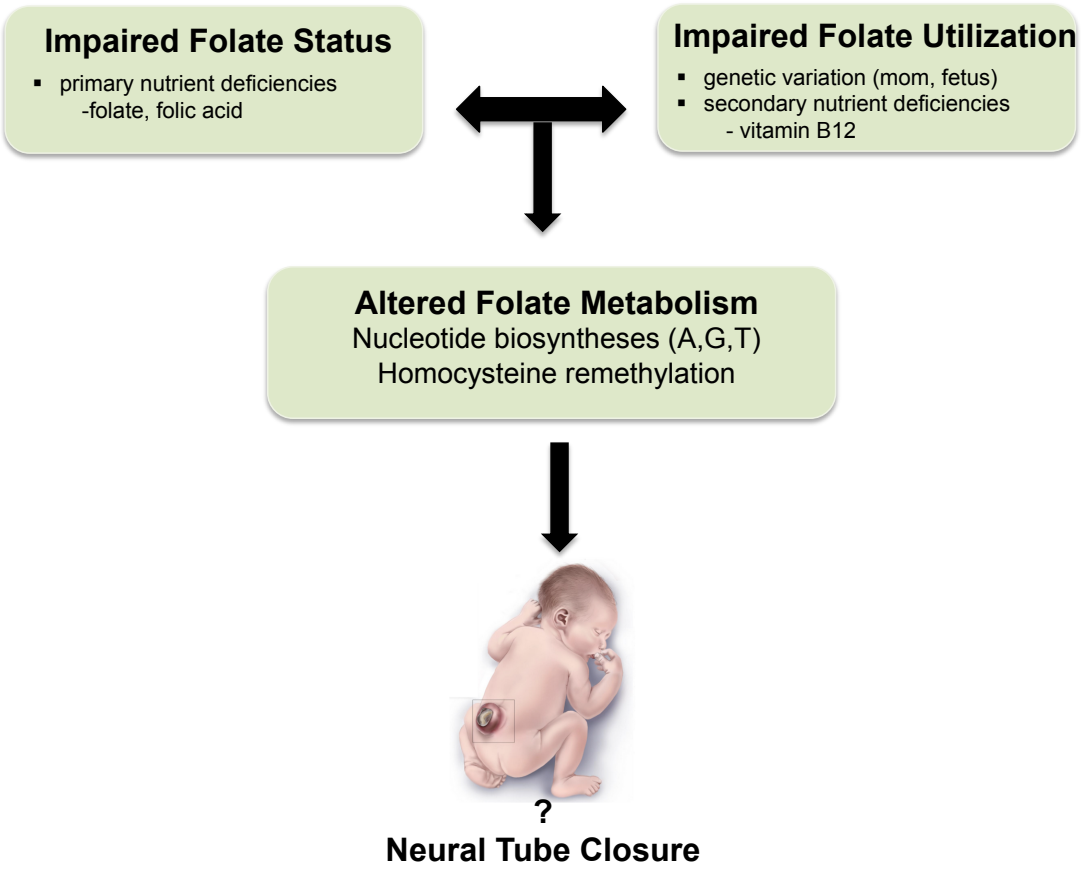

Figure 1.1. Conceptual schematic of neural tube defect etiology. Figure was amended from PJ Stover (personal communication) and inspired by Blom et al. (18). Image source: U.S. Centers for Disease Control and Prevention (CDC).

Folate-mediated one-carbon metabolism is compartmentalized within the cell

Tetrahydrofolates (THF) are a family of metabolic cofactors that carry and activate one-carbon units at three oxidation states: formate (10-formylTHF), formaldehyde (5,10-methyleneTHF), and methanol (5-methylTHF) (Fig. 2) (19). One-carbon units are generated by the catabolism of serine, glycine, sarcosine, dimethylglycine, and histidine, and are required for the *de novo* synthesis of purines and methionine in the cytosol, thymidylate (dTMP) in the nucleus, and formate in the

mitochondria. These biosynthetic pathways comprise a metabolic network referred to as folate-mediated one-carbon metabolism (FOCM). The exchange of folate cofactors is minimal between the cytosol and mitochondria, but one-carbon donors including serine, glycine, and formate may freely traverse between both compartments (20). The concentration of folate-utilizing proteins within the cell exceeds the amount of available folate cofactor, thus creating competition between pathways that is achieved by compartmentalization, which is most apparent in the use of 5,10-methyleneTHF for both the *de novo* dTMP biosynthesis and homocysteine remethylation pathways (Fig. 3). (21)

Mitochondrial FOCM generates formate for the FOCM pathways in the cytosol and nucleus. The hydroxymethyl group of serine is transferred to THF to form 5,10-methyleneTHF and glycine, catalyzed by SHMT2 (19). Glycine can be exported to the cytosol or further metabolized to 5,10-methyleneTHF via the glycine cleavage system (GCS). 5,10-methyleneTHF is oxidized to 10-formylTHF by the 5,10-methyleneTHF dehydrogenase and 5,10-methenylTHF cyclohydrolase activities of the bifunctional isoforms MTHFD2 or MTHFD2L (22). 10-formylTHF is oxidized in a final step by the 10-formylTHF synthetase activities of MTHFD1L to yield THF and formate, with the latter product being exported to the cytosol (23–25). The mitochondrial one-carbon metabolic pathways also synthesize formylated methionine-tRNA for mitochondrial protein biosynthesis. Additionally, a recent discovery has identified a homologous pathway for *de novo* dTMP biosynthesis in mitochondria (19, 26).

In the cytoplasm, *de novo* purine biosynthesis requires 10-formylTHF for the synthesis of adenosine (A) and guanosine (G) nucleotides. There are no functional biomarkers for impaired *de novo* purine biosynthesis.

The homocysteine remethylation pathway is also present in the cytosol and regenerates THF and methionine from 5-methylTHF and homocysteine. 5,10-methyleneTHF is irreversibly reduced to 5-methylTHF by MTHFR. The remethylation of homocysteine to methionine is accomplished by the vitamin B_{12}-dependent enzyme methionine synthase (MTR) and allows for the regeneration of THF for subsequent *de novo* synthesis of nucleotides and methionine for synthesis of S-adenosylmethionine that is used to methylate DNA, histones, proteins, and other small molecules, including neurotransmitters (27). Biomarkers of impaired homocysteine remethylation include elevated homocysteine and decreased methylation potential, as defined by the [AdoMet]/[AdoHcy], which can lead to altered gene expression (28, 29).

In the nucleus, one-carbon units are required for *de novo* dTMP biosynthesis. During S-phase of the cell cycle or in response to DNA damage, the folate-dependent enzymes comprising the *de novo* dTMP biosynthesis pathway translocate to the nucleus after modification by the small ubiquitin-like modifier (SUMO) protein (30, 31). Serine hydroxymethyltransferase (SHMT) serves as a required scaffold protein for thymidylate synthase (TYMS), dihydrofolate reductase (DHFR), and methylenetetrahydrofolate dehydrogenase (MTHFD1) that form a complex at sites of DNA replication and repair (32, 33), and its expression determines *de novo* dTMP capacity but does not provide the majority of one-carbon units in dTMP (34). 5,10-methyleneTHF can be generated by the SHMT-catalyzed cleavage of serine, or formate derived from the mitochondria can be condensed with THF in a reaction catalyzed by MTHFD1 to form 5,10-methyleneTHF (34). Stable isotope tracer studies in MCF-7 cells indicate that MTHFD1 provides 70-90% of the one-carbon units for dTMP from formate, whereas SHMT provides 10-30% of one-carbon units (34). Previous studies demonstrated that SHMT controls the partitioning of one-carbon

units between methylation reactions and *de novo* dTMP biosynthesis, and preferentially supports *de novo* dTMP at the expense of homocysteine remethylation (34). However, recent studies indicate that the MTHFD1 nuclear localization explains this apparent partitioning of 5,10-methyleneTHF. Under conditions of folate deficiency or when total cellular MTHFD1 levels are limited, *de novo* dTMP is prioritized at the expense of homocysteine remethylation through enhanced MTHFD1 nuclear enrichment (33, 35). 5,10-methyleneTHF is both a one-carbon donor and source of electrons used to methylate deoxyuridylate (dUMP) to form thymidylate (dTMP) and dihydrofolate (DHF), in a reaction catalyzed by TYMS. Biomarkers for impaired *de novo* dTMP biosynthesis include elevated levels of uracil content in DNA (35–39) that can lead to the formation of single- and double-stranded breaks (DSBs) in DNA as a result of base excision repair (BER) (36).

Mitochondrial folate-mediated one-carbon metabolism

Although disruptions in FOCM in the mitochondria result in NTDs, there is currently no evidence to suggest that impairments in mitochondrial FOCM underlie folate-responsive NTDs. Recent evidence from human studies and loss-of-function mouse models highlights the critical importance of mitochondrial formate production for neural tube closure, an observation that is not surprising given that mitochondria provide the majority of one-carbon units for the cytosolic and nuclear FOCM pathways. In spite of these encouraging findings, however, none of these mouse models are folate-responsive.

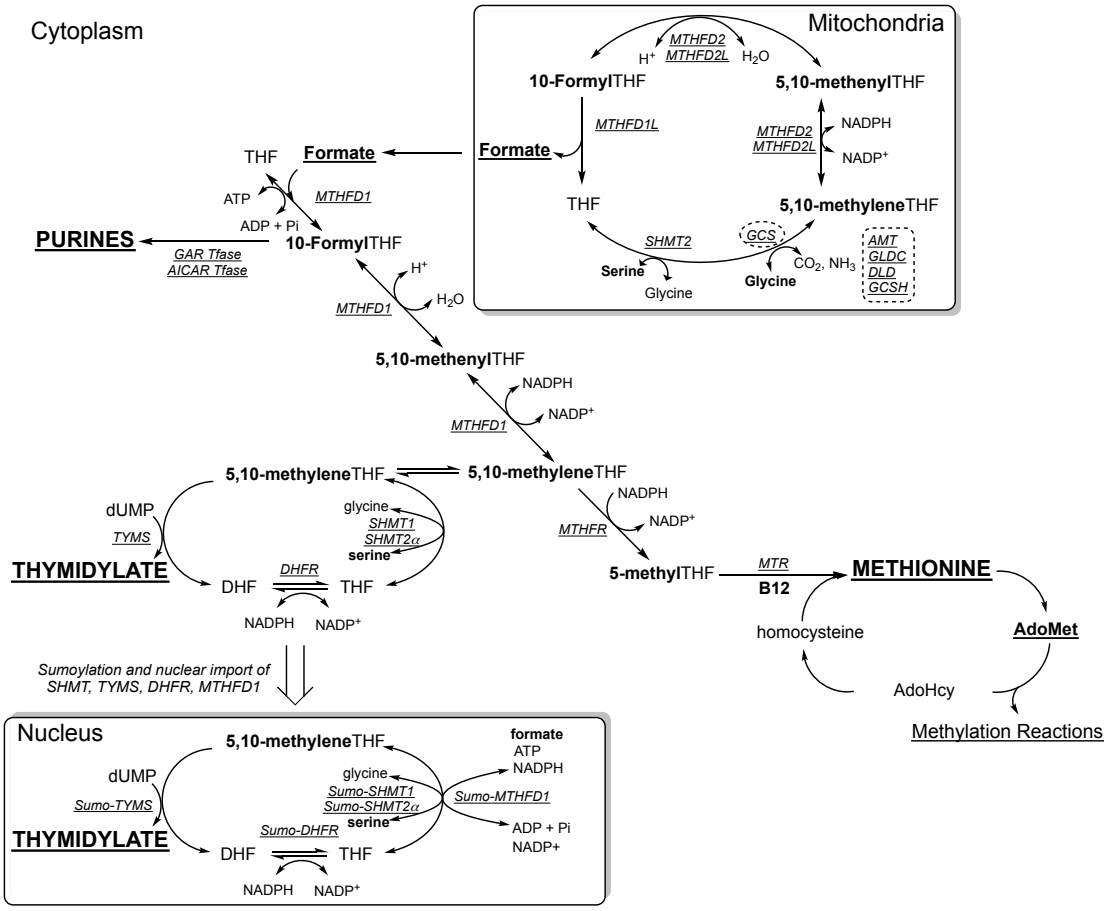

Figure 1.2. Overview of folate-mediated one-carbon metabolism. Folate-activated one-carbon units are required for the synthesis of formate in the mitochondria, purines and methionine in the cytoplasm, and thymidylate in the nucleus. Abbreviations: AdoHcy, *S*-adenosylhomocysteine; AdoMet, *S*-adenosylmethionine; AICAR Tfase, aminoimidazolecarboxamide ribonucleotide transformylase; AMT, aminomethyltransferase; DLD, dihydrolipoamide dehydrogenase; DHF, dihydrofolate; DHFR, dihydrofolate reductase; GAR Tfase, glycinamide ribonucleotide tranformylase; GCS, glycine cleavage system; GCSH, glycine cleavage system protein H; GLDC, glycine decarboxylase; MTHFD1, C1-tetrahydrofolate synthase (formyltetrahydrofolate synthetase, 5,10-methenyltetrahydrofolate cyclohydrolase, 5,10-methylenetetrahydrofolate dehydrogenase); MTHFD1L, formyltetrahydrofolate synthetase; MTHFD2, MTHFD2L, methylenetetrahydrofolate dehydrogenase/methenyltetrahydrofolate cyclohydrolase; MTHFS, methenyltetrahydrofolate synthetase; MTHFR, methylenetetrahydrofolate reductase; MTR, methionine synthase; SHMT, serine hydroxymethyltransferase; SUMO, small ubiquitin-like modifier; THF, tetrahydrofolate; TYMS, thymidylate synthase. Figure adapted from Field et al. (33).

The data from human studies linking impairments in mitochondrial folate metabolism with NTD risk support the idea that alterations in mitochondrial formate production increase risk for NTDs. Exome sequencing of the GCS components in cohorts from the UK, Sweden, and Japan identified novel missense variants in aminomethyltransferase (*AMT*) and glycine decarboxylase (*GLDC*) in NTD patients (Fig 2.) (40). In an Irish population, increased risk for NTDs is associated with homozgosity for an intronic polymorphism affecting splicing efficiency in *MTHFD1L* (41). Taken together, these associations suggest that disruptions in the production of one-carbon units in the mitochondria may increase risk for NTDs.

Several groups have recently demonstrated the essentiality of mitochondrially-derived formate for proper neural tube closure using loss-of-function mouse models, which supports the limited findings from human populations (40, 42, 43). Momb et al. showed that embryos with homozygous deletion of *Mthfd1L* exhibit growth delay and develop NTDs including exencephaly and craniorachiscisis at 100% penetrance, ultimately resulting in embryonic lethality by E13.5 (42). Maternal supplementation with sodium formate significantly rescued the number of expected NTD-affected embryos as well as the growth delay (42). In support of these findings, maternal formate supplementation also rescues NTDs in *curly tail* (*ct/ct*) embryos that have decreased expression of *Mthfd1L* (43). Loss-of-function mouse models for Amt and Gldc, encoded by the *Amt* and *Gldc* genes that participate in the glycine cleavage system (GCS), also demonstrate that mitochondrial formate production is crucial for neural tube closure. Embryos with homozygous gene-trap mutations in *Gldc* and *Amt* develop NTDs at 25-29% and 87% penetrance, respectively (40, 44). The NTDs in $Gldc^{GT,GT}$ can be rescued with exogenous formate (44); however it is not known if $Amt^{-/-}$ embryos respond to maternal formate supplementation (40). These findings,

taken together, strongly indicate that mitochondrial formate production is critical for neural tube closure, but that impairments in mitochondrial FOCM are not folate-responsive and therefore likely do not underlie folate-responsive NTDs.

Cytosolic folate-mediated one-carbon metabolic pathways

De novo Purine Biosynthesis

There is currently little evidence supporting the idea that impairments in folate-dependent *de novo* purine biosynthesis underlie folate-responsive NTDs. Investigating this pathway to better understand its role in NTD pathogenesis has been particularly difficult as data from cross-sectional studies have not identified genetic variants in enzymes in *de novo* purine biosynthesis that are associated with NTD risk.

Untangling the metabolic mechanisms underlying folate-dependent *de novo* purine biosynthesis in mouse models has presented a considerable challenge. Mice homozygous for loss-of-function gene trap alleles in *Mthfs* result in early embryonic lethality (45, 46). These observations likely reflect the essential roles of *Mthfs* in providing 10-formylTHF for *de novo* synthesis of purines (46). *Mthfs*$^{gt/+}$ mouse embryonic fibroblasts (MEFs) revealed a 50% reduction in *de novo* purine biosynthesis capacity, as quantified by a decrease in ^{14}C-formate incorporation into genomic DNA whereas *de novo* dTMP biosynthesis was unaffected (46). *Pax3 splotch* is a folate-responsive mouse model of NTDs that gives rise to spina bifida at 100% penetrance. There are 9 *splotch* alleles that result in *Pax3* mutations that yield a range of defects with variable penetrance and severity. MEFs derived from *Pax3*$^{Sp/Sp}$ embryos demonstrated significant impairments in *de novo* purine biosynthesis and a non-significant trend toward impaired *de novo* dTMP biosynthesis, as evidenced by the decrease in TYMS protein observed in mutant embryos (47).

When *Pax3 Splotch* heterozygotes were crossed with *Shmt1*$^{-/-}$ and *Shmt1*$^{-/+}$, the incidence and severity of NTDs was exacerbated. These findings suggest that *Pax3* may affect both *de novo* purine and dTMP biosyntheses.

Homocysteine Remethylation

There is no evidence that impairments in homocysteine remethylation underlie human folate responsive NTDs. The earliest findings from case-control studies demonstrating associations between elevated maternal plasma homocysteine and NTD risk (48, 49), combined with the knowledge that homocysteine can be lowered with folate supplementation, led to the hypothesis that impaired homocysteine remethylation is causal in NTD pathogenesis. To date, the common *MTHFR* 677 C>T polymorphism has shown the strongest association with NTD risk with contributions from both maternal and fetal alleles, but not all studies agree (18, 50). Furthermore, the prevalence of the *TT* polymorphism does not account for the NTD incidence observed in the population (50). The *TT* genotype is associated with elevated plasma homocysteine (51–53), reduced folate status (53, 54), and DNA hypomethylation (55, 56), especially under conditions of low folate status (53, 55, 56).

Recent findings from a large-scale population-based RCT in China (57) have demonstrated that the *TT* genotype independently predicts response to folic acid supplementation (53). At all doses, the *TT* genotype was associated with lower blood folate and elevated homocysteine concentrations compared to the *CT* or *CC* genotype (*TT*<*CT*<*CC*), indicating that folate supplementation can overcome the low folate and high homocysteine observed in *TT* individuals (53). In support of these findings, a recent systematic review assessing the relationship between MTHFR genotype and blood folate concentrations in women of reproductive age (12-49 years)

demonstrated that the blood folate concentrations are consistently highest in *CC* individuals, followed by *CT* and *TT* individuals (*CC* > *CT* > *TT*) (54). These observations are likely explained by structural studies indicating that the *TT* phenotype results from loss of flavin adenine dinucleotide (FAD) cofactor that can be prevented with folate, and suggest that lower blood folate observed in *TT* individuals may explain the increased risk of NTDs (58). It cannot be fully discounted that the *TT* genotype increases risk for NTDs by impaired methylation or homocysteine accumulation; however, no mechanistic findings have demonstrated support for this alternative.

There is no evidence from studies in mouse models to indicate that impairments in homocysteine remethylation underlie human folate-responsive NTDs. Germ-line deletion of both *Mthfr* alleles in the mouse results in a 10-fold elevation in plasma homocysteine, elevated in AdoHcy and/or decreased AdoMet, and global DNA hypomethylation, but do not develop NTDs (59) even under conditions of folate deficiency (60). Mice nullizygous for cystathionine beta synthase (*Cbs*) exhibit elevated plasma homocysteine but do not develop NTDs (61). Furthermore, mice with reduced expression of methionine synthase reductase (*Mtrr*) exhibit elevated plasma homocysteine, decreased plasma methionine, with tissue-specific alterations in methylation potential, but do not develop NTDs (62). MTR null mice exhibit early embryonic lethality (63).

Nuclear folate-mediated one-carbon metabolic pathways

The evidence to date strongly supports a role for impairments in folate-dependent *de novo* dTMP biosynthesis in the etiology of folate-responsive NTDs. Although the data from cross-sectional studies have not revealed convincing

associations between known genetic variants in the coding regions of folate-metabolizing enzymes comprising the *de novo* dTMP biosynthesis pathway and NTD risk (64–66), known variants do not affect enzyme activity. The strongest evidence to date has focused on the common polymorphism in *MTHFD1*, the 1958G>A variant, that has a homozygosity frequency of 20% in European populations and results in decreased 10-formylTHF synthetase activity but does not affect plasma folate status or homocysteine or impair nuclear localization (35, 67–69). However, the findings from individual studies are contradictory, as significant associations have been demonstrated in the Irish (69, 70) and Italian (71) but not Dutch populations (67, 72).

A 19-base pair deletion in intron 1 of DHFR has yielded inconclusive findings in conferring NTD risk (73–75). No significant differences in *DHFR* expression have been detected between individuals with one or two copies of the 19-base pair deletion polymorphism and those wild-type individuals (73, 74). A common 28-base pair repeat polymorphism in the promoter enhancer region of TYMS has shown conflicting results between studies (76, 77). Functional analyses of the repeat polymorphism indicate that alleles with two copies of the repeat polymorphism (2R) have decreased *TYMS* expression compared to those alleles with three copies (3R) (78)**.**

Evidence demonstrating that impairments in folate-dependent *de novo* dTMP are causal in the etiology of folate-responsive NTDs

There is substantial evidence from loss-of-function mouse models supporting the idea that impairments in nuclear *de novo* dTMP biosynthesis underlie folate-responsive NTDs. There is a loss-of-function mouse model for *Dhfr* exhibiting early embryonic lethality. A loss of function mouse model for *Tyms* generated by an N-ethyl-N-nitrosourea (*ENU*) mutagenesis screen that identified a T > A transversion in

the codon encoding amino acid 106 of TYMS causing a asparagine to lysine change (79). Homozygous embryos die shortly after implantation due to defects in gastrulation; however, heterozygous mice exhibit nearly 3-fold elevations in TYMS protein in liver compared to wild-type mice (79). This increase is likely explained by the fact that TYMS autoregulates its own translation by binding its own mRNA (79). Mice with genetic disruptions in *Shmt1* are viable and fertile (39), and this observation is explained by the fact that SHMT2α is redundant with SHMT1 and contributes 25% to nuclear *de novo* dTMP biosynthesis in *Shmt1*$^{-/-}$ mice (80). Mice with reductions in nuclear SHMT1 exhibit elevated uracil content in DNA, whereas methylation potential is not impaired (37–39).

The impact of maternal folate deficiency causes sporadic folate-responsive exencephaly in *Shmt1*$^{-/-}$ and *Shmt1*$^{-/+}$ embryos at low penetrance (81–83), and maternal supplementation with deoxyuridine (dU) fully rescues the folate-responsive NTDs (83). Tracer experiments in human cells have demonstrated that exogenous dU is incorporated into DNA as dT, and not dU, suggesting that dU supplementation compensates for this impairment by accelerating dTMP biosynthesis (83). When *Shmt1*$^{-/-}$ and *Shmt1*$^{-/+}$ mice were crossed with *Pax3 Spotch* heterozygotes, the incidence and severity of NTDs in offspring was exacerbated (82). PAX3 and SHMT1 co-localize in the neural tube, and genetic disruption of either *Shmt1* or *Pax3* results in a reciprocal increase in protein of the other. This exacerbated phenotype may be due to the decreases in TYMS protein observed when PAX3 and SHMT1 both decrease (82). A different *Pax3 splotch* strain was shown to have impaired *de novo* dTMP biosynthesis that can be rescued with supplemental thymidine and folic acid (84). In support of these findings, apoptosis occurs in the developing neuroepithelium along the lesion of NTD-affected *Pax3*$^{Sp/Sp}$ embryos (85), and deficiency of p53

completely rescues the NTDs observed in *Pax3*$^{Sp/Sp}$ embryos (86).

Mice with reduced expression of *Mthfd1* do not develop folate-responsive NTDs, and these observations may be explained by the observation that *Mthfd1*$^{gt/+}$ mice and human fibroblasts with loss-of-function mutations in *MTHFD1* demonstrate enhanced *de novo* dTMP biosynthesis at the expense of homocysteine remethylation.

Mthfd1$^{gt/+}$ mice exhibit a 40% reduction in hepatic AdoMet concentrations, which is expected because formate is a major source of one-carbon units for methylation reactions but exhibit enhanced *de novo* dTMP biosynthesis, as evidenced by reduction of genomic uracil in liver and colon of *Mthfd1*$^{gt/+}$ mice compared to *Mthfd1*$^{+/+}$ littermates fed either a control or folate-deficient diet (33, 45). This enhancement in *de novo* dTMP biosynthesis is explained by the finding that during folate deficiency, both *Mthfd1*$^{gt/+}$ and *Mthfd1*$^{+/+}$ mice demonstrate increased liver nuclear localization of MTHFD1, and mouse liver nuclei are resistant to folate-depletion compared to the cytosolic compartment (33). These findings, taken together, explain previous observations that 5,10-methyleneTHF is preferentially directed towards *de novo* dTMP biosynthesis under conditions of folate deficiency.

In support of the findings in *Mthfd1*$^{gt/+}$ embryos, recent evidence in human fibroblasts from a proband with inborn errors of metabolism in *MTHFD1* further demonstrate that folate-dependent *de novo* dTMP biosynthesis is prioritized at the expense of homocysteine remethylation (35). The fibroblasts expressing *MTHFD1* with significant reductions in cyclohydrolase and dehydrogenase activities exhibited a two-fold increase in MTHFD1 protein in the nucleus compared to control fibroblasts. Stable isotope tracer studies revealed that the MTHFD1 contributions into thymidine and methionine were reduced by 50% and 90%, respectively, indicating that despite

marked impairments in both pathways, homocysteine remethylation is still prioritized to a lesser degree. A 7-fold decrease in *de novo* dTMP capacity was observed due to a 4-fold increase in the salvage pathway and a 2-fold increase in TK1 levels. Increased nuclear localization of MTHFD1 as well as increased priority conferred to *de novo* dTMP biosynthesis was insufficient to minimize genomic uracil and DNA damage in proband fibroblasts (35).

Conclusions

In closing, the current evidence strongly argues that impairments in folate-dependent *de novo* dTMP biosynthesis underlie folate-responsive NTDs. Reduced rates of *de novo* dTMP biosynthesis can lead to elevated uracil content in DNA, as the replicative polymerases do not discriminate between dUTP and dTTP. The subsequent removal of genomic uracil by repair enzymes generates single- and double-stranded breaks in DNA, thereby compromising genome integrity (36), especially at those fragile sites that may be especially sensitive to replication stress (87). Futile cycles of replication and repair under conditions where dTTP is limiting can therefore lead to cell cycle arrest and apoptosis (88). Alternatively, reduced replication fork stability during S-phase can result in the formation of DSBs, for example in the case of a fork collapse (88). Therefore, impairments in dTMP synthesis, specifically within those cells comprising the developing neuroepithelium that have a high demand for dTMP production, can lead to increased genome instability, decreased rates of cellular proliferation, increased cell cycle arrest, and ultimately apoptosis that may lead to the development of NTDs. Studies to further advance our understanding of this pathway and its role in NTD pathogenesis should consider examining the impact of additional factors that may impair nuclear *de novo* dTMP biosynthesis. It is well-known that a fraction of NTD cases are not folate-

responsive (6), and vitamin B_{12} is an ideal nutrient to investigate, as a maternal deficiency has been identified as an independent risk factor for NTDs in a number of small case-control studies (15, 89–92).

Vitamin B_{12} is large, water-soluble B-vitamin that consists of a central cobalt atom surrounded by a planar corrin ring (93). Vitamin B_{12} participates in FOCM as a required cofactor for MTR in the cytosol that remethylates homocysteine to methionine by using 5-methyltetrahydrofolate (5-methylTHF) and regenerates THF for subsequent nucleotide biosyntheses (Fig. 2). Historically, experimental models aimed at studying the effects of vitamin B_{12} deficiency in animals or cells have utilized nitrous oxide (N_2O) gas treatment (94–97). Oxidation of the cobalt atom in the vitamin B_{12} bound to MTR leads to enzyme inactivation (98); therefore, blocking this step has served as a primary means of establishing experimental systems to study the underlying mechanisms of vitamin B_{12} deficiency in human health and disease. Deficiency of vitamin B_{12} can result from inadequate dietary intake or impaired absorption, with the latter cause accounting for the majority of deficiency cases (99). A clinical vitamin B_{12} deficiency can cause megaloblastic anemia by trapping folate cofactors as 5-methylTHF in the cytosol that leads to an inhibition of DNA synthesis (99). Furthermore, the role of vitamin B_{12} in maintaining genome stability is apparent in a number of cell types (100–104). It is understood that both the folate-dependent *de novo* dTMP biosynthesis and homocysteine remethylation pathways occur in separate compartments, but it is not known how a cytosolic vitamin B_{12} deficiency could impair nuclear *de novo* dTMP biosynthesis. These unanswered questions serve as the motivation for the work in Chapters 2 and 3.

References

1. Christianson A, Howson C, Modell B (2006) *March of Dimes global report on birth defects: the hidden toll of dying and disabled children*.

2. Botto LD, Moore CA, Khoury M, Erickson JD (1999) Neural-Tube Defects. *N Engl J Med* 342(20):1509–1519.

3. Copp AJ, Greene NDE (2013) Neural tube defects – disorders of neurulation and related embryonic processes. *Wiley Interdiscip Rev Dev Biol* 2(2):213–227.

4. Zohn IE, Sarkar AA (2008) Modeling neural tube defects in the mouse. *Curr Top Dev Biol* 84(8):1–35.

5. Grosse SD, Berry RJ, Mick Tilford J, Kucik JE, Waitzman NJ (2016) Retrospective assessment of cost savings from prevention folic acid fortification and spina bifida in the U.S. *Am J Prev Med* 50(5 Suppl 1):S74-80.

6. Group MVSR (1991) Prevention of neural tube defects: Results of the Medical Research Council Vitamin Study. *Lancet* 338(8760):131–137.

7. Czeizel A, Dudas I (1992) Prevention of the first occurrence of neural tube defects by periconceptional vitamin supplementation. *N Engl J Med* 327(26):1832–5.

8. MMWR (2014) Use of Folic Acid for Prevention of Spina Bifida and Other Neural Tube Defects: 1983-1991 Interim CDC Recommendations for Folic Acid Supplementation for Women August 1991. 2–3.

9. CDC Public Health Service (1993) Recommendations for the use of folic acid to reduce the number of cases of spina bifida and other neural tube defects. *JAMA J Am Med Assoc* 269(10):1233–1238.

10. Finglas PM (2000) *Dietary Reference intakes for thiamin, riboflavin, niacin, vitamin B6, folate, vitamin B12, pantothenic acid, biotin and choline* doi:10.1016/S0924-2244(01)00010-3.

11. EPA US, Mandates FU, Office GA (1996) Federal Register / Vol. 61, No. 151 / Monday, August 5, 1996 / Rules and Regulations. *Fed Regist* 61(151):1996.

12. Williams J, et al. (2015) Updates estimates of neural tube defects prevented by mandatory folic acid fortification - United States, 1995-2011. *MMWR Morb Mortal Wkly Rep* 64(1):1–5.

13. Cordero A, et al. (2010) CDC Grand Rounds: additional opportunities to prevent neural tube defects with folic acid fortification. *Morb Mortal Wkly Rep* 59(31):980–984.

14. Scott J, et al. (1994) Folic acid metabolism and mechanisms of neural tube defects. *Ciba Found Symp* 181:180–191.

15. Kirke PN, Daly LE, Burke H, Weir DC (1993) Maternal plasma folate and vitamin B12 are independent risk factors for neural tube defects. *Q J Med* 86(11):703–708.

16. Heid MK, Bills ND, Hinrichs SH, Clifford AJ (1992) Biochemical and Molecular Roles of Nutrients Folate Deficiency Alone Does Not Produce Neural Tube Defects in Mice1. *J Nutr* 122(4):888–894.

17. Mitchell LE, et al. (2004) Spina bifida. *Lancet* 364(9448):1885–1895.

18. Blom HJ, Shaw GM, den Heijer M, Finnell RH (2006) Neural tube defects and folate: case far from closed. *Nat Rev Neurosci* 7(9):724–731.

19. Fox JT, Stover PJ (2008) Chapter 1 Folate-Mediated One-Carbon Metabolism. 79(8):1–44.

20. Tibbetts AS, Appling DR (2010) Compartmentalization of Mammalian folate-mediated one-carbon metabolism. *Annu Rev Nutr* 30:57–81.

21. Stover PJ, Field MS (2011) Trafficking of intracellular folates. *Adv Nutr* 2(4):325–331.

22. Bolusani S, et al. (2011) Mammalian MTHFD2L encodes a mitochondrial methylenetetrahydrofolate dehydrogenase isozyme expressed in adult tissues. *J Biol Chem* 286(7):5166–5174.

23. Christensen KE, Patel H, Kuzmanov U, Mejia NR, MacKenzie RE (2005) Disruption of the Mthfd1 gene reveals a monofunctional 10-formyltetrahydrofolate synthetase in mammalian mitochondria. *J Biol Chem* 280(9):7597–7602.

24. Prasannan P, Pike S, Peng K, Shane B, Appling DR (2003) Human mitochondrial C1-tetrahydrofolate synthase: gene structure, tissue distribution of the mRNA, and immunocolocalization in CHO cells. *J Biol Chem* 278(44):43178–43187.

25. Pike ST, Rajendra R, Artzt K, Appling DR (2010) Mitochondrial C1-tetrahydrofolate synthase (MTHFD1L) supports the flow of mitochondrial one-carbon units into the methyl cycle in embryos. *J Biol Chem* 285(7):4612–4620.

26. Anderson DD, Quintero CM, Stover PJ (2011) Identification of a de novo thymidylate biosynthesis pathway in mammalian mitochondria. *Proc Natl Acad Sci* 108(37):15163–15168.

27. Bailey LB, Gregory JF (1999) Polymorphisms of methylenetetrahydrofolate reductase and other enzymes: metabolic significance, risks and impact on folate requirement. *J Nutr* 129(5):919–922.

28. Finkelstein JD (1998) The metabolism of homocysteine: pathways and regulation. *Eur J Pediatr* 157 Suppl:S40–S44.

29. Kim YI, et al. (1997) Folate deficiency in rats induces DNA strand breaks and hypomethylation within the p53 tumor suppressor gene. *Am J Clin Nutr* 65(1):46–52.

30. Woeller CF, Anderson DD, Szebenyi DME, Stover PJ (2007) Evidence for small ubiquitin-like modifier-dependent nuclear import of the thymidylate biosynthesis pathway. *J Biol Chem* 282(24):17623–17631.

31. Fox JT, Shin WK, Caudill MA, Stover PJ (2009) A UV-responsive internal ribosome entry site enhances serine hydroxymethyltransferase 1 expression for DNA damage repair. *J Biol Chem* 284(45):31097–108.

32. Anderson DD, Woeller CF, Chiang EP, Shane B, Stover PJ (2012) Serine hydroxymethyltransferase anchors de novo thymidylate synthesis pathway to nuclear lamina for DNA synthesis. *J Biol Chem* 287(10):7051–7062.

33. Field MS, et al. (2014) Nuclear enrichment of folate cofactors and methylenetetrahydrofolate dehydrogenase 1 (MTHFD1) protect de novo thymidylate biosynthesis during folate deficiency. *J Biol Chem* 289(43):29642–29650.

34. Herbig K, et al. (2002) Cytoplasmic serine hydroxymethyltransferase mediates competition between folate-dependent deoxyribonucleotide and S-adenosylmethionine biosyntheses. *J Biol Chem* 277(41):38381–38389.

35. Field MS, Kamynina E, Watkins D, Rosenblatt DS, Stover PJ (2014) Human mutations in methylenetetrahydrofolate dehydrogenase 1 impair nuclear de novo thymidylate biosynthesis. *Proc Natl Acad Sci U S A* 112(2):1–6.

36. Blount B, et al. (1997) Folate deficiency causes uracil misincorporations into human DNA and chromosome breakage: implications for cancer and neuronal damage. *Proc Natl Acad Sci U S A* 94(7):3290–5.

37. MacFarlane AJ, et al. (2011) Nuclear localization of de novo thymidylate biosynthesis pathway is required to prevent uracil accumulation in DNA. *J Biol Chem* 286(51):44015–44022.

38. MacFarlane AJ, Perry CA, McEntee MF, Lin DM, Stover PJ (2011) Shmt1 Heterozygosity Impairs Folate-Dependent Thymidylate Synthesis Capacity and Modifies Risk of Apcmin-Mediated Intestinal Cancer Risk. *Cancer Res* 71(6):2098–2107.

39. MacFarlane AJ, et al. (2008) Cytoplasmic serine hydroxymethyltransferase regulates the metabolic partitioning of methylenetetrahydrofolate but is not essential in mice. *J Biol Chem* 283(38):25846–25853.

40. Narisawa A, et al. (2012) Mutations in genes encoding the glycine cleavage system predispose to neural tube defects in mice and humans. *Hum Mol Genet* 21(7):1496–503.

41. Parle-McDermott A, et al. (2009) A common variant in MTHFD1L is associated with neural tube defects and mRNA splicing efficiency. *Hum Mutat* 30(12):1650–1656.

42. Momb J, et al. (2013) Deletion of Mthfd1l causes embryonic lethality and neural tube and craniofacial defects in mice. *Proc Natl Acad Sci U S A* 110(2):549–54.

43. Sudiwala S, et al. (2015) Formate supplementation enhances folate-dependent nucleotide biosynthesis and prevents spina bifida in a mouse model of folic acid-resistant neural tube defects. *Biochimie* 126:63–70.

44. Pai YJ, et al. (2015) Glycine decarboxylase deficiency causes neural tube defects and features of non-ketotic hyperglycinemia in mice. *Nat Commun* 6:6388.

45. MacFarlane AJ, et al. (2009) Mthfd1 is an essential gene in mice and alters biomarkers of impaired one-carbon metabolism. *J Biol Chem* 284(3):1533–1539.

46. Field MS, Anderson DD, Stover PJ (2011) Mthfs is an essential gene in mice and a component of the purinosome. *Front Genet* 2(36):1–13.

47. Beaudin AE, et al. (2011) Shmt1 and de novo thymidylate biosynthesis underlie folate-responsive neural tube defects in mice. *Am J Clin Nutr* 93(4):789–98.

48. Steegers-Theunissen RPM, Boers G, Trijbels FJ, Eskes TKAB (1991) Neural-tube defects and the derangement of homocysteine metabolism.

49. Mills JL et al. (1995) Homocysteine metabolism neural-tube defects in pregnancies complicated by. *Q J Med*:149–151.

50. Botto LD, Yang Q (2000) 5,10-methylenetetrahydrofolate reductase gene variants and congenital anomalies: A HuGE review. *Am J Epidemiol* 151(9):862–877.

51. Frosst P, et al. (1995) A candidate genetic risk factor for vascular disease: a common mutation in methylenetetrahydrofolate reductase. *Nat Genet* 10:196–201.

52. Harmon D, et al. (1996) The commmon “thermolabile” variant of methylenetetrahydrofolate reducase is a major determinant of mild hyperhomocysteinaemia. *Q J Med* 89(8):571–577.

53. Crider KS, et al. (2011) MTHFR 677C>T genotype is associated with folate and homocysteine concentrations in a large, population-based, double-blind trial of folic. *Am J Clin Nutr* 93(6):1365–1372.

54. Tsang BL, et al. (2015) Assessing the association between the methylenetetrahydrofolate reductase (MTHFR) 677C>T polymorphism and blood folate concentrations: a systematic review and meta-analysis of trials and observational studies. *Am J Clin Nutr* 101(6):1286–1294.

55. Stern LL, Mason JB, Selhub J, Choi SW (2000) Genomic DNA hypomethylation, a characteristic of most cancers, is present in peripheral leukocytes of individuals who are homozygous for the C677T polymorphism in the Methylenetetrahydrofolate reductase gene. *Cancer Epidemiol Biomarkers Prev* 9(8):849–853.

56. Friso S, et al. (2002) A common mutation in the 5,10-methylenetetrahydrofolate reductase gene affects genomic DNA methylation through an interaction with folate status. *Proc Natl Acad Sci U S A* 99(8):5606–5611.

57. Hao L, et al. (2008) Folate status and homocysteine response to folic acid doses and withdrawal among young Chinese women in a large-scale randomized double-blind trial. *Am J Clin Nutr* 88(2):448–457.

58. Guenther BD, et al. (1999) The structure and properties of methylenetetrahydrofolate reductase from Escherichia coli suggest how folate ameliorates human hyperhomocysteinemia. *Nat Struct Biol* 6(4):359–365.

59. Chen Z, et al. (2001) Mice deficient in methylenetetrahydrofolate reductase exhibit hyperhomocysteinemia and decreased methylation capacity, with neuropathology and aortic lipid deposition. *Hum Mol Genet* 10(5):433–443.

60. Li D, Pickell L, Liu Y, Rozen R (2006) Impact of methylenetetrahydrofolate reductase deficiency and low dietary folate on the development of neural tube defects in Splotch mice. *Birth Defects Res Part A - Clin Mol Teratol* 76(1):55–59.

61. Watanabe M, et al. (1995) Mice deficient in cystathionine beta-synthase: animal models for mild and severe homocyst(e)inemia. *Proc Natl Acad Sci U S A* 92(5):1585–9.

62. Elmore CL, et al. (2007) Metabolic derangement of methionine and folate metabolism in mice deficient in methionine synthase reductase. *Mol Genet Metab* 91(1):85–97.

63. Swanson D, Liu M, Baker P (2001) Targeted disruption of the methionine synthase gene in mice. *Mol Cell Biol* 21(4):1058–1065.

64. Heil SG, et al. (2001) Is mutated serine hydroxymethyltransferase (SHMT) involved in the etiology of neural tube defects? *Mol Genet Metab* 73:164–172.

65. Relton CL, et al. (2004) Gene-gene interaction in folate-related genes and risk of neural tube defects in a UK population. *J Med Genet* 41(4):256–260.

66. Relton CL, et al. (2004) Low erythrocyte folate status and polymorphic variation in folate-related genes are associated with risk of neural tube defect pregnancy. *Mol Genet Metab* 81(4):273–281.

67. Hol FA, et al. (1998) Molecular genetic analysis of the gene encoding the trifunctional enzyme MTHFD (methylenetetrahydrofolate-dehydrogenase, methenyltetrahydrofolate-cyclohydrolase, formyltetrahydrofolate synthetase) in patients with neural tube defects. *Clin Genet* 53(2):119–125.

68. Christensen KE, et al. (2009) The MTHFD1 p.Arg653Gln variant alters enzyme function and increases risk for congenital heart defects. *Hum Mutat* 30(2):212–220.

69. Brody LC, et al. (2002) A polymorphism, R653Q, in the trifunctional enzyme methylenetetrahydrofolate dehydrogenase/methenyltetrahydrofolate cyclohydrolase/formyltetrahydrofolate synthetase is a maternal genetic risk factor for neural tube defects: report of the Birth Defects Res. *Am J Hum Genet* 71(5):1207–1215.

70. Parle-McDermott A, et al. (2006) Confirmation of the R653Q polymorphism of the trifunctional C1-synthase enzyme as a maternal risk for neural tube defects in the Irish population. *Eur J Hum Genet* 14(6):768–772.

71. De Marco P, et al. (2006) Evaluation of a methylenetetrahydrofolate-dehydrogenase 1958G>A polymorphism for neural tube defect risk. *J Hum Genet* 51(2):98–103.

72. van der Linden IJM, Heil SG, Kouwenberg IC, Den Heijer M, Blom HJ (2007) The methylenetetrahydrofolate dehydrogenase (MTHFD1) 1958G> A variant is not associated with spina bifida risk in the Dutch population. *Clin Genet* 72(6):599–600.

73. van der Linden IJM, et al. (2007) Variation and expression of dihydrofolate reductase (DHFR) in relation to spina bifida. *Mol Genet Metab* 91(1):98–103.

74. Parle-McDermott A, et al. (2007) The 19-bp deletion polymorphism in intron-1 of dihydrofolate reductase (DHFR) may decrease rather than increase risk for spina bifida in the Irish population. *Am Mournal Med Genet Part A* 143A(11):1174–1180.

75. Johnson WG, et al. (2004) New 19 bp deletion polymorphism in intron-1 of dihydrofolate reductase (DHFR): a risk factor for spina bifida acting in mothers during pregnancy? *Am J Med Genet Part A* 124A(4):339–45.

76. Wilding CS, et al. (2004) Thymidylate synthase repeat polymorphisms and risk of neural tube defects in a population from the northern United Kingdom. *Birth Defects Res A Clin Mol Teratol* 70(7):483–5.

77. Volcik KA, et al. (2003) Associations between polymorphisms within the thymidylate synthase gene and spina bifida. *Birth Defects Res Part A - Clin Mol Teratol* 67(11):924–8.

78. Horie N, Aiba H, Oguro K, Hojo H, Takeishi K (1995) Functional analysis and DNA polymorphism of the tandemly repeated sequences in the 5'-terminal regulatory region of the human gene for thymidylate synthase. *Cell Struct Funct* 20(3):191–197.

79. Ching Y-H, et al. (2010) High resolution mapping and positional cloning of ENU-induced mutations in the Rw region of mouse chromosome 5. *BMC Genet* 11:106.

80. Anderson DD, Stover PJ (2009) SHMT1 and SHMT2 are functionally redundant in nuclear de novo thymidylate biosynthesis. *PLoS One* 4(6):e5839.

81. Beaudin AE, et al. (2012) Dietary folate, but not choline, modifies neural tube defect risk in Shmt1 knockout mice. *Am J Clin Nutr* 95(1):109–114.

82. Beaudin AE, et al. (2011) Shmt1 and de novo thymidylate biosynthesis underlie folate-responsive neural tube defects in mice. *Am J Clin Nutr* 93(4):789–798.

83. Martiniova L, Field MS, Finkelstein JL, Perry CA, Stover PJ (2015) Maternal dietary uridine causes, and deoxyuridine prevents, neural tube closure defects in a mouse model of folate-responsive neural tube defects. *Am J Clin Nutr* 101(4):860–9.

84. Fleming A, Copp AJ (1998) Embryonic Folate Metabolism and Mouse Neural Tube Defects. *Science (80-)* 280(5372):2107–2109.

85. Phelan SA, Ito M, Loeken MR (1997) Neural tube defects in embryos of diabetic mice. *Diabetes* 46(7):1189–1197.

86. Pani L, Horal M, Loeken MR (2002) Rescue of neural tube defects in Pax-3-deficient embryos in p53 loss of function: implications for Pax-3-dependent development and tumorigenesis. *Genes Dev* 16(6):676–680.

87. Reidy JA (1987) Deoxyuridine increases folate-sensitive fragile site expression in human lymphocytes. *Am J Med Genet* 26(1):1–5.

88. Berger SH, Pittman DL, Wyatt MD (2008) Uracil in DNA: Consequences for carcinogenesis and chemotherapy. *Biochem Pharmacol* 76(6):697–706.

89. Gaber K, Farag M, Soliman S, El-Bassyouni H, El-Kamah G (2007) Maternal vitamin B12 and the risk of fetal neural tube defects in Egyptian patients. *Clin Lab* 53(1–2):69–75.

90. Groenen PMW, et al. (2004) Marginal maternal vitamin B12 status increases the risk of offspring with spina bifida. *Am J Obstet Gynecol* 191(1):11–17.

91. Molloy AM, et al. (2009) Maternal vitamin B12 status and risk of neural tube defects in a population with high neural tube defect prevalence and no folic acid fortification. *Pediatrics* 123(3):917–23.

92. Ray JG, et al. (2007) Vitamin B12 and the risk of neural tube defects in a folic-acid-fortified population. *Epidemiology* 18(3):362–366.

93. Scott JM (1999) Folate and vitamin B12. *Proc Nutr Soc* 58(2):441–448.

94. Christensen B, Ueland PM (1993) Methionine synthase inactivation by nitrous oxide during methionine loading of normal human fibroblasts. Homocysteine remethylation as determinant of enzyme inactivation and homocysteine export. *J Pharmacol Exp Ther* 267(3):1298–303.

95. Ermens AAM, Schoester M, Lindemans J, Abels J (1991) Effect of nitrous oxide and methotrexate on folate coenzyme pools of blast cells from leukemia patients. *Leuk Res* 15(2–3):165–171.

96. Wilson SD, Horne DW (1986) Effect of nitrous oxide inactivation of vitamin B12 on the levels of folate coenzymes in rat bone marrow, kidney, brain, and liver. *Arch Biochem Biophys* 244(1):248–53.

97. Walker PR, et al. (1997) Induction of apoptosis in neoplastic cells by depletion of vitamin B12. *Cell Death Differ* 4(3):233–41.

98. Burman JF (1978) Megaloblastic Haemopoiesis in Patients Receiving Nitrous Oxide. 339–342.

99. Stabler SP (2013) Vitamin B12 Deficiency. *N Engl J Med* 368(2):149–160.

100. Jensen MK (1977) Cytogenetic findings in pernicious anaemia. Comparison between results obtained with chromosome studies and the micronucleus test. *Mutat Res Mol Mech Mutagen* 45(2):249–252.

101. Minnet C, Koc A, Aycicek A, Kocyigit A (2011) Vitamin B12 treatment reduces mononuclear DNA damage. *Pediatr Int* 53(6):1023–7.

102. Rana S, Colman N, Goh KO, Herbert V, Klemperer M (1983) Transcobalamin II deficiency associated with unusual bone marrow findings and chromosomal abnormalities. *Am J Hematol* 14(1):89–96.

103. Wickramasinghe SN, Fida S (1994) Bone marrow cells from vitamin B12- and folate-deficient patients misincorporate uracil into DNA. *Blood* 83(6):1656–61.

104. Kapiszewska M, Kalemba M, Wojciech U, Milewicz T (2005) Uracil misincorporation into DNA of leukocytes of young women with positive folate balance depends on plasma vitamin B12 concentrations and methylenetetrahydrofolate reductase polymorphisms. A pilot study. *J Nutr Biochem* 16(8):467–78.

CHAPTER 2: MATERNAL VITAMIN B_{12} DEFICIENCY CAUSES EXENCEPHALY IN A MOUSE MODEL OF FOLATE-RESPONSIVE NEURAL TUBE DEFECTS

Authors: Ashley M. Palmer[a], Julia L. Finkelstein[a], Sally P. Stabler[c], Robert H. Allen[c], Margaret E. Brosnan[d], John T. Brosnan[d], Martha S. Field[a], Patrick J. Stover[a,b]

Affiliations: [a]Division of Nutritional Sciences and [b]Graduate Field of Biochemistry, Molecular, and Cell Biology, Cornell University, Ithaca, NY 14853, [c]Department of Medicine and Division of Hematology, University of Colorado Health Sciences Center, Aurora, CO 80045 and [d]Department of Biochemistry, Memorial University of Newfoundland, St. John's, Newfoundland A1B X39, Canada

Abstract:

Background: Folic acid intake in the periconceptional period significantly reduces the risk of neural tube defect (NTD) occurrence and recurrence by up to 70%, and identification of other modifiable risk factors may further prevent NTD-affected pregnancies. Observational studies have shown an association between maternal vitamin B_{12} status and NTD risk in both folate-fortified and non-fortified populations. Vitamin B_{12} participates in folate-mediated one-carbon metabolism, and a vitamin B_{12} deficiency causes an accumulation of cellular folate as 5-methylTHF, making folate cofactors unavailable for nucleotide biosyntheses. Serine hydroxymethyltransferase (SHMT) serves as an essential scaffold for the assembly of a nuclear multienzyme complex comprising the folate-dependent *de novo* thymidylate (dTMP) biosynthesis pathway enzymes; mice with reduced *Shmt1* expression have elevated uracil content in DNA and embryos are sensitized to NTDs under conditions of maternal folate deficiency. Therefore, this model system is ideal for examining the role of vitamin B_{12}

deficiency in NTD pathogenesis, specifically in relation to folate-dependent *de novo* dTMP biosynthesis.

Objective: The impact of mild maternal vitamin B_{12} deficiency, under folate-replete and deficient conditions, on NTD incidence was investigated in the *Shmt1* mouse model.

Design: *Shmt1*$^{-/-}$ and *Shmt1*$^{-/+}$ female mice were randomized to 1 of 4 diets: 1) AIN93G, 2) AIN93G - folate, 3) AIN93G - vitamin B_{12}, and 4) AIN93G lacking vitamin B_{12} and folate for a minimum of 8 weeks. Females (12 – 24 weeks) fed the AIN93G diet deficient in folate and/or vitamin B_{12} were mated to *Shmt1*$^{-/+}$ males, and embryos were examined for the presence of NTDs at E12.5. The following outcomes were also measured: plasma metabolites (plasma folate, vitamin B_{12}, formate, and transsulfuration pathway biomarkers), the number of resorptions and implants, crown-rump (CR) length, and embryonic *Shmt1* genotype.

Results: The vitamin B_{12}- and folate-deficient diets reduced mean serum vitamin B_{12} and/or folate concentrations by 72 and 79%, respectively. NTDs were observed in *Shmt1*$^{-/-}$ and *Shmt1*$^{-/+}$ embryos from dams fed the vitamin B_{12} deficient diet. Dietary folate and maternal folate status did not cause a significant difference in NTD incidence between the vitamin B_{12} deficient groups. Transsulfuration pathway metabolites (homocysteine, cystathionine, and cysteine) were significantly predicted by maternal folate status but not by maternal vitamin B_{12} status. Maternal dietary folate deficiency and embryonic *Shmt1* genotype, but not vitamin B_{12} status, predicted CR length.

Conclusions: Vitamin B_{12} deficiency is an independent risk factor for NTDs in the *Shmt1* mouse model, and NTDs were observed in both *Shmt1*$^{-/-}$ and *Shmt1*$^{-/+}$. No

differences were observed in rates of NTDs between the vitamin B_{12}-deficient, folate-replete and the vitamin B_{12}- and folate-deficient dams. Although maternal vitamin B_{12} deficiency caused NTDs, it did not significantly impair growth or increase plasma homocysteine, indicating that neural tube closure is more sensitive to mild maternal vitamin B_{12} deficiency compared to embryonic growth and homocysteine remethylaton.

Keywords: SHMT | neural tube defects | vitamin B_{12} | folic acid | thymidylate

Introduction

Neural tube defects (NTDs), including spina bifida and anencephaly, occur when the neural folds fail to fuse during early embryogenesis (1). The etiology of NTDs is multifactorial and involves interactions among both genetic and environmental factors, although the underlying mechanisms are not fully understood (2). The methylenetetrahydrofolate reductase (MTHFR) C677T polymorphism is associated with NTDs in some populations due to its effect on reducing folate status (3–5); however, much of the genetic basis of NTDs remains unidentified.

Maternal folic acid supplementation prevents NTD occurrence and recurrence (6, 7). In the period immediately following the mandatory folic acid fortification of enriched flour (1999-2000), the prevalence of NTDs in the US was reduced to a baseline rate of 0.6/1,000 live births (8, 9). However, NTD prevalence has remained relatively stable in the years following, as not all NTD cases are folate-responsive (9). Therefore, identifying the remaining non-genetic risk factors may inform new interventions to further reduce the incidence of NTD-affected pregnancies. Particular attention has focused on better understanding those risk factors that are closely

interrelated with folate-mediated one-carbon metabolism that may impair either folate status or metabolism (10–13).

Maternal vitamin B_{12} deficiency is a proposed NTD risk factor. Several small case-control studies show an association between low maternal vitamin B_{12} status and increased risk for NTDs (14–23). In the period following mandatory folic acid fortification in Canada, second trimester mothers in the lowest quartile of holotranscobalamin (holo-TC, a biomarker of vitamin B_{12} status) exhibited a nearly 3-fold greater risk for having an NTD-affected pregnancy compared to the reference quartile, with no difference in folate status among the groups (20, 24). In a non-folate-fortified population, Molloy and colleagues demonstrated a 2.5 to 3-fold increase in NTD risk among Irish mothers with low serum vitamin B_{12} at 15 weeks gestation when comparing lowest and highest quartiles of serum vitamin B_{12} (19). No prospective studies have assessed the causal relationship between maternal vitamin B_{12} status and NTD risk in human populations nor has this question been investigated in animal models.

Within the cell, folates carry and activate one-carbon units for *de novo* synthesis of nucleotides (purines and dTMP) and remethylation of homocysteine to methionine (25) (Fig. 2.1). Increasing evidence from both epidemiologic and animal studies suggests that impairments in *de novo* dTMP biosynthesis underlie folate-responsive NTDs (26–28). SHMT is a required scaffold protein for other components of the nuclear *de novo* dTMP biosynthesis pathway, including TYMS, DHFR, and MTHFD1 (29, 30) (Fig. 2.1). In mice, *Shmt1* loss-of-function leads to increased uracil content in DNA, but does not cause homocysteine remethylation cycle impairments (31). The *Shmt1* mouse is the only mouse model with a genetic disruption in a gene encoding a folate-dependent enzyme that causes folic acid-responsive NTDs, and

this NTD phenotype is observed in both *Shmt1* homozygotes and heterozygotes embryos. This mouse model reflects the pathogenesis of folate-responsive human NTD cases that arise from gene by diet interactions at a low penetrance with only minor alterations in biomarkers of one-carbon metabolism (2, 26, 28, 32). Maternal dietary deoxyuridine (dU) supplementation rescues NTDs observed in *Shmt1*$^{-/-}$ and *Shmt1*$^{-/+}$ embryos carried by folate-deficient dams, and tracer studies in cultured human cells have shown that dU is ultimately incorporated into DNA as deoxythymidine (dT) (28). Taken together, these findings suggest that *de novo* dTMP biosynthesis underlies folate-responsive NTDs, and that exogenous dU may prevent these NTDs by correcting the metabolic impairment in *de novo* dTMP biosynthesis. In support of these studies in mouse models, a subset of human fibroblast lines derived from terminated NTD-affected pregnancies revealed significantly impaired *de novo* thymidylate biosynthesis. This observed impairment in *de novo* dTMP capacity was not correlated with alterations in methylation cycle metabolites (27). Furthermore, several mouse models with impairments in homocysteine remethylation demonstrate elevated circulating homocysteine levels without NTDs (33–36), even under conditions of maternal folate deficiency (35), suggesting that this pathway is not causal in NTD pathogenesis.

Vitamin B_{12} functions within folate-mediated one-carbon metabolism as a required cofactor for methionine synthase (MTR), which catalyzes the remethylation of homocysteine to methionine and regenerates tetrahydrofolate (THF) for nucleotide biosyntheses (Fig. 2.1). Impaired MTR function leads to a trapping of folate cofactors as 5-methylTHF within the cell and subsequent depressed rates of nucleotide biosynthesis and impaired methylation reactions (37–39). This consequence is most readily apparent in highly proliferative cell types, where there exists a substantial

metabolic demand for nucleotide production, and inadequate THF leads to impaired cell division, dTMP synthesis and DNA replication, as in the case of megaloblastic anemia that results from a deficiency of either vitamin B_{12} or folate (37, 38).

We investigated the impact of maternal vitamin B_{12} deficiency on NTD incidence in embryos with disruptions in *Shmt1* expression. Associations between maternal vitamin B_{12} deficiency and increased risk for NTDs in humans (15, 16, 18–20), coupled with the knowledge that vitamin B_{12} is required to maintain *de novo* dTMP biosynthesis, prompted us to test the *a priori* hypothesis that a maternal B_{12} deficiency sensitizes *Shmt1*$^{-/-}$ and *Shmt1*$^{-/+}$ embryos to NTDs. Our second *a priori* comparison asked whether incidence of NTDs differed between embryos from dams fed a vitamin B_{12}-deficient, folate-replete diet compared to a combined vitamin B_{12}- and folate-deficient diet. The second comparison was prompted by recent findings from cross-sectional studies that have suggested low vitamin B_{12} and high folate status exacerbates symptoms of several common vitamin B_{12}-associated pathologies, including anemia and cognition (40, 41).

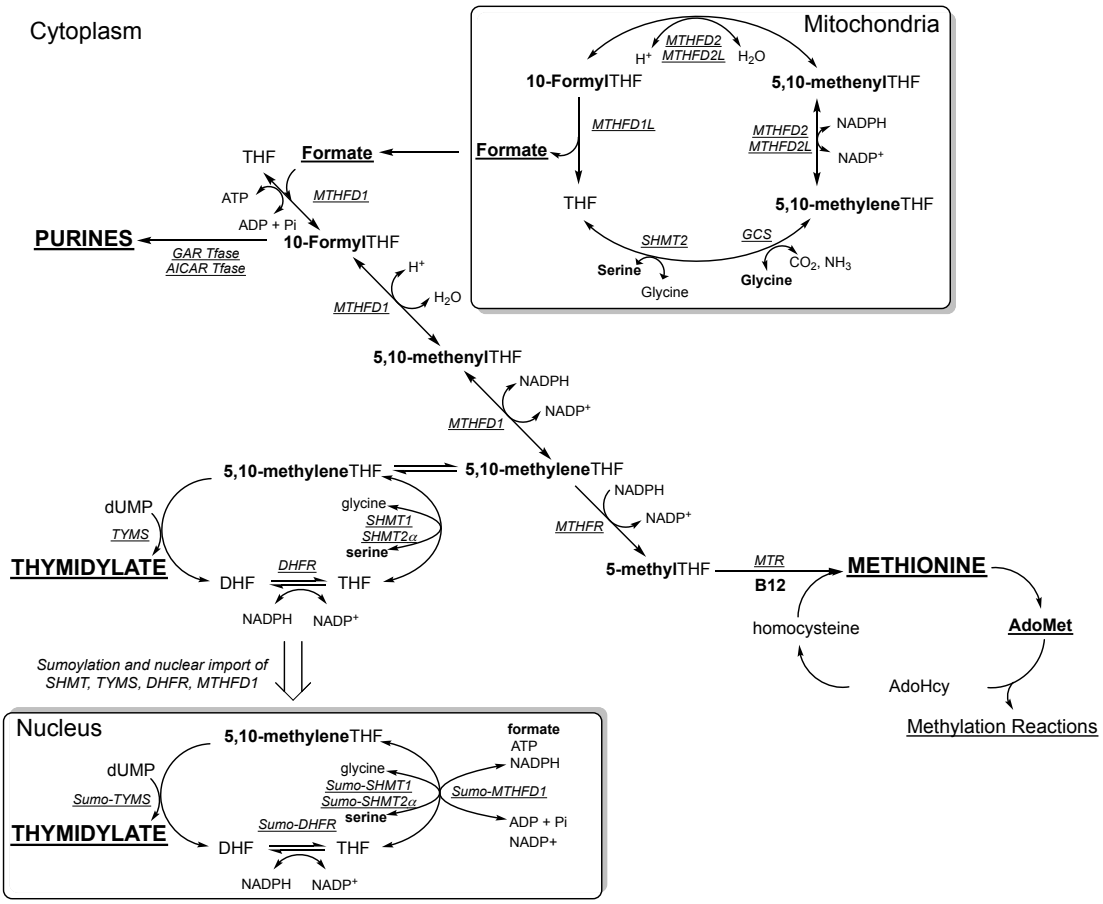

Figure 2.1. One-carbon metabolism in the nucleus, cytosol, and mitochondria. Folate- and vitamin B_{12}-mediated one-carbon metabolism is compartmentalized within the cell. The hydroxymethyl group of serine is a primary source of 1C units, and can enter the pool of activated 1C units by SHMT-catalyzed cleavage of serine. Otherwise, serine and glycine are converted to formate in mitochondria, which traverses to the cytosol and nucleus where it is condensed with THF by MTHFD1. 1C metabolism in the cytosol includes the *de novo* synthesis of purines and the remethylation of homocysteine to methionine. Vitamin B_{12} is a required cofactor for MTR. *De novo* dTMP biosynthesis occurs in the nucleus, catalyzed by the enzymes SHMT1, SHMT2α, TYMS, and DHFR, which undergo SUMOylation leading to nuclear import in S-phase. 5,10-methyleneTHF is synthesized by SHMT or MTHFD1 for *de novo* dTMP synthesis. AdoHcy, *S*-adenosylhomocysteine; AdoMet, *S*-adenosylmethionine; AICAR Tfase, aminoimidazolecarboxamide ribonucleotide transformylase; DHF, dihydrofolate; DHFR, dihydrofolate reductase; GAR Tfase, glycinamide ribonucleotide tranformylase; GCS, glycine cleavage system; MTHFD1, methylenetetrahydrofolate dehydrogenase 1; MTHFD1L, methylenetetrahydrofolate dehydrogenase 1-like; MTHFD2 & MTHFD2L, methylenetetrahydrofolate dehydrogenase 2 and 2-like; MTHFR, methylenetetrahydrofolate reductase; MTR, methionine synthase; SHMT, serine hydroxymethyltransferase; SUMO, small ubiquitin-like modifier; THF, tetrahydrofolate; TYMS, thymidylate synthase. Figure adapted from Field et al. (30).

Methods

Mouse models: The *Shmt1* mouse model and its sensitivity to folate deficiency in the etiology of NTDs has been described previously (26, 28, 32). *Shmt1*$^{-/+}$ females were generated by intercrossing *Shmt1*$^{-/+}$ breeding pairs maintained on a pure 129SvEv background. *Shmt1*$^{-/-}$ females were generated by intercrossing *Shmt1*$^{-/-}$ breeding pairs on the 129SvEv background.

Experimental animals and diets: All animal experiments were approved by the Cornell Institutional Animal Care and Use Committee (Cornell University, Ithaca, NY) according to the guidelines of the Animal Welfare Act and all applicable federal and state laws. Mice were maintained on a 12-h light/dark cycle in a temperature-controlled room. All female *Shmt1*$^{-/-}$ and *Shmt1*$^{-/+}$ mice derived from *Shmt1*$^{-/+}$ and *Shmt1*$^{-/-}$ crosses were weaned onto an AIN93G diet lacking folic acid and vitamin B_{12} (Dyets, Bethlehem, PA). Weekly supplementation of vitamin B_{12} and/or folate comprised a total of 4 diet groups determined *a priori*: 1) AIN93G (control diet; CD), 2) AIN93G - folate (folate-deficient diet; FDD), 3) AIN93G - vitamin B_{12} (vitamin B_{12} deficient diet; B_{12}DD), 4) AIN93G – folate & vitamin B_{12} (combined vitamin B_{12} and folate deficient diet; B_{12}FDD) (refer to **Supplemental Information**). At weaning, mice were randomized to one of the 4 diets, and, once weekly, were fasted overnight (12-h). The following morning, mice were individually housed in an empty cage with access to water, and administered a supplement corresponding to the appropriate diet. Following consumption of the supplement, mice were returned to their cages; all mice housed within a cage were assigned to the same diet regimen. Those mice that failed to consume the weekly supplement in 3 consecutive weeks were removed from the study. All mice were maintained on these diets from weaning until sacrifice. Following 8 weeks on experimental dietary regime, virgin *Shmt1*$^{+/-}$ and *Shmt1*$^{-/-}$ dams

were mated to *Shmt1*$^{+/-}$ males overnight, and examined each morning for the presence of a vaginal plug to determine gestational age. Pregnant females were sacrificed at E12.5 by cervical dislocation. Maternal blood was collected by cardiac puncture, plasma and red blood cells were separated, and all samples were stored at -80°C. Gravid uteri were removed, and all implant and resorption sites were recorded. Live embryos were examined for the presence of malformations; a subset of those NTD-affected embryos were fixed in 10% neutral buffered formalin. Crown-rump length was determined and yolk sacks were collected for embryo *Shmt1* genotyping.

Genotype analysis: Genotyping for *Shmt1*$^{-/-}$, *Shmt1*$^{-/+}$, *and Shmt1*$^{+/+}$ alleles was performed using established protocols (31).

Determination of metabolites:

Plasma folate: Total serum folate concentrations were quantified by the *Lactobacillus casei* microbiological assay as described previously (42).

Serum vitamin B_{12}: Total serum vitamin B_{12} was measured by a modification of published procedures (43). Briefly, serum was thawed on ice and diluted 10-fold in extraction buffer containing sodium hydroxide (8.3 mM), acetic acid (20.7 mM), and sodium cyanide (0.45 mM), pH 4.5 to liberate protein-bound vitamin B_{12} in serum. Samples were autoclaved for 20 minutes at 121°C, cooled on ice, and spun down for 15 minutes at maximum speed in a tabletop centrifuge at 4°C. The supernatant was removed, and the extracted volume recorded. The concentration of serum vitamin B_{12} in individual samples was determined using a standard curve that consisted of 1 pg/μL, 20 pg/μL, 40 pg/μL, 60 pg/μL, and 80 pg/μL cyanocobalamin standards added to respective standard tubes at a final concentration of 0-80 pg as appropriate. Vitamin B_{12} Assay Media (Becton-Dickinson, #245710) was prepared according to the

manufacturer's instructions. In glass borosilicate tubes, 10 mL assay mixtures were prepared for the following: 1) *samples* (B_{12} assay media: 5 mL, extracted plasma: 40 μL, deionized water: 4.86 mL), 2) *standards* (B_{12} assay media: 5 mL, diluted cyanocobalamin in extraction buffer: 50 μL, deionized water: 4.85 mL), 3) *blank* (B_{12} assay media: 5 mL, extraction buffer: 40 μL, deionized water: 4.86 mL), and 4) *zero standard* (B_{12} assay media: 5 mL, extraction buffer: 40 μL, deionized water: 4.86 mL). The tubes containing assay mixtures were autoclaved for 20 minutes at 121°C and allowed to cool to room temperature before inoculation with 100 μL of either 0.9% saline (blank) or *L. leischmanii* diluted 1:50 in 0.9% saline (zero, standards, samples). Cultures were incubated at 37°C for 18 hours. The following day, tubes were vortexed and subsequently plated in triplicate into 96-well plates (300 μL/well), that included a standard curve on each plate. All plates were read at 595 nm on a Gen5 microplate reader (BioTek). One standard curve was constructed by averaging the standard curve readings from all plates, and the vitamin B_{12} concentrations in the extracted samples were determined from this single curve.

Plasma formate: Plasma formate was quantified in a subset of samples (n=10 dams comprising a mixture of both *Shmt1*$^{-/-}$ and *Shmt1*$^{-/+}$ genotypes) from pregnant study dams from each of the 4 diet groups as described previously (Table 2.4) (44).

Plasma homocysteine panel: Plasma homocysteine, cystathionine, cysteine, methionine, glycine, serine, and α-aminobutyric acid metabolites were quantified in a subset of samples (n=10) from pregnant study dams in each of the 4 diets as described previously (45, 46). Each diet contained a subset of both *Shmt1*$^{-/-}$ and *Shmt1*$^{-/+}$ genotypes (Table 2.4).

Statistical analyses:

Plasma metabolites: Analyses of plasma metabolites were assessed using a two-way analysis of variance (ANOVA) with Tukey's honestly significant difference (HSD) test for post-hoc analysis. Independent variables included maternal *Shmt1* genotype, maternal diet, as well as the interaction between genotype and diet. If the interaction term was not significant, it was removed, and the model was fit again to test the main effects of maternal diet and genotype. Metabolites with non-normal distributions were either log- or rank-transformed to improve the normal distribution assumption. Linear contrasts were used to assess the influence of individual nutrients (e.g., vitamin B_{12}) on metabolite response in the case of plasma [serine]/[glycine].

NTDs: Fisher's exact test for independence with Bonferroni's correction (n=2) was used to assess the following comparisons for NTD incidence from dams fed the B_{12}DD compared to that from dams fed the: 1) CD and 2) B_{12}FDD. Because we did not expect the rates of NTDs in offspring from vitamin B_{12} deficient dams to be less than the rates of NTDs for offspring from the CD, a one-sided Fisher's Exact Test was used to assess the impact of maternal vitamin B_{12} deficiency versus the CD. The impact of embryonic *Shmt1* genotype on NTD incidence was assessed using exact tests.

Crown-rump length: Mixed models evaluated the fixed effects of maternal *Shmt1* genotype, embryonic *Shmt1* genotype, maternal diet, and two relevant interaction terms, namely, maternal genotype x diet and embryonic genotype x diet on crown-rump (CR) length. Litter was included in the model and treated as a random effect. The interaction term was removed from the model when it was not significant and

main effects were tested again. A Tukey's HSD test for post-hoc analysis was used to assess differences when main effects were significant.

Resorptions: Generalized estimating equations models were used to evaluate the fixed effects of maternal *Shmt1* genotype, maternal diet, and the interaction between genotype and diet on the odds of resorption for all implanted embryos. These models assumed binomial errors and used a logit link function. Implants were considered repeated measures within litter. Differences in observed versus expected embryonic genotype distributions in litters from *Shmt1*$^{-/-}$ and *Shmt1*$^{-/+}$ dams were analyzed by a Chi-Square test.

Results

Supplemented diets modulate plasma folate and vitamin B_{12} in study dams

Plasma folate concentrations were influenced by *Shmt1* disruption ($F = 10.02$, $p = 0.002$; Table 2.1) and dietary folate deficiency ($F = 166$, $p < 0.0001$). The interaction between both diet and genotype was significant ($F = 4.78$; $p = 0.003$; Table 2.1). The mean plasma folate concentrations in dams fed the folate deficient diets (FDD and B_{12}FDD) were reduced by approximately 79% compared to the mean serum folate concentrations in dams fed the folate-replete diets (B_{12}DD and CD) (Table 2.1). Serum vitamin B_{12} concentrations were influenced by maternal *Shmt1* genotype ($F = 23.7$; $p<0.0001$) and a dietary vitamin B_{12} deficiency ($F = 129.3$; $p<0.0001$; Table 2.1). There was a significant interaction between *Shmt1* genotype and maternal diet ($F = 3.37$; $p = 0.02$). Both vitamin B_{12} deficient diets (B_{12}DD and B_{12}FDD) were significantly different from the vitamin B_{12}-replete (CD and FDD) diets ($p<0.0001$). Dietary maternal vitamin B_{12} deficiency reduced mean serum vitamin B_{12}

concentrations by 72% when comparing the vitamin B_{12} replete (CD and FDD) and deficient (B_{12}DD and B_{12}FDD) diet groups.

Vitamin B_{12} deficiency causes NTDs in Shmt1$^{-/-}$ and Shmt1$^{-/+}$ embryos

Maternal diet was significant at the litter level (p = 0.01). Maternal vitamin B_{12} deficiency significantly predicted NTD risk compared to the CD (p = 0.008). There was no difference in the rates of NTDs between the B_{12}DD and the B_{12}FDD groups (p > 0.05). Embryonic genotype significantly predicted NTD response (p = 0.001), and deletion of both *Shmt1* alleles significantly increased NTD risk compared to *Shmt1*$^{-/+}$ (p = 0.004) and *Shmt1*$^{+/+}$ (p=0.005) embryos (Table 2.3). Maternal *Shmt1* genotype did not significantly influence NTD incidence (p > 0.05), which is consistent with previous observations. Therefore, all maternal genotypes within individual diets were combined for further analyses.

Crown-rump length and resorptions

Maternal diet (F= 5.42; p = 0.0013) and embryonic *Shmt1* genotype (F= 4.77; p=0.0087) significantly predicted embryonic CR length but maternal *Shmt1* genotype did not (p > 0.05) (Table 2.2). There was no significant interaction detected for either maternal *Shmt1* genotype and diet (p > 0.05) or embryonic *Shmt1* genotype and diet (p > 0.05). Embryos from dams consuming folate deficient diets (FDD and B_{12}FDD) were significantly smaller compared to those from to dams fed the B_{12}DD, indicating that maternal folate deficiency is likely responsible for the observed growth restriction. *Shmt1*$^{-/-}$ embryos were significantly smaller compared to *Shmt1*$^{-/+}$ and *Shmt1*$^{+/+}$ embryos. Neither maternal genotype nor diet had a significant effect on rates of resorption (p > 0.05). There were no differences between the observed and expected

embryonic genotypes in litters from *Shmt1*$^{-/-}$ and *Shmt1*$^{-/+}$ dams (p = 0.47 and p = 0.71, respectively, chi-square test).

Maternal dietary folate deficiency influences plasma transsulfuration pathway metabolites

Plasma concentrations of transsulfuration pathway metabolites were influenced by dietary folate deficiency, but not maternal *Shmt1* genotype. The interaction term between maternal genotype and diet was not significant (p>0.05). Maternal folate deficiency increased plasma homocysteine concentrations, with significant differences observed between the folate-deficient (FDD and B_{12}FDD) and replete (CD and B_{12}DD) diets (F = 21.97; p<0.0001 (Table 2.4). Plasma cystathionine was significantly influenced by maternal diet (F = 6.49, p = 0.0014) with significant decreases observed in the folate-deficient diets (B_{12}FDD and FDD) compared to the CD (Table 2.4). Maternal folate deficiency also predicted plasma cysteine concentrations with decreases observed in the FDD compared to the B_{12}DD and CD (F = 4.18, p = 0.013). Plasma concentrations of methionine, α-aminobutryic acid, serine, glycine, or the ratio of serine-to-glycine ([serine]/[glycine]) were not influenced by either maternal diet or *Shmt1* genotype (p>0.05; Table 2.4), but a linear contrast performed between the vitamin B_{12}-deficient (B_{12}FDD and B_{12}DD) and replete (FDD and CD) diets revealed significant differences in the plasma [serine]/[glycine] ratio (F = 4.56, p=0.04). The mean ratio of [serine]/[glycine] in plasma increased by approximately 25% under conditions of maternal vitamin B_{12} deficiency (Table 2.4).

Maternal dietary vitamin B_{12} deficiency influences plasma formate concentrations

Plasma formate concentrations in pregnant study dams were significantly influenced by both maternal diet (F = 7.36, p = 0.01; Table 2.4) and *Shmt1* genotype

(F = 4.48, p = 0.009); however, no significant interaction between maternal genotype and diet was detected (p>0.05). Plasma formate concentrations in dams from the B_{12}DD were significantly different from those in the FDD and CD. Plasma formate in *Shmt1*$^{-/+}$ dams on the B_{12}DD was reduced by one-third compared to those in *Shmt1*$^{-/-}$ dams.

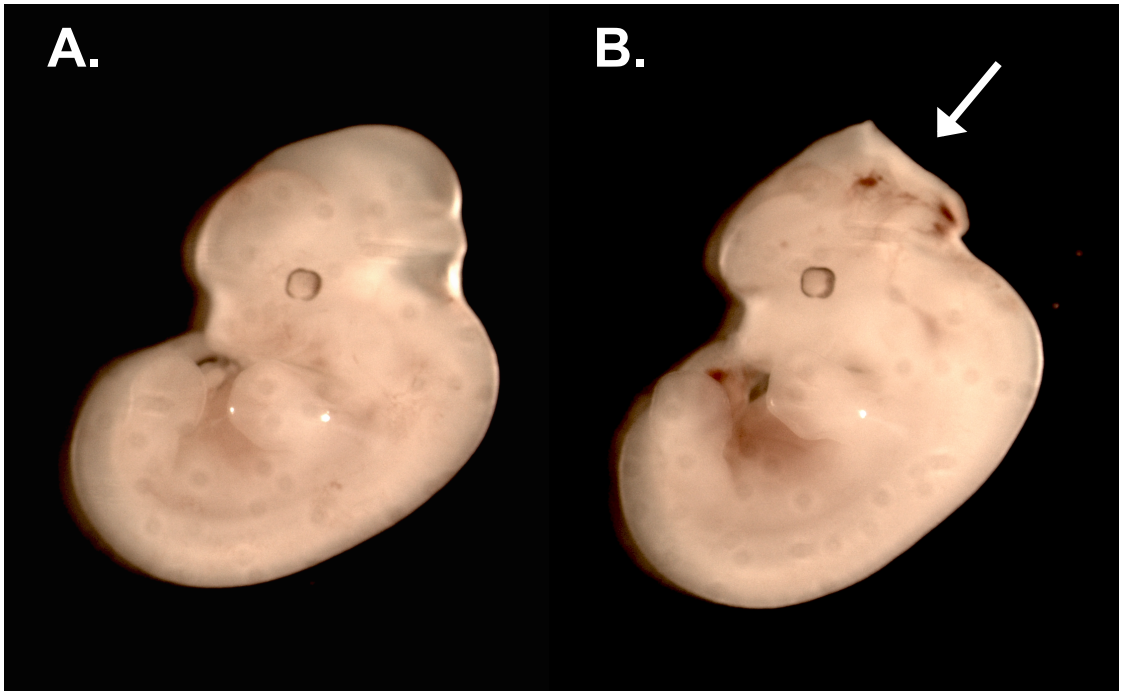

Figure 2.2. Neural tube defects in *Shmt1*-deficient embryos at gestational day 12.5 (E12.5). (A) Representative unaffected *Shmt1*$^{-/+}$ embryo and (B) *Shmt1*$^{-/-}$ littermate that exhibited failure of rostral neural tube closure both from a *Shmt1*$^{-/+}$ dam fed a vitamin B_{12}-deficient diet. Arrows indicate location of lesion.

Table 2.1. Effects of maternal diet on plasma folate and vitamin B_{12} concentrations by maternal *Shmt1* genotype.[1]

Diet and Maternal Genotype		n	Folate, ng/mL	Ln (Folate)[2,3,4]	n	Vitamin B_{12}, pg/μL	Ln (B_{12})[5,6,7]
Control (CD)	(n=68)	50	28.74 (1.45)	3.29 (0.05)	59	7.29 (0.45)	1.88 (0.06)
	Shmt1$^{+/-}$	35	28.82 (1.66)	3.30 (0.06)	43	7.11 (0.58)	1.84 (0.08)
	Shmt1$^{-/-}$	15	28.58 (3.01)	3.26 (0.12)	16	7.76 (0.61)	2.00 (0.08)
Vitamin B_{12} Deficient (B_{12}DD)	(n=69)	60	31.96 (1.60)	3.37 (0.06)	63	2.38 (0.12)	0.80 (0.05)
	Shmt1$^{+/-}$	46	31.67 (1.86)	3.35 (0.08)	48	2.33 (0.14)	0.77 (0.05)
	Shmt1$^{-/-}$	14	32.94 (3.26)	3.43 (0.10)	15	2.56 (0.26)	0.87 (0.10)
Folate Deficient (FDD)	(n=64)	56	5.99 (0.42)	1.65 (0.07)	57	10.32 (0.63)	2.21 (0.07)
	Shmt1$^{+/-}$	44	6.40 (0.47)	1.74 (0.08)	45	9.64 (0.70)	2.13 (0.08)
	Shmt1$^{-/-}$	12	4.51 (0.76)	1.33 (0.18)	12	12.88 (1.26)	2.50 (0.11)
Folate and B_{12} Deficient (B_{12}FDD)	(n=68)	65	6.92 (0.46)	1.75 (0.08)	68	2.60 (0.12)	0.88 (0.05)
	Shmt1$^{+/-}$	46	7.90 (0.53)	1.94 (0.08)	48	2.15 (0.11)	0.71 (0.05)
	Shmt1$^{-/-}$	19	4.56 (0.64)	1.30 (0.17)	20	3.67 (0.14)	1.29 (0.04)

[1] Values are shown as means (S.E.). A two-way ANOVA assessed the effects of maternal *Shmt1* genotype, maternal diet, and the interaction between genotype and diet on log-transformed values for serum folate and vitamin B_{12}. Post-hoc comparisons were analyzed using a Tukey's honestly significant difference (HSD) test.
[2] *Shmt1*$^{-/-}$ was different from *Shmt1*$^{-/+}$ ($p = 0.002$)
[3] The FDD and B_{12}FDD were significantly different from the CD and B_{12}DD ($p<0.0001$).
[4] *Shmt1*$^{-/+}$ was different from *Shmt1*$^{-/-}$ for the B_{12}FDD only ($p = 0.003$).
[5] *Shmt1*$^{-/-}$ was different from *Shmt1*$^{-/+}$ ($p<0.0001$)
[6] The FDD and CD were significantly different from the B_{12}FDD and B_{12}DD ($p<0.0001$).
[7] *Shmt1*$^{-/-}$ was different from *Shmt1*$^{-/+}$ in the B_{12}FDD only ($p = 0.02$).

Table 2.2. Average embryonic crown-rump (CR) length, average resorption rate, average litter size, and percent NTDs as a function of maternal *Shmt1* genotype and diet.[1]

Diet and Maternal Genotype	Litters, *n*	Implants, *n*	Litter Size	Embryos, *n*	NTDs[2], n (%)	Resorptions[3], n (%)	CR Length[4], mm
Control (CD)[5]	68	445	6.5 ± 0.3	314	0 (0.0)	131 (29.4)	8.24 ± 0.04 (292)
Shmt1$^{+/-}$	46	299	6.5 ± 0.3	220	0 (0.0)	79 (26.4)	8.32 ± 0.05 (198)
Shmt1$^{-/-}$	22	146	6.6 ± 0.5	94	0 (0.0)	52 (35.6)	8.07 ± 0.07 (94)
Vitamin B_{12} Deficient (B_{12}DD)	69	475	6.9 ± 0.2	338	4 (1.2)	137 (28.8)	8.39 ± 0.04 (272)
Shmt1$^{+/-}$	54	369	6.8 ± 0.2	260	3 (1.2)	109 (29.5)	8.34 ± 0.05 (195)
Shmt1$^{-/-}$	15	106	7.1 ± 0.5	78	1 (1.3)	28 (26.4)	8.54 ± 0.09 (77)
Folate Deficient (FDD)	64	403	6.3 ± 0.3	251	9 (3.6)	152 (37.7)	7.98 ± 0.06 (208)
Shmt1$^{+/-}$	50	317	6.3 ± 0.3	194	6 (3.1)	123 (38.8)	8.02 ± 0.07 (152)
Shmt1$^{-/-}$	14	86	6.1 ± 0.7	57	3 (5.3)	29 (33.7)	7.86 ± 0.12 (56)
Fol. and B_{12} Deficient (B_{12}FDD)	68	481	7.1 ± 0.2	318	4 (1.3)	163 (33.9)	7.91 ± 0.05 (262)
Shmt1$^{+/-}$	48	350	7.3 ± 0.3	226	1 (0.4)	124 (35.4)	7.97 ± 0.06 (170)
Shmt1$^{-/-}$	20	131	6.6 ± 0.4	92	3 (3.3)	39 (29.8)	7.80 ± 0.09 (92)

[1] Mean ± standard error of mean (S.E.)

[2] Percent of embryos. The difference in rates of NTDs between the CD and B_{12}DD was significant (p=0.008; Bonferroni-corrected). There was no difference in NTD rates between the B_{12}DD and B_{12}FDD (p>0.05; Bonferroni-corrected).

[3] Percent of resorptions is determined by dividing the number of resorbed embryos by the total number of implant sites (number of live embryos and resorbed embryos). Maternal *Shmt1* genotype, diet, and the genotype by diet interaction did not significantly predict rates of resorptions (p>0.05).

[4] Mean ± S.E. (n with measured length available). Maternal diet (p=0.0013) and embryonic genotype (p=0.0087) had a significant effect on CR length, and the interaction terms were not significant (p>0.05). Maternal genotype (p>0.05) was not significant. The folate-deficient diets (FDD and B_{12}FDD) were smaller than the B_{12}DD. *Shmt1*$^{-/-}$ embryos were smaller than *Shmt1*$^{-/+}$ and *Shmt1*$^{+/+}$ embryos.

[5] Rates of NTDs were determined from a total of 200 dams fed the CD. A subset of these litters (n=68) was used in the analyses.

Table 2.3. Frequency of NTDs as a function of embryonic *Shmt1* genotype.[1]

		Embryo *Shmt1*$^{+/+}$		Embryo *Shmt1*$^{+/-}$		Embryo *Shmt1*$^{-/-}$	
Diet and Maternal Genotype[2]		**NTDs, *n* (%)**	**Embryos, *n***	**NTDs, *n* (%)**	**Embryos, *n***	**NTDs, *n* (%)**	**Embryos, *n***
Control (CD)		0	54	0	154	0	101
	Shmt1$^{+/-}$	0	54	0	109	0	52
	Shmt1$^{-/-}$	–	–	0	45	0	49
Vitamin B_{12} Deficient (B_{12}DD)		0	62	2 (1.34)	149	2 (1.89)	106
	Shmt1$^{+/-}$	0	62	1 (0.88)	113	2 (3.13)	64
	Shmt1$^{-/-}$	–	–	1 (2.78)	36	0	42
Folate Deficient (FDD)		0	43	2 (1.55)	129	6 (8.81)	73
	Shmt1$^{+/-}$	0	43	2 (2.00)	100	3 (6.66)	45
	Shmt1$^{-/-}$	–	–	0	29	3 (10.71)	28
Folate and B_{12} Deficient (B_{12}FDD)		0	55	0	167	4 (4.21)	95
	Shmt1$^{+/-}$	0	55	0	123	1 (2.13)	47
	Shmt1$^{-/-}$	–	–	0	44	3 (6.25)	48

[1] The effect of overall embryonic *Shmt1* genotype on NTD incidence was significant p=0.0009. *Shmt1*$^{-/-}$ embryos were significantly different from *Shmt1*$^{-/+}$ (p=0.004) and *Shmt1*$^{+/+}$ embryos (p=0.005) as determined by exact tests.
[2] Maternal *Shmt1* genotype did not predict rates of NTDs (p>0.05).

Table 2.4. Concentrations of plasma metabolites in pregnant *Shmt1*$^{-/-}$ and *Shmt1*$^{-/+}$ dams at E12.5 fed a control, folate-deficient, combined vitamin B_{12} & folate deficient, or vitamin B_{12}-deficient diet.[1]

Metabolite	Maternal Genotype	Diet			
		CD	FDD	B_{12}DD	B_{12}FDD
HCYS[2,5] (μmol/L)	Total	8.1 ± 0.8	21.7 ± 3.5	8.0 ± 0.7	21.2 ± 1.5
	Shmt1$^{+/-}$	7.6 ± 1.6	22.4 ± 4.2	9.0 ± 0.9	22.7 ± 2.2
	Shmt1$^{-/-}$	8.3 ± 0.9	19.2 ± 7.1	6.4 ± 0.8	19.5 ± 2.0
CYSTAT[2,6] (nmol/L/)	Total	1151 ± 108	1800 ± 218	1343 ± 134	2042 ± 240
	Shmt1$^{+/-}$	1104 ± 79	1738 ± 235	1256 ± 67	2297 ± 347
	Shmt1$^{-/-}$	1175 ± 39	2046 ± 727	1475 ± 338	1658 ± 224
CYS[7] (μmol/L)	Total	187.1 ± 6.0	160.2 ± 7.2	184.2 ± 5.1	174.2 ± 6.8
	Shmt1$^{+/-}$	177.3 ± 8.5	161.8 ± 8.9	193.5 ± 4.7	178.7 ± 10.9
	Shmt1$^{-/-}$	191.3 ± 7.5	154.0 ± 7.0	170.3 ± 5.6	167.5 ± 4.8
ABUT[4] (μmol/L)	Total	8.5 ± 0.4	9.1 ± 0.5	9.4 ± 0.5	9.0 ± 0.3
	Shmt1$^{+/-}$	7.8 ± 0.8	9.0 ± 0.7	9.6 ± 0.3	9.2 ± 0.4
	Shmt1$^{-/-}$	8.8 ± 0.4	9.6 ± 0.5	9.0 ± 1.2	8.7 ± 0.5
MET[4] (μmol/L)	Total	56.6 ± 3.7	53.0 ± 3.5	61.2 ± 3.8	61.6 ± 5.9
	Shmt1$^{+/-}$	60.9 ± 9.2	50.6 ± 3.7	59.3 ± 4.5	64.3 ± 8.8
	Shmt1$^{-/-}$	54.8 ± 4.0	62.3 ± 7.6	64.0 ± 7.1	57.7 ± 7.5
GLY[3,4] (μmol/L)	Total	102.1 ± 11.3	107.1 ± 12.7	89.6 ± 8.8	97.7 ± 9.1
	Shmt1$^{+/-}$	100.0 ± 9.6	105.0 ± 13.6	84.3 ± 10.8	101.0 ± 15.1
	Shmt1$^{-/-}$	103.0 ± 16.1	115.6 ± 44.5	97.5 ± 16.2	92.8 ± 5.4
SER[4] (μmol/L)	Total	168.7 ± 16.6	182.6 ± 13.0	177.0 ± 14.0	207.9 ± 15.1
	Shmt1$^{+/-}$	144.0 ± 8.7	176.6 ± 15.7	166.8 ± 11.7	213.7 ± 20.1
	Shmt1$^{-/-}$	179.3 ± 22.7	206.5 ± 0.5	192.3 ± 31.4	199.3 ± 25.8
[SER]/[GLY][4,8]	Total	1.70 ± 0.11	1.85 ± 0.19	2.14 ± 0.23	2.28 ± 0.25
	Shmt1$^{+/-}$	1.46 ± 0.10	1.79 ± 0.19	2.14 ± 0.28	2.34 ± 0.37
	Shmt1$^{-/-}$	1.80 ± 0.14	2.10 ± 0.81	2.14 ± 0.46	2.19 ± 0.35
FORMATE[9,10] (μmol/L)	Total	203.5 ± 22.1	196.6 ± 11.6	140.9 ± 12.7	162.4 ± 16.1
	Shmt1$^{+/-}$	191.3 ± 36.9	196.2 ± 13.7	122.2 ± 8.9	123.4 ± 20.3
	Shmt1$^{-/-}$	221.9 ± 7.9	198.5 ± 27.9	184.4 ± 22.9	193.5 ± 12.1

Abbreviations: HCYS, homocysteine; CYSTAT, cystathionine; CYS, cysteine; ABUT, α-aminobutyric acid; MET, methionine; GLY, glycine; SER, serine; [SER/GLY], serine/glycine; CD, control diet; FDD, folate-deficient diet; B_{12}FDD, vitamin B_{12}- and folate-deficient diet; B_{12}DD, vitamin B_{12}-deficient diet; E, embryonic day.

[1] All values are shown as means ± S.E. n=10 samples per diet group were analyzed for plasma metabolites. For plasma formate, the number of dams within each diet is as follows: CD (n=4 *Shmt1*$^{-/-}$, n=6 *Shmt1*$^{-/+}$), FDD (n=2 *Shmt1*$^{-/-}$, n=8 *Shmt1*$^{-/+}$), B_{12}DD (n=3 *Shmt1*$^{-/-}$, n=7 *Shmt1*$^{-/+}$), B_{12}FDD (n=5 *Shmt1*$^{-/-}$, n=4 *Shmt1*$^{-/+}$). For all other metabolites: CD (n=7 *Shmt1*$^{-/-}$, n= 3 *Shmt1*$^{-/+}$), FDD (n=2 *Shmt1*$^{-/-}$, n=8 *Shmt1*$^{-/+}$), B_{12}DD (n=4 *Shmt1*$^{-/-}$, n=6 *Shmt1*$^{-/+}$), B_{12}FDD (n=4 *Shmt1*$^{-/-}$, n=6 *Shmt1*$^{-/+}$). Independent effects of maternal *Shmt1* genotype, diet, and the interaction between genotype and diet were assessed using a two-way ANOVA and a Tukey's HSD test for post-hoc analysis.

[2] Metabolite values were log-transformed to improve the normal distribution assumption of the model. Values displayed are the non-transformed means ± S.E.

[3] Metabolite values were rank-tranformed to improve the normal distribution assumption of the model. Values are displayed as the non-transformed means ± S.E.

[4] There was no significant effect of *Shmt1* genotype, diet, or genotype x diet

interaction detected.
[5] The FDD and B_{12}FDD were significantly different from the CD and B_{12}DD ($p<0.0001$).
[6] The B_{12}FDD and FDD were significantly different from the CD ($p = 0.0014$).
[7] The FDD differed significantly from the CD and B_{12}DD ($p = 0.013$).
[8] No significant effect of maternal diet on log[serine/glycine] was detected. A linear contrast made between vitamin B_{12}-deficient (B_{12}FDD + B_{12}DD) and replete (FDD + CD) diets revealed significant differences in log[serine/glycine] ($p = 0.04$).
[9] *Shmt1*$^{-/-}$ was significantly different from *Shmt1*$^{-/+}$ ($p = 0.009$)
[10] The B_{12}DD was significantly different from the FDD and CD ($p = 0.01$).

Discussion

There exists a need to identify additional risk factors for NTDs, as folic acid has not reduced the birth prevalence of NTDs below an incidence of 0.6/1,000 live births in the post-fortification era, equating to an estimated 2,600 NTD-affected pregnancies in the U.S annually (9). Maternal vitamin B_{12} deficiency has emerged as a highly attractive candidate risk factor given its participation in folate metabolism as well as the findings from cross-sectional studies that demonstrate association between maternal deficiency and NTD risk (14–23). In spite of this knowledge, no prospective studies have assessed the role of maternal vitamin B_{12} deficiency in conferring NTD risk. Additional concerns raised in the period following mandatory folic acid fortification suggest that high folate status and vitamin B_{12} deficiency may be detrimental for some clinical outcomes (40, 41). No mechanistic understanding exists to explain this concern, nor has the vitamin B_{12}-folate interrelationship been systematically examined.

In this study, we demonstrate that maternal vitamin B_{12} deficiency is an independent risk factor for NTDs in embryos with reduced *Shmt1* expression (Table 2.2, Fig. 2.2). Interestingly, maternal vitamin B_{12} deficiency did not affect CR length (Table 2.2) or levels of plasma transsulfuration pathway metabolites (Table 2.4), but

did significantly predict rates of NTDs (Table 2.2), suggesting that the developing neuroepithelium is the most sensitive to vitamin B_{12} deficiency. The fact that plasma homocysteine was not predicted by maternal vitamin B_{12} deficiency suggests a marked, but not severe, deficiency of vitamin B_{12} (Table 2.4). Only two case-control studies demonstrating a significant association between maternal vitamin B_{12} deficiency and NTD risk, independently of folate status, include plasma homocysteine measurements (15, 16). One study showed that maternal vitamin B12 deficiency did not significantly modulate plasma homocysteine levels (16) whereas the second one did (15).

The incidence of NTDs between the two vitamin B_{12}-deficient diets was not different ($p>0.05$; Table 2.2), indicating that dietary folate repletion does not exacerbate symptoms of disease pathogenesis in vitamin B_{12} deficiency, and therefore addresses post-folic-acid-fortification concerns regarding effects of elevated folate intakes and low vitamin B_{12} status. Additional clinical implications emerge from these findings, as folic acid supplementation did not affect incidence of NTDs in vitamin B_{12} deficiency (Table 2.2). Folic acid has been proposed to compensate for vitamin B_{12} deficiency, as elevated intakes of folic acid can mask symptoms of vitamin B_{12} deficiency by overcoming impairments in *de novo* dTMP biosynthesis in vitamin B_{12}-deficient hematopoietic cells, as is observed in megaloblastic anemia, but not in the central nervous system (CNS) (38, 47). Our findings that supplemental folic acid did not rescue NTDs in vitamin B_{12} deficiency suggests that folic acid intake cannot compensate for vitamin B_{12} deficiency in the neuroepithelium, similar to what is observed in vitamin B_{12}-associated neuropathies (38).

This study demonstrates that maternal vitamin B_{12} deficiency sensitizes embryos with reductions in *Shmt1* expression to NTDs that could not be rescued by

folic acid. Therefore, these findings illustrate the need to investigate the mechanism by which vitamin B_{12} and folate interact in nuclear *de novo* dTMP biosynthesis, given that specific cell types, including hematopoietic cells and CNS tissue, differentially respond to vitamin B_{12}-deficiency. This need is further supported by the conflicting observations suggesting that supplemental folic acid can either correct or exacerbate metabolic impairments in vitamin B_{12} deficiency. The vitamin B_{12}-dependent homocysteine remethylation and *de novo* dTMP biosynthesis are compartmentalized in the cytosol and nucleus, respectively, and it is not known how the former impacts nuclear one-carbon metabolism for dTMP synthesis. The finding that maternal vitamin B_{12} deficiency caused NTDs but did not influence plasma homocysteine levels suggests that the nuclear compartment may exhibit increased sensitivity to the 5-methylTHF trap. Lastly, these findings emphasize the need to consider fortification as an opportunity to reduce those vitamin B_{12}-responsive NTDs that cannot be rescued with supplemental folic acid (52). Future large-scale, population-based studies designed to investigate the effect of periconceptional vitamin B_{12} supplementation may result in the development of efficacious interventions to further reduce NTD incidence.

Contributions: AMP collected primary data. SPS & RHA provided metabolite measurements for plasma homocysteine panel (Table 2.4); MEB & JTB provided metabolite measurements for plasma formate (Table 2.4). AMP performed statistical analyses; JLF performed analyses for resorptions.(Table 2.2).

Supplemental Information

Formulation of one-carbon and vitamin B_{12} weekly supplements: *Formulation of one-carbon & vitamin* B_{12} *fortified mini-marshmallows:* Commercially made mini-

marshmallows (Kraft™) were fortified with the following pure compounds obtained from Sigma-Aldrich: vitamin B_{12} (cyanocobalamin), folic acid, or 2% ascorbate depending on the dietary scheme. Mini-marshmallows were selected as a vehicle for delivering the weekly dietary supplements, as they do not contain B-vitamins that would interfere with biomarker readouts according to the most recent Food Composition Tables from the U.S. Department of Agriculture. Furthermore, we used the *L. casei* assay to establish that marshmallows are folate-free (data not shown). The concentration of individual compounds were determined and diluted 1:1 in a 4% ascorbate solution. The final solution in 2% ascorbate was filtered under sterile conditions and injected into marshmallows to deliver 0.7 micrograms of cyanocobalamin and 56 micrograms of folic acid in 5 microliters of 2% ascorbate solution prior to storage at -80°C. These weekly supplements of dietary cyanocobalamin, folic acid, and 2% ascorbate added to the marshmallows were determined based on the composition of these vitamin and one-carbon sources in the AIN93G diet as well as unpublished data from our laboratory that have determined the amount of food (grams)/week an individual mouse consumes. Following preparation, the fortified marshmallows were treated with 5-20 kilograys (kGy) of gamma irradiation, the same range and value of gamma irradiation used to treat our commercially prepared diets at an offsite facility to be in agreement with Cornell IACUC protocols. This route of administration was preferred over gavage or intraperitoneal (IP) injection of aforementioned compounds as it minimizes stress to the animal and represents a more realistic dietary scenario. We determined, using established methods in our laboratory, that gamma ray treatment does not degrade the injected compounds. Dams in the control diet (CD) group received a weekly supplement containing both cyanocobalamin and folic acid. Dams in the combined

vitamin B_{12} and folate deficient diet (B_{12}FDD) group received a weekly supplement containing 2% ascorbate. Dams in the folate-deficient diet (FDD) or vitamin B_{12} deficient diet (B_{12}DD) groups received supplements containing cyanocobalamin or folic acid, respectively.

References

1. Christianson A, Howson C, Modell B (2006) *March of Dimes global report on birth defects: the hidden toll of dying and disabled children*.

2. Beaudin AE, Stover PJ (2009) Insights into metabolic mechanisms underlying folate-responsive neural tube defects: a minireview. *Birth Defects Res A Clin Mol Teratol* 85(4):274–84.

3. Crider KS, et al. (2011) MTHFR 677C>T genotype is associated with folate and homocysteine concentrations in a large, population-based, double-blind trial of folic. *Am J Clin Nutr* 93(6):1365–1372.

4. Tsang BL, et al. (2015) Assessing the association between the methylenetetrahydrofolate reductase (MTHFR) 677C>T polymorphism and blood folate concentrations: a systematic review and meta-analysis of trials and observational studies. *Am J Clin Nutr* 101(6):1286–1294.

5. Blom HJ, Shaw GM, den Heijer M, Finnell RH (2006) Neural tube defects and folate: case far from closed. *Nat Rev Neurosci* 7(9):724–731.

6. Czeizel A, Dudas I (1992) Prevention of the first occurrence of neural tube defects by periconceptional vitamin supplementation. *N Engl J Med* 327(26):1832–5.

7. Group MVSR (1991) Prevention of neural tube defects: Results of the Medical Research Council Vitamin Study. *Lancet* 338(8760):131–137.

8. Centers for Disease Control and Prevention (2004) Spina bifida and anencephaly before and after folic acid mandate — United States, 1995-1996 and 1999-2000. *Morbiidty Mortal Wkly Rep* 53(17):362–365.

9. Williams J, et al. (2015) Updates estimates of neural tube defects prevented by mandatory folic acid fortification - United States, 1995-2011. *MMWR Morb Mortal Wkly Rep* 64(1):1–5.

10. Gelineau-van Waes J, Voss KA, Stevens VL, Speer MC, Riley RT (2009) *Chapter 5 Maternal Fumonisin Exposure as a Risk Factor for Neural Tube Defects* (Elsevier Inc.). 1st Ed.

11. Ray JG, Blom HJ (2003) Vitamin B12 insufficiency and the risk of fetal neural tube defects. *Q J Med* 96(4):289–295.

12. Tanoshima M, et al. (2015) Risks of congenital malformations in offspring exposed to valproic acid in utero: A systematic review and cumulative meta-analysis. *Clin Pharmacol Ther* 98(4):417–441.

13. Mazumdar M, et al. (2015) Polymorphisms in maternal folate pathway genes interact with arsenic in drinking water to influence risk of myelomeningocele. *Birth Defects Res Part A - Clin Mol Teratol* 103(9):754–762.

14. Felkner M, Suarez L, Canfield MA, Brender JD, Sun Q (2009) Maternal serum homocysteine and risk for neural tube defects in a Texas-Mexico border population. *Birth Defects Res Part A - Clin Mol Teratol* 85(6):574–581.

15. Gaber K, Farag M, Soliman S, El-Bassyouni H, El-Kamah G (2007) Maternal vitamin B12 and the risk of fetal neural tube defects in Egyptian patients. *Clin Lab* 53(1–2):69–75.

16. Groenen PMW, et al. (2004) Marginal maternal vitamin B12 status increases the risk of offspring with spina bifida. *Am J Obstet Gynecol* 191(1):11–17.

17. Gu Q, Li Y, Cui Z, Luo X (2012) Homocysteine, folate, vitamin B12 and B6 in mothers of children with neural tube defects in Xinjiang, China. *Acta Paediatr* 101(11):e486–e490.

18. Kirke PN, Daly LE, Burke H, Weir DC (1993) Maternal plasma folate and vitamin B12 are independent risk factors for neural tube defects. *Q J Med* 86:703–708.

19. Molloy AM, et al. (2009) Maternal vitamin B12 status and risk of neural tube defects in a population with high neural tube defect prevalence and no folic acid fortification. *Pediatrics* 123(3):917–23.

20. Ray JG, et al. (2007) Vitamin B12 and the risk of neural tube defects in a folic-acid-fortified population. *Epidemiology* 18(3):362–366.

21. Wilson A, et al. (1999) A common variant in methionine synthase reductase combined with low cobalamin (vitamin B12) increases risk for spina bifida. *Mol Genet Metab* 67(4):317–323.

22. Suarez L, Hendricks K, Felkner M, Gunter E (2009) Maternal serum B12 levels and risk for neural tube defects in a Texas-Mexico border population. *Birth Defects Res Part A - Clin Mol Teratol* 85(6):574–581.

23. Zhang T, et al. (2008) Maternal serum vitamin B12, folate and homocysteine and the risk of neural tube defects in the offspring in a high-risk area of China. *Public Health Nutr* 12(5):680–686.

24. Thompson MD, Cole DEC, Ray JG (2009) Vitamin B-12 and neural tube defects: the Canadian experience. *Am J Clin Nutr* 89(2):697S–701S.

25. Stover PJ, Field MS (2011) Trafficking of intracellular folates. *Adv Nutr* 2(4):325–331.

26. Beaudin AE, et al. (2011) Shmt1 and de novo thymidylate biosynthesis underlie folate-responsive neural tube defects in mice. *Am J Clin Nutr* 93(4):789–98.

27. Dunlevy LPE, et al. (2007) Abnormal folate metabolism in foetuses affected by neural tube defects. *Brain* 130:1043–1049.

28. Martiniova L, Field MS, Finkelstein JL, Perry CA, Stover PJ (2015) Maternal dietary uridine causes, and deoxyuridine prevents, neural tube closure defects in a mouse model of folate-responsive neural tube defects. *Am J Clin Nutr* 101(4):860–9.

29. Anderson DD, Woeller CF, Chiang EP, Shane B, Stover PJ (2012) Serine hydroxymethyltransferase anchors de novo thymidylate synthesis pathway to nuclear lamina for DNA synthesis. *J Biol Chem* 287(10):7051–7062.

30. Field MS, et al. (2014) Nuclear enrichment of folate cofactors and methylenetetrahydrofolate dehydrogenase 1 (MTHFD1) protect de novo thymidylate biosynthesis during folate deficiency. *J Biol Chem* 289(43):29642–29650.

31. MacFarlane AJ, et al. (2008) Cytoplasmic serine hydroxymethyltransferase regulates the metabolic partitioning of methylenetetrahydrofolate but is not essential in mice. *J Biol Chem* 283(38):25846–25853.

32. Beaudin AE, et al. (2012) Dietary folate, but not choline, modifies neural tube defect risk in Shmt1 knockout mice. *Am J Clin Nutr* 95(1):109–114.

33. Watanabe M, et al. (1995) Mice deficient in cystathionine beta-synthase: animal models for mild and severe homocyst(e)inemia. *Proc Natl Acad Sci U S A* 92(5):1585–9.

34. Chen Z, et al. (2001) Mice deficient in methylenetetrahydrofolate reductase exhibit hyperhomocysteinemia and decreased methylation capacity, with neuropathology and aortic lipid deposition. *Hum Mol Genet* 10(5):433–443.

35. Li D, Pickell L, Liu Y, Rozen R (2006) Impact of methylenetetrahydrofolate reductase deficiency and low dietary folate on the development of neural tube defects in Splotch mice. *Birth Defects Res Part A - Clin Mol Teratol* 76(1):55–59.

36. Elmore CL, et al. (2007) Metabolic derangement of methionine and folate metabolism in mice deficient in methionine synthase reductase. *Mol Genet Metab* 91(1):85–97.

37. Metz J, Kelly A, Swett V, Waxman S, Herbert V (1968) Deranged DNA synthesis by bone marrow from vitamin B12-deficient humans. *Br J Haematol* 14(6):575–592.

38. Stabler SP (2013) Vitamin B12 Deficiency. *N Engl J Med* 368(2):149–160.

39. Shane B, Stokstad ELR (1985) Vitamin B12-Folate Interrelationships. *Annu Rev Nutr* 5(1):115–141.

40. Selhub J, Morris MS, Jacques PF, Rosenberg IH (2009) Folate-vitamin B12 interaction in relation to cognitive impairment, anemia, and biochemical indicators of vitamin B12 deficiency. *Am J Clin Nutr* 89:702–707.

41. Morris MS, Jacques PF, Rosenberg IH, Selhub J (2007) Folate and vitamin B-12 status in relation to anemia, macrocytosis, and cognitive impairment in older Americans in the age of folic acid fortification. *Am J Clin Nutr* 85(1):193–200.

42. Molloy AM, Scott JM (1997) Microbiological assay for serum, plasma, and red cell folate using cryopreserved, microtiter plate method. *Methods Enzymol* 281:43–53.

43. Kelleher BP, Broin SD (1991) Microbiological assay for vitamin B12 performed in 96-well microtitre plates. *J Clin Pathol* 44(7):592–595.

44. Lamarre SG, et al. (2012) Formate can differentiate between hyperhomocysteinemia due to impaired remethylation and impaired transsulfuration. *Am J Physiol Endocrinol Metab* 302(1):E61-7.

45. Allen RH, Stabler SP, Lindenbaum J (1993) Serum betaine, N,N-dimethylglycine, and N-methylglycine levels in patients with cobalamin and folate deficiency and related inborn errors of metabolism. 42(11):1448–1460.

46. Stabler SP, Lindenbaum J, Savage DG, Allen RH (1993) Elevation of serum cystathionine levels in patients with cobalamin and folate deficiency. *Blood* 81(12):3404–13.

47. Marshall R, Jandl J (1960) Responses to “physiologic” doses of folic acid in megaloblastic anemias. *Arch Intern Med* 105(3):352–360.

48. Herbert V, Zalusky R (1962) Interrelations of vitamin B12 and folic acid metabolism: folic acid clearance studies. *J Clin Invest* 41(6):1263–76.

49. Stover P, Schirch V (1991) 5-formyltetrahydrofolate polyglutamates are slow tight binding inhibitors of serine hydroxymethyltransferase. *J Biol Chem* 266(3):1543–1550.

50. Morrow GP, et al. (2015) In vivo kinetics of formate metabolism in folate-deficient and folate-replete rats. *J Biol Chem* 290(4):2244–50.

51. Lamarre SG, et al. (2012) Formate can differentiate between hyperhomocysteinemia due to impaired remethylation and impaired transsulfuration. *Am J Physiol Endocrinol Metab* 302(1):E61-7.

52. Green R (2009) Is it time for vitamin B-12 fortification? What are the questions? *Am J Clin Nutr* 89(2):712S–716S.

CHAPTER 3: FOLATE AND VITAMIN B_{12} INTERACT IN NUCLEAR FOLATE METABOLISM LEADING TO GENOME INSTABILITY

Authors: Ashley M. Palmer[a], Elena Kamynina[a], Martha S. Field[a], and Patrick J. Stover[a,b]

Affiliations: [a]Division of Nutritional Sciences and [b]Graduate Field of Biochemistry, Molecular, and Cell Biology, Cornell University, Ithaca, NY 14853

Abstract:

Clinical vitamin B_{12} deficiency can result in megaloblastic anemia, which results from the inhibition of DNA synthesis by trapping folate cofactors in the form of 5-methyltetrahydrofolate (5-methylTHF) and subsequent inhibition of *de novo* thymidylate (dTMP) biosynthesis. In the cytosol, vitamin B_{12} functions in the remethylation of homocysteine to methionine, which regenerates tetrahydrofolate (THF) from 5-methylTHF. In the nucleus, THF is required for *de novo* dTMP biosynthesis, but it is not understood how 5-methylTHF accumulation in the cytosol impairs nuclear dTMP biosynthesis. The impact of vitamin B_{12} depletion on nuclear *de novo* dTMP biosynthesis was investigated in methionine synthase (MTR)-null human fibroblast and nitrous oxide-treated HeLa cell models. The nucleus was the most sensitive cellular compartment to 5-methylTHF accumulation, with levels increasing greater than 4-fold. Vitamin B_{12} depletion decreased *de novo* dTMP biosynthesis capacity by 5-35%, whereas *de novo* purine synthesis, which occurs in the cytosol, was not affected. Phosphorylated histone H2AX (γH2AX), a marker of DNA double-strand breaks (DSBs), was increased in vitamin B_{12} depletion, and this effect was exacerbated by folate depletion. These studies also revealed that 5-formylTHF, a slow, tight-binding inhibitor of SHMT, was enriched in nuclei, accounting for 35% of

folate cofactors, explaining previous observations that nuclear SHMT is not a robust source of one-carbons for *de novo* dTMP biosynthesis. These findings indicate that a nuclear 5-methylTHF trap occurs in vitamin B_{12} depletion, which suppresses *de novo* dTMP biosynthesis and causes DNA damage, accounting for the pathophysiology of megaloblastic anemia observed in vitamin B_{12} and folate deficiency.

Keywords: folate | vitamin B_{12} | 5-methyltetrahydrofolate trap | thymidylate | γH2AX |

Significance Statement: Vitamin B_{12} deficiency causes hematological and neurological pathologies by impairing DNA synthesis. The nucleus is shown to be highly sensitive to 5-methyltetrahydrofolate accumulation induced by vitamin B_{12} depletion in the cytosol, leading to impaired nuclear *de novo* thymidylate synthesis and genome instability. These effects of the 5-methyltetrahydrofolate trap are exacerbated by folate depletion in nitrous oxide-treated HeLa cells and methionine synthase (MTR) loss-of-function fibroblasts. These results provide a mechanism underlying vitamin B_{12}-folate interrelationships that underlie megaloblastic anemia and neural tube defects (NTDs).

Introduction

Vitamin B_{12} (cobalamin) deficiency disproportionately affects older adults and pregnant women (1). It can arise from inadequate dietary intake or impaired absorption, with the latter accounting for the majority of cases (2, 3). Vitamin B_{12} is essential for maintaining nervous system function as well as hematopoiesis, as the classic sequelae of deficiency include irreversible neurological damage and/or reversible hematological changes (2, 4). The clinical manifestations of vitamin B_{12} deficiency have been known for decades, and it is known that high levels of folate intake can mask megaloblastic anemia (5), indicating that increased intracellular

folate levels can rescue some metabolic consequences of vitamin B_{12} deficiency. Conversely, data from cross-sectional studies suggest that low vitamin B_{12} and elevated folate status exacerbate symptoms of cognition and anemia (6, 7) as well as biochemical indicators of vitamin B_{12} deficiency (7); however, there is no mechanistic understanding in support these observations.

There are two enzymes that require vitamin B_{12} as a cofactor in mammals: methionine synthase (MTR), which functions in the cytosol, and L-methylmalonyl-coenzyme A (coA) mutase (MUT), which functions in the mitochondria (4). MTR is both vitamin B_{12}- and folate-dependent, and catalyzes the conversion of homocysteine to methionine in a two-step process. In the first step, the methyl group from 5-methylTHF is transferred to cobalamin, thereby creating methylcobalamin and releasing THF. In the second step, the methyl group from methylcobalamin is transferred to homocysteine for methionine synthesis (4). Consequences of reduced MTR activity include elevated homocysteine in tissue and plasma, a biomarker associated with adverse health outcomes including risk for neural tube defects (NTDs) (8), and impaired methylation status, as methionine is required for the synthesis of *S*-adenosylmethionine (AdoMet), the universal methyl donor required for over 100 cellular methylation reactions (9). Reduced MTR activity also leads to the trapping of cellular folate as 5-methyltetrahydrofolate (5-methylTHF), as the methylenetetrahydrofolate reductase (MTHFR)-catalyzed conversion of 5,10-methyleneTHF to 5-methylTHF is irreversible *in vivo* (Fig. 3.1) (10). The "5-methylTHF trap" is associated with the onset of megaloblastic anemia, which is characterized by an enlarged reticulocyte cytosol, immature nuclei, and incomplete DNA replication and cell division due to inadequate dTMP biosynthesis (Fig. 3.1) (2, 5, 11).

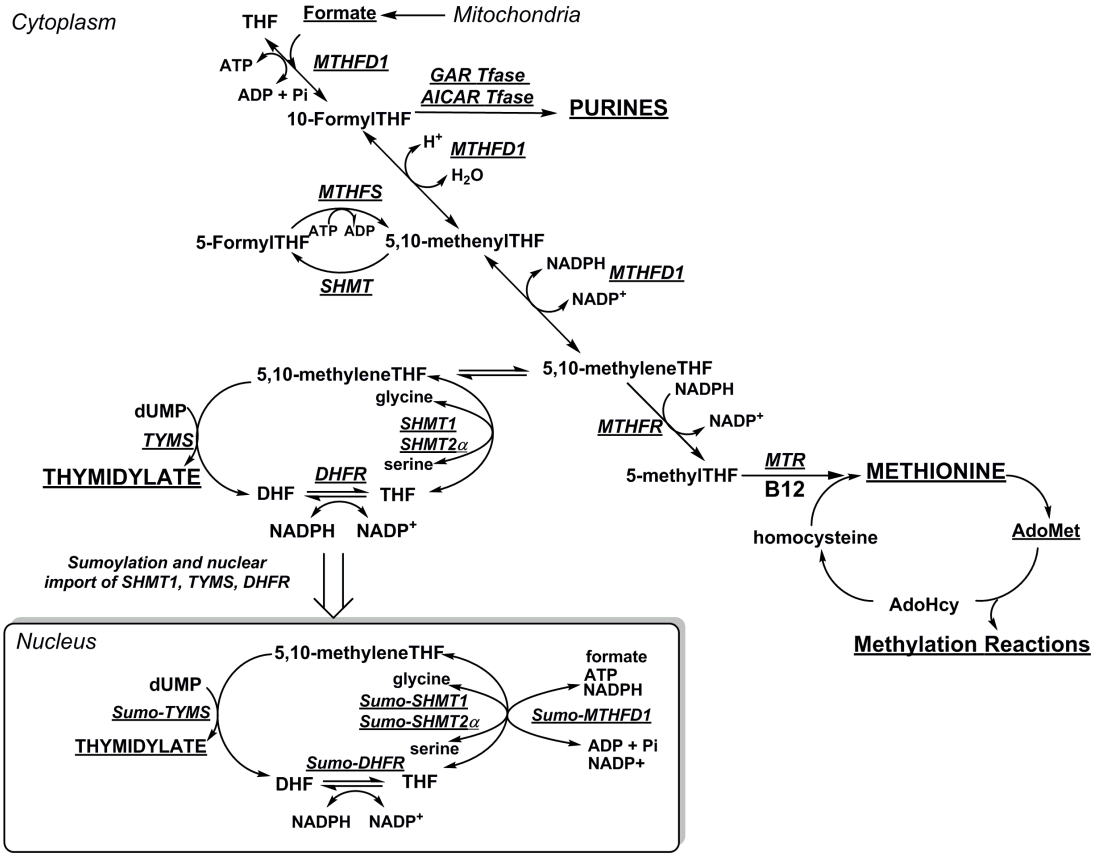

Figure 3.1. Folate- and vitamin B_{12}-mediated one-carbon (1C) metabolism is compartmentalized within the cell. The hydroxymethyl group of serine is a primary source of 1C units, and can enter the pool of activated 1C units by SHMT-catalyzed cleavage of serine. Otherwise, serine and glycine are converted to formate in mitochondria, which traverses to the cytosol and nucleus where it is condensed with THF by MTHFD1. 1C metabolism in the cytosol includes the *de novo* synthesis of purines and the remethylation of homocysteine to methionine. Vitamin B_{12} is a required cofactor for MTR. *De novo* dTMP biosynthesis occurs in the nucleus, catalyzed by the enzymes SHMT1, SHMT2α, TYMS, and DHFR, which undergo SUMOylation leading to nuclear import in S-phase. 5,10-methyleneTHF is synthesized by SHMT or MTHFD1 for *de novo* dTMP synthesis. AdoHcy, *S*-adenosylhomocysteine; AdoMet, *S*-adenosylmethionine; AICAR Tfase, aminoimidazolecarboxamide ribonucleotide transformylase; DHF, dihydrofolate; DHFR, dihydrofolate reductase; GAR Tfase, glycinamide ribonucleotide tranformylase; MTHFS, methenyltetrahydrofolate synthetase; MTHFR, methylenetetrahydrofolate reductase; MTR, methionine synthase; SHMT, serine hydroxymethyltransferase; SUMO, small ubiquitin-like modifier; THF, tetrahydrofolate; TYMS, thymidylate synthase. Figure adapted from Field et al. 2015 (47).

The proposed mechanisms underlying vitamin B_{12} deficiency-induced megaloblastic anemia are based on an assumption that both the homocysteine remethylation and *de novo* dTMP biosynthesis pathways function in the cytosol (12, 13). However, there is increasing evidence that *de novo* dTMP biosynthesis occurs in the nucleus at sites of DNA synthesis (14). The enzymes that participate in *de novo* dTMP biosynthesis, serine hydroxymethyltransferase 1 and 2α (SHMT1, SHMT2α), dihydrofolate reductase (DHFR), methylenetetrahydrofolate dehydrogenase 1 (MTHFD1), and thymidylate synthase (TYMS) undergo modification by the small ubiquitin-like modifier (SUMO) protein, and translocate to the nucleus where they form a complex at sites of DNA replication and repair (Fig. 3.1) during S-phase or in response to DNA damage (14–17). SHMT serves as an essential scaffold protein that connects this multienzyme complex to the nuclear lamina (14), but does not serve as a primary source of one-carbon units, as most one-carbons incorporated into dTMP are derived from formate via MTHFD1 (18). TYMS methylates deoxyuridylate (dUMP) using 5,10-methyleneTHF as the cofactor to produce dTMP and dihydrofolate (DHF). DHF is reduced to THF by DHFR, which is NADPH-dependent (Fig. 3.1). Insufficient concentrations of intracellular folate or impairments in nuclear localization of the *de novo* dTMP biosynthesis complex can lead to elevated uracil levels in DNA (19, 20). Low intracellular vitamin B_{12} concentrations and/or status can increase markers of genome instability including chromosomal abnormalities (21, 22), DNA strand breaks (23), and uracil content in DNA (24, 25). The mechanisms underlying the interactions between folate and vitamin B_{12} in maintaining genome stability and their contributions to human disease are unresolved. There is evidence that the cytosolic and nuclear folate cofactor pools are distinct. Unlike the cytosol, the nucleus is resistant to folate depletion when total cellular folates are depleted (26). Therefore, it is not clear if an

accumulation of 5-methylTHF in the cytosol during vitamin B_{12} depletion influences folate cofactor pools in the nucleus.

We investigated the impact of vitamin B_{12} depletion on nuclear dTMP synthesis in two models of vitamin B_{12} deficiency: human fibroblasts with loss-of-function mutations in *MTR* that comprise the inborn errors of cobalamin metabolism complementation group G (cblG) (27), and HeLa cells treated with nitrous oxide. The nucleus was observed to be highly sensitive to 5-methylTHF accumulation in vitamin B_{12} depletion, which led to depressed rates of *de novo* dTMP biosynthesis and increased genome instability. We also demonstrate that the nucleus is enriched in 5-formylTHF cofactors, which are slow, tight-binding inhibitors of SHMT (28). This observation accounts for the lack of nuclear SHMT catalytic activity in *de novo* dTMP biosynthesis. These findings link vitamin B_{12} depletion to nuclear 5-methylTHF accumulation, impaired DNA synthesis, and genome instability, and provide a mechanism underpinning vitamin B_{12}-associated pathologies.

Results

5-methylTHF is enriched in nuclei of vitamin B_{12}-depleted HeLa cells and in cblG patient fibroblasts. Intracellular 5-methylTHF was 2.5-fold higher in cblG (WG4215) compared to control (MCH058) fibroblasts (p=0.01), with the elevation in 5-methylTHF occurring at the expense of 10-formylTHF (p=0.009) and 5-formylTHF (p=0.03) (Fig. 3.2*A*). THF was not detected in either MTR-null or control fibroblasts. HeLa cells cultured in vitamin B_{12}-depleted conditions exhibited a 1.75-fold increase in intracellular 5-methylTHF (p=0.0002), and a 50% decrease in THF (p=0.001) compared to HeLa cells maintained in vitamin B_{12}-replete media (Fig. 3.2*B*). Nuclei isolated from vitamin B_{12}-depleted HeLa cells exhibited a more than 4-fold enrichment

of 5-methylTHF (p=0.002), whereas THF levels decreased by greater than 50% (p=0.02) (Fig. 3.2*C*) compared to vitamin B_{12}-replete HeLa cells. Nuclear 10-formylTHF pools were 7.5-fold lower in nuclei isolated from HeLa cells maintained in vitamin B_{12}-depleted conditions compared to vitamin B_{12}-replete cells (p=0.02). Interestingly, 5-formylTHF was enriched in nuclei compared to total cellular 5-formylTHF levels in HeLa cells (p=0.002) (Fig. 3.2*B,C*).

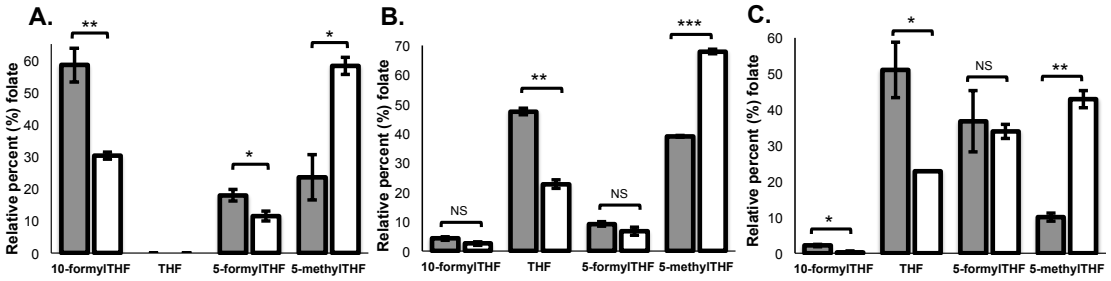

Figure 3.2. Vitamin B_{12} depletion or MTR disruption results in elevated 5-methylTHF in cells (A,B) and nuclei (C). *(A) Distribution of folate one-carbon forms in human fibroblasts*. The percentages of folate forms are shown for one cell line of each cblG (WG4215, white bars) and control (MCH058, gray bars). *(B,C) Nitrous oxide-induced changes in folate one-carbon distribution in HeLa cells (B) and nuclei (C).* The percentages of folate forms present in HeLa cells and nuclei maintained in vitamin B_{12}-depleted (white bars) or replete (gray bars) conditions are shown. All measurements were made in duplicate. Data are shown as mean ± standard deviation (S.D.). Differences in folate forms between replete and depleted conditions were determined by a Student's 2-tailed t-test. For (C), a Western blot confirmed that nuclei were free of cytoplasmic contamination (Fig. S3.5). In A-C, statistical significance is denoted as follows: NS = Not significant ($p > 0.05$); * = $0.01 < p < 0.05$; ** = $0.01 < p < 0.001$; *** = $p < 0.001$.

Folate and vitamin B_{12} depletion interact to increase DNA damage in HeLa cells.

Both folate depletion and vitamin B_{12} depletion independently increased γH2AX immunostaining (Fig. 3.3, 2*B-E* and 3*B-E*). Intracellular folate concentrations were 8-fold lower in cells cultured in folate-depleted media (5 nM) compared to cells cultured in folate-replete (25 nM) media at the time of γH2AX staining and quantification ($p<0.0001$) (Fig. S3.6). Vitamin B_{12} depletion significantly increased the percentage of

cells with high γH2AX immunostaining, a marker of DNA DSBs, in all phases of the cell cycle compared to vitamin B_{12}- and folate-replete conditions (Fig. 3.3, 1*B*-*E* vs. 3*B*-*E*). This effect was exacerbated by folate deficiency (Fig. 3.3, 1*B*-*E* vs. 4*B*-*E*). Importantly, the difference in the percentage of cells with high γH2AX immunostaining between vitamin B_{12}-depleted conditions was statistically significant (Fig. 3.3, 3*B*-*E* vs. 4*B*-*E*) (Table S3.1, 5*B*-*E*). Within treatment conditions, the greatest increase in the percentage of cells with high γH2AX immunostaining was observed during G2/M (Fig. 3.3, 1-4*E*).

Folate depletion, but not MTR loss-of-function, increases DNA damage in human fibroblasts. In fibroblasts, folate depletion significantly increased γH2AX immunostaining, as quantified by the percentage of nuclear area with γH2AX ($p<0.0001$) (Fig. 3.4*A*). MTR loss-of-function did not significantly affect γH2AX levels when comparing cblG (WG4215 & WG4460) and control fibroblast lines (MCH058 & MCH064) cultured under either folate-replete or depleted culture conditions ($p>0.05$) (Fig. 3.4*A*).

Vitamin B_{12} and folate depletion impair *de novo* dTMP biosynthesis. In HeLa cells, vitamin B_{12} depletion impaired *de novo* dTMP synthesis by 5% compared to vitamin B_{12}-replete cells ($p=0.02$) (Fig. 3.4*B*). A combined folate and vitamin B_{12} depletion decreased *de novo* dTMP capacity by 35% ($p<0.0001$). In cblG fibroblasts, MTR loss-of-function decreased the relative rate of *de novo* dTMP synthesis by approximately 25% ($p<0.0001$) (Fig. 3.4*C*).

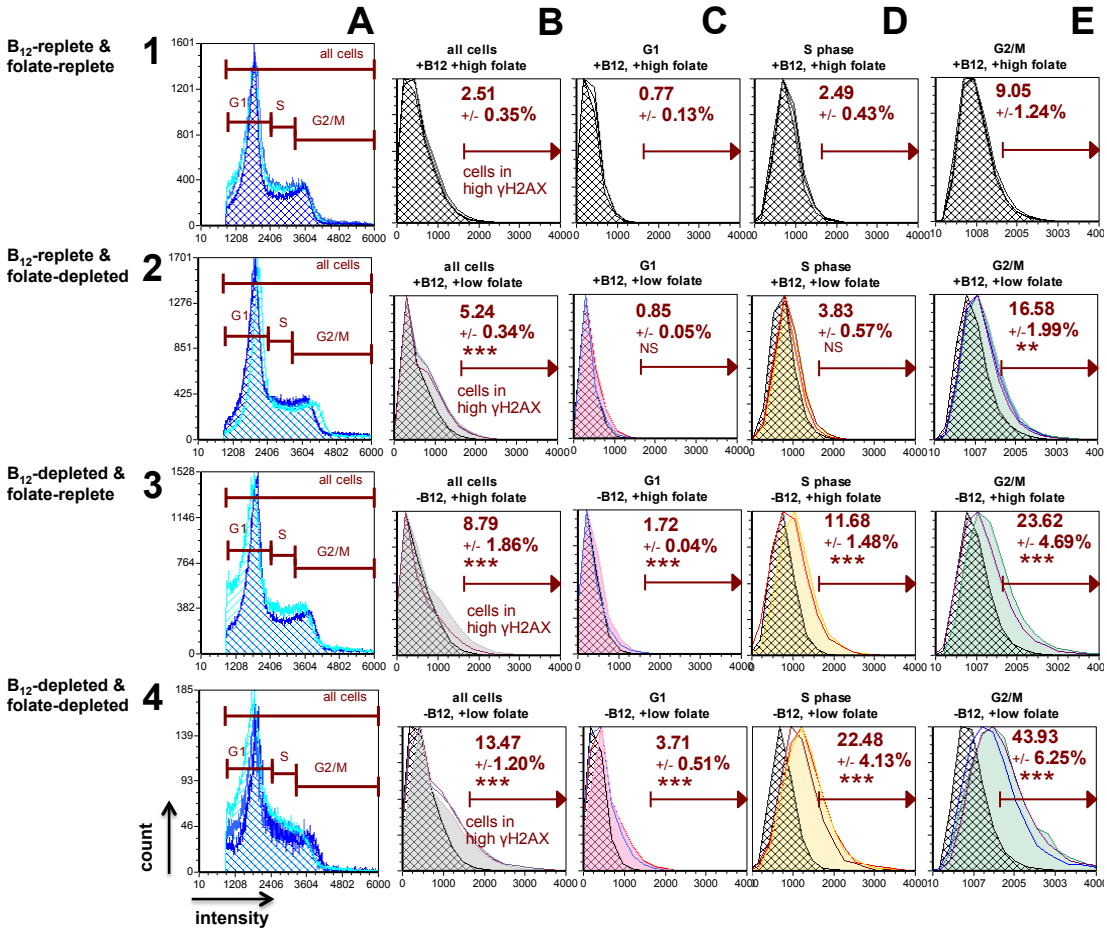

Figure 3.3. Vitamin B_{12} depletion induces changes in γH2AX, a marker of DNA damage in HeLa cells. Cells were stained for DNA content (Vybrant Violet; 1-4A) and γH2AX (FITC; 1-4 B-E); individual plots depict the cell count (Y-axis) versus fluorescence intensity (X-axis). The high γH2AX parameter is a threshold defined by the mean top 2.5% of cells in G1, S, and G2/M ('all cells') stained for γH2AX in the vitamin B_{12}- and folate-replete condition (1B), and this gate was uniformly applied to all conditions and cell cycle phases. Each plot shows the mean percent high γH2AX ± S.D. for triplicate measurements for each experimental condition and cell cycle phase. Individual triplicate measurements for each condition are plotted relative to the corresponding mean γH2AX values in the vitamin B_{12}- and folate-replete condition (hatched histograms, 1B-E). The grey, pink, yellow, and green colors correspond to the γH2AX fluorescence intensity for all cells, G1, S, and G2/M cell cycle phases, respectively. Asterisks designate statistical significance in percent high γH2AX values between treatment conditions and cell cycle phases compared to the corresponding phases in the vitamin B_{12}- and folate-replete condition (Table S3.1). The greatest percentage of cells with high γH2AX within conditions was observed in G2/M under vitamin B_{12}- and folate-depleted conditions ($p<0.001$; 4E). The vitamin B_{12}-depleted and folate-replete condition in row 3 contains duplicate measurements. The experiment was performed twice (see Fig. S3.7). Folate-replete, 25 nM (6S) 5-formylTHF in culture media; Folate-depleted, 5 nM (6S) 5-formylTHF in culture media.

The statistical significance is represented as follows: NS = Not significant ($p > 0.05$); * = $0.01 < p < 0.05$; ** = $0.01 < p < 0.001$; *** = $p < 0.001$.

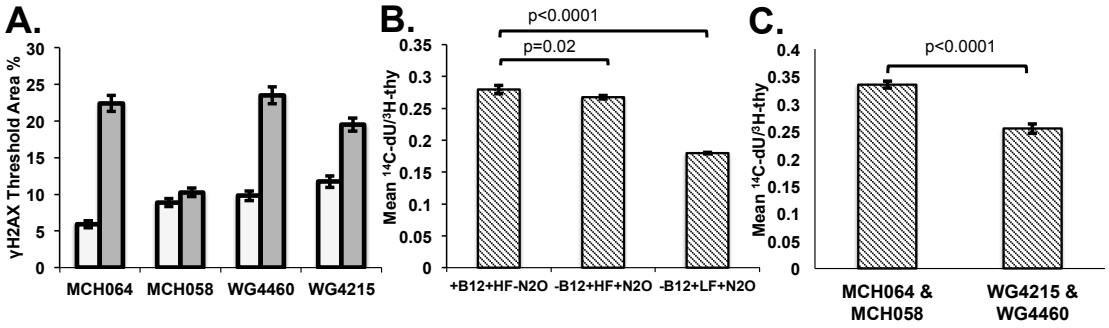

Figure 3.4. Metabolic effects of vitamin B_{12} depletion are exacerbated by folate depletion. *(A)* Folate depletion (gray bars) significantly increases the formation of γH2AX in MTR-null and control fibroblasts compared to those maintained in folate-replete conditions (white bars). Data are shown as mean percent thresholded area ± S.E. The number of cells analyzed per fibroblast line and treatment was: MCH064 25 nM folate: 648; MCH064 5nM folate: 542; MCH058 25 nM folate: 623; MCH058 5 nM folate: 773; WG4460 25 nM: 884; WG4460 5 nM folate: 851; WG4215 25 nM folate: 645; WG4215 5 nM folate: 625. Folate exposure predicted γH2AX response ($p<0.0001$) in three of the four cell lines, but MTR loss-of-function did not ($p>0.05$), as determined by a linear mixed-effects model. (*B)* Rates of *de novo* dTMP biosynthesis relative to salvage pathway synthesis in HeLa cells maintained in vitamin B_{12}- and folate-replete or depleted conditions. Vitamin B_{12} depletion and folate-replete conditions impaired *de novo* dTMP synthesis capacity by 5% compared to vitamin B_{12}- and folate-replete conditions ($p=0.02$). A combined vitamin B_{12} and folate depletion decreased rates of *de novo* dTMP synthesis by 35% ($p<0.0001$). Data are shown as mean ± S.D. *(C)* Rates of *de novo* dTMP biosynthesis relative to salvage pathway synthesis in cblG (WG4215 & WG4460) and control (MCH058 & MCH064) human fibroblasts maintained in vitamin B_{12}-replete or depleted media without folate. cblG fibroblasts exhibited a 25% reduction in *de novo* dTMP capacity compared to control fibroblasts ($p<0.0001$). Data are shown as means ± S.E. (n=12 per group). HF, 25 nM (6S) 5-formylTHF in culture media; LF, 5 nM (6S) 5-formylTHF in culture media; N_2O, nitrous oxide.

MTR loss-of-function and folate depletion do not impair *de novo* purine biosynthesis. Intracellular folate depletion did not significantly impair *de novo* purine biosynthesis in human fibroblasts ($p>0.05$). One control and two cblG cell lines exhibited similar rates of *de novo* purine biosynthesis, as determined by the ratio of ^{14}C-formate/^{3}H-hypoxanthine incorporation into nuclear DNA (Fig. S3.8). One control cell line showed reduced *de novo* purine biosynthesis.

Vitamin B_{12} depletion and intracellular folate concentrations influence the source of one-carbon units for dTMP biosynthesis. The incorporation of one-carbons derived from L-[2,3,3-$^2H_3$]-serine into the *de novo* dTMP biosynthesis pathway either as formate (CD1 via MTHFD1) or the hydroxymethyl group of serine (CD2 via SHMT), as indicated by the ratio of CD1/(CD1+CD2) was increased by 12% in HeLa cells grown under vitamin B_{12}-depleted and folate-replete conditions compared to HeLa cells cultured in vitamin B_{12}- and folate-replete media (p=0.007) (Fig. S3.9*A*). The difference between vitamin B_{12} depleted conditions was significant (p=0.002) (Fig. S3.9*A*). These findings indicate that vitamin B_{12} depletion and folate-replete conditions decrease the contribution of SHMT-derived single carbons (CD2) compared to folate- and vitamin B_{12}-depleted conditions. There was no difference in the CD1/(CD1+CD2) ratio between cblG (WG4215 & WG4460) and control (058MCH & MCH064) fibroblasts cultured in folate-replete conditions (Fig. S3.9*B*).

Discussion

Previous studies have described the impact of the vitamin B_{12} deficiency-induced “5-methylTHF trap” in terms of limiting available cytosolic THF cofactors for dTMP synthesis (5, 11). Our work was motivated by recent findings that the *de novo* dTMP biosynthesis pathway is present in the nucleus during S-phase of the cell cycle and forms a complex at sites of DNA replication and repair (14, 16, 29). SHMT serves as an essential scaffold for the assembly of this complex but makes only minor contributions as a source of one-carbon units for dTMP synthesis (14, 18). Proper assembly of the metabolic complex and adequate levels of unsubstituted THF cofactors in the nucleus are required to maintain adequate dTMP synthesis and genome integrity (19, 20). Mice with reduced *Shmt1* expression exhibit 2.5- to 4.5-fold

elevations in levels of uracil in nuclear DNA (22), and elevated levels of uracil incorporation into DNA result in loss of DNA integrity (20).

This study demonstrates that vitamin B_{12} depletion in HeLa cells traps nuclear folate as 5-methylTHF, impairs rates of *de novo* dTMP biosynthesis, and leads to genome instability. These effects of vitamin B_{12} depletion were exacerbated by folate depletion. In vitamin B_{12}-depleted HeLa cells, the elevations in 5-methylTHF were more pronounced in nuclei compared to whole cells, with a greater than 4-fold increase in nuclear 5-methylTHF (Fig. 3.2*B,C*). The sensitivity of the nucleus to 5-methylTHF accumulation is striking, given that 5-methylTHF is synthesized in the cytosol. CblG fibroblasts, which lack MTR activity, exhibit elevated levels of 5-methylTHF compared to control fibroblasts, and therefore serve as a model of severe vitamin B_{12} depletion (Fig. 3.2*A*). Loss of MTR activity seen in cblG fibroblasts was also associated with reduced *de novo* dTMP biosynthesis capacity compared with control fibroblasts (Fig. 3.4*C*). In contrast to HeLa cells, the reduction in *de novo* dTMP biosynthesis did not result in elevations in γH2AX immunostaining (Fig. 3.4*A)* in MTR loss-of-function fibroblasts. These observations may account for differences in the clinical manifestation of vitamin B_{12} deficiency in that specific cell types, including neural tissue and bone marrow, exhibit increased sensitivity to vitamin B_{12} deficiency (2).

The effect of impaired *de novo* dTMP biosynthesis on increasing genome instability as evidenced by increased γH2AX immunostaining could result from two potential mechanisms. γH2AX levels may increase as a result of reduced replication fork movement (31), or due to base excision repair pathways that remove uracil from DNA (32). Reduced replication fork movement has been reported in lymphocytes

from patients with megaloblastic anemia (33). When stratified by cell cycle, the γH2AX immunostaining observed as a result of vitamin B_{12}- and folate depletion occurred primarily during S-phase and G2/M phase of the cell cycle (Fig. 3.3). The presence of a stalled replication fork may be responsible for the increased γH2AX immunostaining that is observed during S-phase, as vitamin B_{12} depletion decreases the amount of nuclear THF available for subsequent nucleotide biosynthesis (Fig. 3.2*C* & 4*B,C*). Alternatively, it is possible that the DSBs observed in S- and G2/M phases of the cell cycle may arise as a result of base-excision repair of genomic uracil in DNA (32). In HeLa cells, folate depletion exacerbated genome instability associated with vitamin B_{12} depletion, with high rates of genome instability observed in all phases of the cell cycle including G1 phase (Fig. 3.3, 4*B-E*). Our findings are in contrast to observational studies reporting that high folate status worsens clinical symptoms (6, 7) and biochemical indicators of vitamin B_{12} deficiency (7).

This study provides a new role for 5-formylTHF in *de novo* dTMP synthesis, as it revealed that nuclear folate pools are enriched in 5-formylTHF. The role of 5-formylTHF in mammalian one-carbon metabolism has been elusive. It does not serve as a metabolic cofactor, but rather has been proposed to serve as a stable, storage form of folate, and is an inhibitor of folate-dependent enzymes including SHMT (34). SHMT and MTHFS participate in a futile cycle that regulates cellular 5-formylTHF levels. SHMT synthesizes 5-formyTHF, whereas MTHFS converts 5-formylTHF back to a metabolically active cofactor (Fig. 3.1) (35). 5-formylTHF is a minor component of the total cellular folate pool (8%), but accounts for 35% in nuclei. The enrichment of 5-formylTHF in HeLa nuclei provides a mechanism for previous observations that the majority of one-carbon units incorporated into dTMP are derived from formate via MTHFD1 and not from serine via SHMT1 and/or SHMT2α (Fig. 3.1) (15, 18). The 5-

formylTHF present in the nucleus is expected to inhibit SHMT1 and SHMT2α, as 5-formylTHF is a slow, tight-binding inhibitor of SHMT (28). The increase in incorporation of one-carbons from MTHFD1 into dTMP in folate-replete and vitamin B_{12}-deficient HeLa cells is likely explained by the increased pool of 5-methylTHF, which also binds and inhibits SHMT (Fig. S3.9*A*) (28). It is unclear if nuclear SHMT activity and, hence, *de novo* dTMP biosynthesis is regulated by changes in nuclear 5-formylTHF levels.

This study provides a mechanism whereby vitamin B_{12} depletion in the cytosol impairs *de novo* dTMP synthesis in the nucleus by trapping folate as 5-methylTHF, and this discovery can be extended to other vitamin B_{12}-associated human pathologies. Megaloblastic anemia is characterized by impaired maturation and proliferation of red blood cell precursors during hematopoiesis that results in an accumulation of cells in S-phase, as the G2 to M transition cannot be completed for cell division because of inadequate THF pools (2). Furthermore, maternal vitamin B_{12} deficiency has been associated with NTDs (36–38). NTDs arise when the neural folds fail to fuse entirely during neurulation in early embryogenesis, a period of rapid growth that places demands on nucleotide pools for the cell division required to complete neural tube closure. Folic acid supplementation reduces the occurrence and recurrence of NTDs by up to 70% (39, 40). Impairments in *de novo* dTMP synthesis, have been implicated in the etiology of folate-responsive NTDs, both in human studies and in animal models (41–43). The role of a nuclear 5-methylTHF trap resulting from vitamin B_{12} depletion in neural tube closure warrants further investigation.

Contributions: AMP performed all experiments in Chapter 3. EK provided technical advice and expertise, helpful discussions, and contributed to the data analysis in the experiments in Fig. 3.3 & 3.4*A*.

Experimental Procedures

Cell Culture. Two patient [WG4215 & WG4460 cblG (MTR loss-of-function)] and two Montreal Children's Hospital (MCH) control fibroblast cell lines (MCH058 and MCH064) were maintained in MEM, α-modification (α-MEM; HyClone) supplemented with 10% (vol/vol) fetal bovine serum (FBS, Hyclone) and 1X Pen-Strep (Mediatech). For all studies, cells were maintained in custom defined media (Hyclone, #SH3A4302.01) with 10% (vol/vol) dialyzed FBS (Hyclone). Culture medium contained 2 mM glycine (MP Biomedicals), 1 mg/L pyridoxine (Sigma), 250 μM methionine (Sigma), 1.35 μM cyanocobalamin (vitamin B_{12}-replete, Sigma), and either 5 nM (6S) 5-formylTHF (folate-deplete) or 25 nM (6S) 5-formylTHF (folate-replete) (Schircks Laboratories).

Nitrous Oxide (N_2O)-induced Inactivation of Methionine Synthase (MTR). To inactivate MTR activity, HeLa cells were placed in a hypoxia incubator chamber (Stemcell Technologies), and treated with a nitrous oxide (N_2O) gas mixture consisting of 50% N_2O, 45% balance air, and 5% CO_2 (Airgas). At time zero, the N_2O gas mixture was delivered to the chamber at 20 psi for 5 min according to manufacturer's instructions, and this step was repeated 1 h later; the chamber was flushed with the N_2O gas mixture for 5 min twice every 24 h. Prior to initiating treatment with N_2O, culture medium on appropriate plates was replaced with culture medium purged with N_2O for 5 min, and fresh media was administered to plates that did not undergo N_2O treatment.

Determination of Folate Cofactor One-carbon Distribution. HeLa cells ($4.5x10^5$) were seeded in 10-cm tissue culture plates (Corning), cultured in folate-free modified culture medium with or without cyanocobalamin, and cultured to 60-80% confluency. Plates were rinsed twice with 1X PBS (Cellgro) and replaced with 3 mL of medium containing 50 nM [^{3}H]-folinic acid (Moravek Biochemicals). Following a 24 h incubation, 7 mL of vitamin B_{12}-replete or depleted medium purged with N_2O gas was added to the appropriate plates, which were cultured for 24 hours in the hypoxia chamber. Cell monolayers were washed, harvested, and intracellular folates were extracted as previously described (44). Fibroblasts were cultured with labeled folates as described elsewhere (44). Folate one-carbon forms were separated and quantified using reverse phase HPLC as previously described (45).

Determination of Nuclear Folate Cofactor One-carbon Distribution. HeLa cells ($4x10^5$) were plated as described above. Following 48 h in culture, plates were labeled with 50 nM [^{3}H]-folinic acid (Moravek Biochemicals) for 24 h, and then maintained as previously described for another 48 h. Nuclei were extracted using the REAP method (46). The nuclear pellet was resuspended in 200 μL folate extraction buffer (44) and sonicated twice using a Branson Sonifier 150 on level V3 for 5 seconds on ice. Folate one-carbon forms were separated and quantified using reverse phase HPLC as previously described (45).

Immunoblotting. Proteins (20 μg per lane) were separated on a 4-20% (vol/vol) SDS-PAGE gel (Novex), and transferred onto Immobilon-P PVDF membranes (Millipore). Membranes were blocked overnight in 5% (wt/vol) bovine serum albumin (BSA; Sigma) in PBS with 0.2% Tween-20 (Amresco) and 0.02% sodium azide (Sigma). Full-length α-tubulin protein (52 kD) was detected using mouse anti-human

monoclonal primary antibody (mAb) at 1:1000 dilution (Active Motif), and a 1:10,000 dilution of HRP conjugated goat-anti mouse secondary antibody (Pierce). Full-length Lamin B1 protein (68 kD) was detected using a rabbit anti-human monoclonal antibody (Cell Signaling) at 1:1000 dilution, and a 1:5,000 dilution of HRP-conjugated donkey anti-rabbit secondary (Pierce). Secondary antibodies were incubated in 10% (wt/vol) nonfat dry milk in PBS and 0.1% NP-40 (US Biologicals). The membranes were incubated in SuperSignal West Pico Chemiluminescent Substrate (Pierce), and exposed to autoradiography.

dU Suppression Assay. The contributions of the *de novo* and salvage pathways to dTMP biosynthesis were measured in cells by exposure to [^{14}C]-deoxyuridine and [^{3}H]-thymidine, as described elsewhere (47). Briefly, fibroblasts ($2x10^4$ cells/well) were plated in triplicate in 6-well plates (Corning) and allowed to undergo two doublings in vitamin B_{12}-replete or depleted modified media lacking folate and containing 500 nM [^{3}H]-thymidine (Perkin-Elmer) and 10 μM [^{14}C]-deoxyuridine (Moravek). HeLa cells were plated in modified media containing vitamin B_{12} and/or folate for 24 h. The appropriate treatment groups were exposed to nitrous oxide gas for 48 h, which represented two cell doublings. Cells were re-plated in triplicate ($2x10^5$ cells/well) in 6-well plates containing [^{14}C]-dU and [^{3}H] thymidine. Cells in N_2O treatment groups were returned to the chamber and exposed to N_2O gas mixture for an additional 48 h. Cells were harvested and genomic DNA extracted with a DNA Isolation Kit for Cells and Tissues (Roche). The radioisotope quantification was performed as described previously (47). Statistical analyses were performed on HeLa cell data using a Student's two-tailed t-test. Significance in fibroblasts was assessed using two-way ANOVA in JMP Pro 12 Software (SAS Corporation). Independent variables were fibroblast genotype, vitamin B_{12} (replete or deplete), and the

interaction term; the dependent variable was the ratio of ^{14}C-dU to ^{3}H-thymidine in nuclear DNA.

Quantification of γH2AX by Flow Cytometry. The impact of vitamin B_{12} and/or folate depletion on γH2AX formation in HeLa cells was assessed using flow cytometry (48). Briefly, cells (1 x 10^6) were seeded in 10 cm plates in modified media supplemented with folate and/or cyanocobalamin. Vitamin B_{12} depletion was induced with the N_2O gas mixture at 24 h post-plating and held for 48 h. Cells were re-seeded at a 1:5 density in triplicate, and treated with N_2O gas mixture for an additional 48 h. One aliquot of cells per treatment group was saved at harvest for the microbiological assay to quantify intracellular folate. For the positive control: 100 μM etoposide (Sigma) was added to culture medium in the positive control plate for 1 h prior to trypsinizing cells. For preparation of all samples: Cells were washed twice with 1X PBS and harvested with 1X Trypsin-EDTA for no longer than 5 min. Cells were pelleted at 3,700 rpm for 4 min at room temperature. Cell pellets were washed once with PBS prior to a final centrifugation. The supernatant was discarded, and pellets were incubated on ice until staining. For γH2AX staining: 150 μL of master mix containing Block-9 buffer, FITC-conjugated α-γH2AX antibody (1:3000; Millipore), and Vybrant Violet DNA stain (1:1000; Life Sciences) was added to each sample. Cell pellets were gently resuspended by vortexing and incubated on ice in the dark for 3 h. Samples were resuspended 1XPBS and strained immediately before each analysis. The samples were analyzed on a BD FACSAria flow cytometer using 488 and 405 nm lasers for excitation of FITC and Vybrant Violet Dye Cycle Stain, respectively. Data was recorded for approximately 200,000 events per replicate, and initial gating excluded any debris and clumped cells. This population was further gated to exclude

those cells with a large area and width to obtain the parent gated population for γH2AX analyses.

Quantification of high γH2AX. All post-run analyses for flow cytometry data files were performed in FCS Express 5 (De Novo Software). The parent population of cells stained for both DNA content (Vybrant Violet) and γH2AX (FITC) was gated for cell cycle (G1, S, and G2/M). The gate for 'all cells' comprised the G1, S, and G2/M phases analyzed together. Two gates for γH2AX included total γH2AX and high γH2AX. Total γH2AX refers to absolute FITC intensity. The gate for high γH2AX was determined by applying a threshold cutoff at the mean top 2.5% of cells across triplicates in the vitamin B_{12}- and folate-replete (control) condition stained for total γH2AX (Fig. 3.3, 1B). This gate for high γH2AX was applied to replicates in all treatment conditions and cell cycle phases. Significance between the control and other treatment conditions in 'all cells', G1, S, and G2/M was assessed using a 2-way ANOVA. In this model, the independent variables included folate, vitamin B_{12}, and the interaction term (folate x vitamin B_{12}); the dependent variable was the percent high γH2AX for individual triplicates in each treatment and cell cycle. The percent high γH2AX values for triplicates were log-transformed to better satisfy the assumptions of the model. Specific pair-wise *post-hoc* comparisons were made between the percent high γH2AX in the control condition for all cells, G1, S, or G2/M to that observed in the corresponding cell cycle phase for each treatment column. A Bonferroni correction was applied to account for the multiple comparisons between conditions (n=4).

Microbiological *L. casei* Assay. The concentration of total folate in HeLa cells was determined using the microbiological *L. casei* assay as described elsewhere (49).

Formate Suppression Assay. Flux through the *de novo* and salvage purine biosynthetic pathways was measured in human fibroblasts by quantifying the amount of ^{14}C-formate (*de novo*) and ^{3}H-hypoxanthine (salvage) incorporated into nuclear DNA as previously described (47). Cells ($2x10^4$) were seeded in triplicate in 6-well plates in folate-replete or folate-depleted culture medium with cyanocobalamin and containing 20 μM [^{14}C]-formate (Moravek) and 200 nM [^{3}H]-hypoxanthine (Moravek). Cells were cultured for 2 doublings. Cell pellets, DNA extraction, and radioisotope abundance in DNA were performed as described elsewhere (see **dU Suppression Assay**). Statistical analyses were performed using a two-way ANOVA to assess the impact of folate, fibroblast genotype, as well as the interaction term on the mean ratio of ^{14}C-formate/^{3}H-hypoxanthine. The mean ^{14}C/^{3}H values were rank transformed to improve the normal distribution assumption of the model.

γH2AX Immunostaining and Quantification. Cells ($2x10^4$) were seeded in duplicate on #1.5 microscope cover glass slides (Fisher Scientific) in 6-well plates, and maintained in modified folate-replete or deplete culture medium with cyanocobalamin until approximately 80% confluent. Cell fixation and immunostaining was performed as previously described (47) with the modification that 0.5% Triton in PBS was added for permeabilizing cells and diluting the primary antibody. Representative images (n=10 per slide) were recorded with a Leica TCS SP2 confocal microscope. Quantification of the percent γH2AX positive area for each cell was performed as previously described (47). The percent thresholded area of γH2AX staining for each cell within an image were averaged to improve the normal distribution assumption, and statistical analyses were performed using the averaged values across all treatments (n=160). A linear mixed-effects model assessed the impact of folate and vitamin B_{12} status on γH2AX response (mean % threshold area). Fixed effects

included: folate, vitamin B_{12}, and the interaction term. Random effects included: subject and slide. Slide was nested within subject.

Stable Isotope Tracer Studies. The flux of isotopically labeled one-carbon units into the *de novo* dTMP biosynthesis pathway was quantified in thymidine in DNA using L-[2,3,3-$^2H_3$]-serine as described previously (18). Briefly, human fibroblasts (8 x 10^5) were plated in duplicate in folate-replete modified culture medium containing cyanocobalamin (See **Cell Culture**) supplemented with 250 μM L-[2,3,3-$^2H_3$]-serine (Cambridge Isotope Laboratories) and allowed to undergo 2 doublings. HeLa cells ($4x10^5$) were plated in duplicate for three media conditions: 1) vitamin B_{12}- and folate-replete, 2) vitamin B_{12}-deplete and folate-replete, and 3) vitamin B_{12}- and folate-deplete. Vitamin B_{12} depleted conditions were treated with nitrous oxide for 48 h following 24 h in culture. All groups were then seeded at a 1:4 density in duplicate into appropriate media containing 250 μM L-[2,3,3-$^2H_3$]-serine, treated with nitrous oxide for an additional 48 h to allow for 2 population doublings. The cell pellets were washed twice with PBS, and genomic DNA was isolated as previously described (see **dU Suppression Assay**).

Supplemental Information

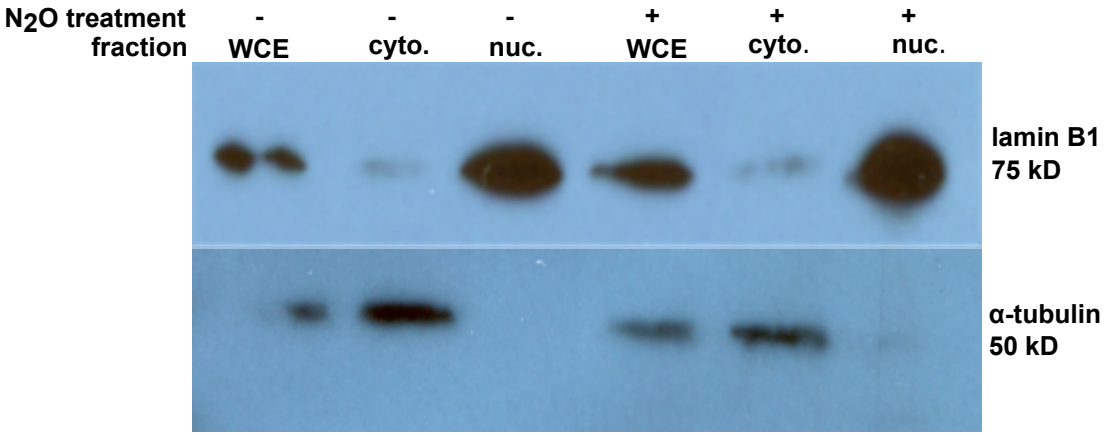

Figure S3.5. Western blot of whole cell, cytosolic, and nuclear fractions for nuclear (lamin B1) and cytosolic (α-tubulin) marker proteins from HeLa cells harvested in tandem with those cells used for quantifying nuclear one-carbon folate forms (refer to Fig. 3.2C). The absence of α-tubulin in the lanes corresponding to nuclear fractions confirms the lack of cytosolic contamination in nuclei. Lane designations: WCE, whole cell extract; cyto, cytosolic; nuc, nuclear. N_2O, nitrous oxide.

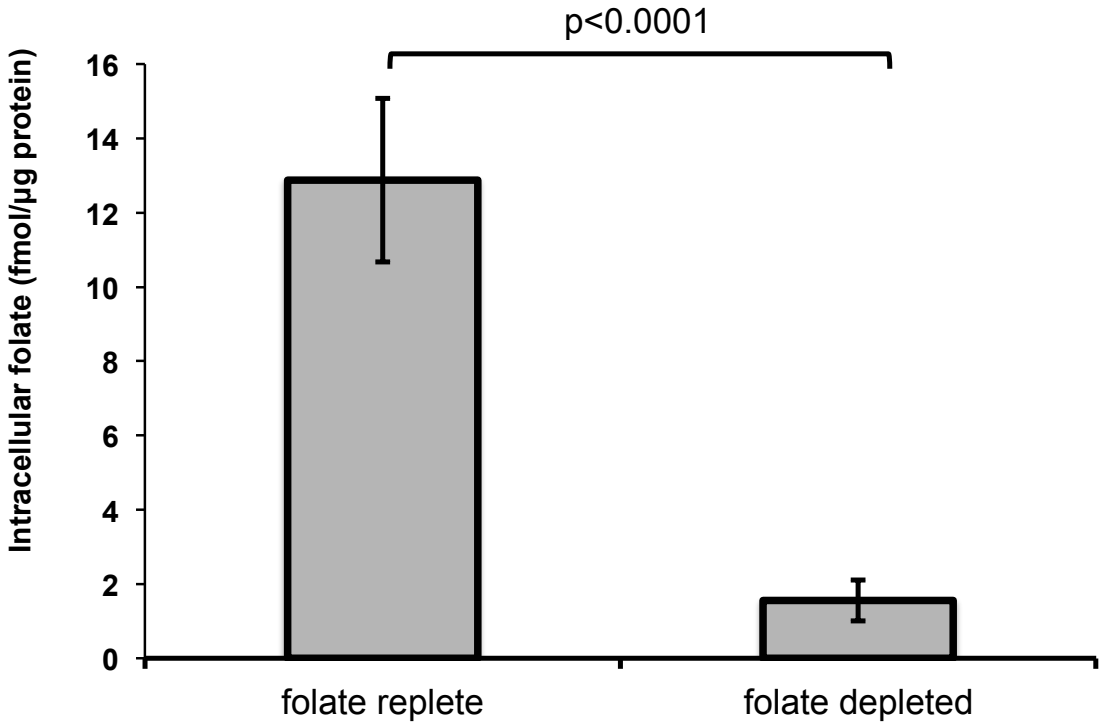

Figure S3.6. Intracellular folate concentrations in HeLa cells assayed for γH2AX at the time of staining and quantification (refer to Fig. 3.3). The intracellular folate concentrations were 8-fold higher in HeLa cells maintained in folate-replete (25 nM) media compared to those cultured in folate-depleted (5 nM) conditions ($p<0.0001$). Data are shown as the mean ± S.D. of n=4 groups for each folate replete or folate depleted condition. Significance was determined by using a Student's two-tailed t-test.

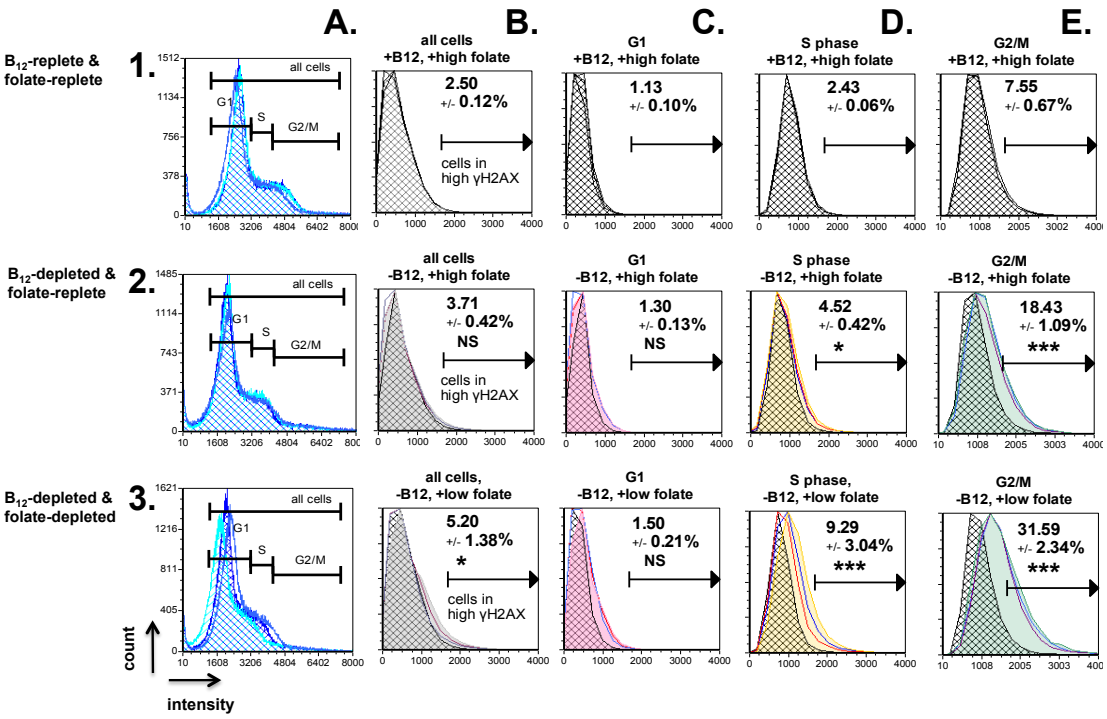

Figure S3.7. Vitamin B_{12} depletion induces changes in γH2AX, a marker of DNA damage, in the S and G2/M phases of the cell cycle in HeLa cells. Cells were stained for DNA content (Vybrant Violet; 1-3A) and γH2AX (FITC; 1-3 B-E); individual plots depict the cell count (Y-axis) versus fluorescence intensity (X-axis). The high γH2AX parameter is a threshold defined by the mean top 2.5% of cells in the G1, S, and G2/M ('all cells') stained for γH2AX in the vitamin B_{12}- and folate-replete condition (1B), and this gate was uniformly applied to all conditions and cell cycle phases. Each plot shows the mean percent high γH2AX ± S.D. for triplicates for each experimental condition and cell cycle phase. Individual triplicates stained for γH2AX in each condition are plotted relative to the corresponding mean γH2AX values in the vitamin B_{12}- and folate-replete condition (hatched histograms, 1B-E). Asterisks designate statistical significance in percent high γH2AX values between treatment conditions and cell cycle phase compared to the corresponding phases in the vitamin B_{12}- and folate-replete condition (1B-E). The grey, pink, yellow, and green colors correspond to the γH2AX fluorescence intensity for all cells, G1, S, and G2/M cell cycle phases, respectively. The greatest percentage of cells in high γH2AX within conditions was observed in G2/M under vitamin B_{12}- and folate-depleted conditions ($p<0.001$; 3E). A combined vitamin B_{12} and folate depletion exacerbated the percent high γH2AX observed in HeLa cells compared to cells maintained in vitamin B_{12}-depleted and folate-replete culture conditions in all cells, S, and G2/M (compare 2A,D-E to 3A,D-E), and this difference in high γH2AX between conditions was significant for S phase ($p=0.01$) and G2/M ($p=0.0003$). Statistical significance was determined using a one-way ANOVA. The dependent variable was log-transformed percent high γH2AX, and the independent variable was vitamin B_{12} and folate level. Folate-replete, 25 nM (6S) 5-formylTHF in culture media; Folate-depleted, 5 nM (6S) 5-formylTHF in culture media. The statistical significance is represented as follows: NS = Not significant ($p > 0.05$); * = $0.01 < p < 0.05$; ** = $0.01 < p < 0.001$; *** = $p < 0.001$.

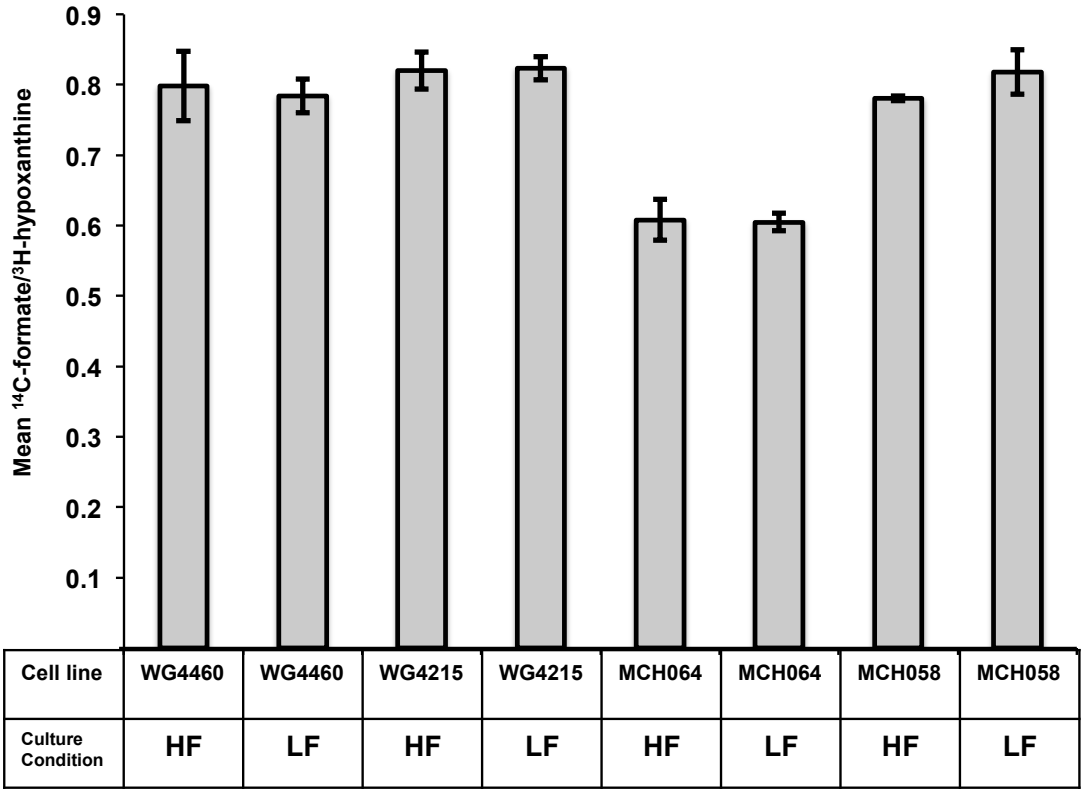

Figure S3.8. Mean ratio of ^{14}C-formate/^{3}H-hypoxanthine incorporation into nuclear DNA in cblG (WG4215 and WG4460) and control (MCH064 and MCH058) fibroblasts. Data are shown as mean ± S.D. for fibroblast line and treatment. A two-way ANOVA revealed a non-significant effect of folate exposure ($p>0.05$) and a significant effect of fibroblast genotype ($p=0.02$) on the rank-transformed mean ratios of ^{14}C/^{3}H incorporated into nuclear DNA. HF, 25 nM (6S) 5-formylTHF; LF, 5 nM (6S) 5-formylTHF.

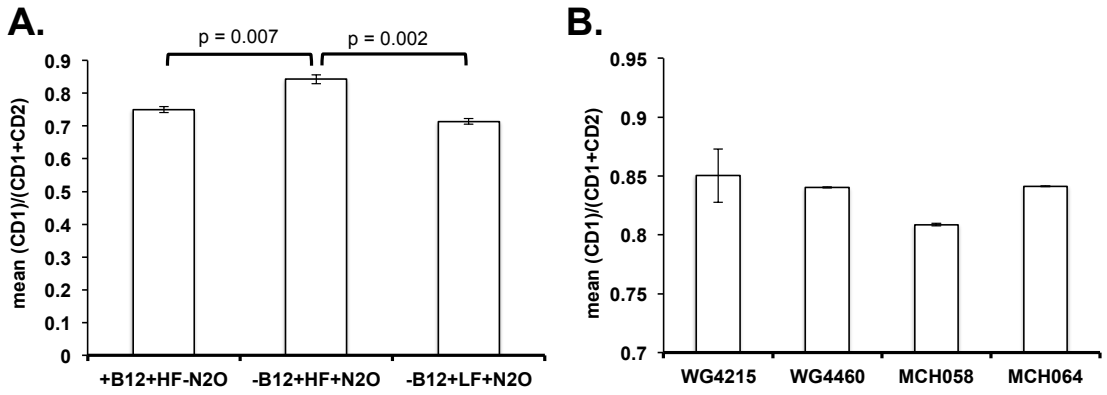

Figure S3.9. Mean ratio of isotopically labeled one-carbon units from MTHFD1 (CD1) to the total number of labeled one-carbons containing 1 or 2 deuterium atoms generated from MTHFD1 (CD1) or SHMT (CD2), respectively, into thymidine in nuclear DNA in (A) HeLa cells and (B) human fibroblasts. *(A)* Vitamin B_{12}-depleted and folate-replete conditions increased the contribution of labeled one-carbon units from MTHFD1 relative to SHMT by 12% compared to vitamin B_{12} and folate-replete conditions in HeLa cells (p=0.007). The ratios between vitamin B_{12}-depleted conditions were significant (p=0.002). *(B)* In human cblG (WG4215 and WG4460) and control fibroblasts (MCH058 and MCH064) grown under high folate conditions, there was no difference in the contributions of one-carbon units from MTHFD1 (p>0.05). For (A) and (B), cells were plated in duplicate, and the data are shown as mean ± S.D. Statistical significance between conditions was assessed using a one-way ANOVA. The dependent variable was the log-transformed ratio of mean CD1/(CD1+CD2) and the independent variable was folate and vitamin B_{12} exposure. HF, 25 nM (6S) 5-formylTHF; LF, 5 nM (6S) 5-formylTHF.

Table S3.1. Fold differences in percent high γH2AX[1] between control and experimental conditions[2] within cell cycle phase (to accompany Fig. 3.3).

	All cells	**G1**	**S**	**G2/M**
	Least Square (LS) Mean 95% CI (Lower, Upper)	LS Mean 95% CI (L,U)	LS Mean 95% CI (L,U)	LS Mean 95% CI (L,U)
Treatment	**B**	**C**	**D**	**E**
(1) B_{12}- and folate-replete (control)	**2.50**	**0.76**	**2.46**	**8.99**
(2) B_{12}-replete, folate-depleted	2.10*** (1.65, 2.66)	1.12^{NS} (0.89, 1.40)	1.55^{NS} (1.11, 2.16)	1.84** (1.39, 2.43)
(3) B_{12}-depleted, folate-replete	3.16*** (2.42, 4.13)	2.25*** (1.74, 2.90)	4.50*** (3.10, 6.52)	2.80*** (2.05, 3.84)
(4) B_{12}- and folate-depleted	5.38*** (4.23, 6.83)	4.83*** (3.85, 6.06)	9.02*** (6.47, 12.59)	4.85*** (3.66, 6.42)
(5) B_{12}-depleted: folate-replete vs. depleted (row 3 vs. 4)	1.70** (1.30, 2.23)	2.15*** (1.67, 2.77)	2.01* (1.38, 2.91)	1.73* (1.26, 2.37)

[1]Percent (%) high γH2AX refers to the percentage of HeLa cells stained for γH2AX above the mean top 2.5% total γH2AX intensity in 'all cells' in the vitamin B_{12}- and folate-replete (control) condition (Fig. 3.3, 1B). Columns show the back-transformed least-squares (LS) means and 95% confidence intervals (CI) for Log_e transformed mean % high γH2AX for specific contrasts, indicating fold differences in % high γH2AX. Values for LS means in row 1B-E for control conditions are those mean % high γH2AX predicted by the model. LS means and 95% CI were back-transformed = exp^(LS Mean) = geometric mean % high γH2AX.

[2]*Post-hoc* comparisons (n=3) were made within cell cycle phase ('all cells', G1, S, G2/M) and compared the % high γH2AX in the control to that in row: 2) B_{12}-replete, folate-depleted, 3) B_{12}-depleted, folate-replete, and 4) B_{12}- and folate-depleted conditions. A final comparison considered the difference in % high γH2AX between B_{12} depleted conditions (row 3 vs. 4). A Bonferroni correction was applied to all p-values to account for multiple comparisons (n=4).

Legend: NS = Not significant ($p \geq 0.05$); * = $0.01 < p < 0.05$; ** = $0.01 < p < 0.001$; *** = $p < 0.001$.

References

1. Finkelstein JL, Layden AJ, Stover PJ (2015) Vitamin B-12 and Perinatal Health. *Adv Nutr* 6(5):552–63.

2. Stabler SP (2013) Vitamin B12 Deficiency. *N Engl J Med* 368(2):149–160.

3. Carmel R (2008) Nutritional Anemias and the Elderly. *Semin Hematol* 45(4):225–234.

4. Nielsen MJ, Rasmussen MR, Andersen CBF, Nexø E, Moestrup SK (2012) Vitamin B12 transport from food to the body's cells--a sophisticated, multistep pathway. *Nat Rev Gastroenterol Hepatol* 9(6):345–54.

5. Marshall R, Jandl J (1960) Responses to "physiologic" doses of folic acid in megaloblastic anemias. *Arch Intern Med* 105(3):352–360.

6. Morris MS, Jacques PF, Rosenberg IH, Selhub J (2007) Folate and vitamin B-12 status in relation to anemia, macrocytosis, and cognitive impairment in older Americans in the age of folic acid fortification. *Am J Clin Nutr* 85(1):193–200.

7. Selhub J, Morris MS, Jacques PF, Rosenberg IH (2009) Folate-vitamin B12 interaction in relation to cognitive impairment, anemia, and biochemical indicators of vitamin B12 deficiency. *Am J Clin Nutr* 89:702–707.

8. Mills JL, et al. (1996) Homocysteine and Neural Tube Defects. *J Nutr* 126:756–60.

9. Bailey LB, Gregory JF (1999) Folate Metabolism and Requirements. *J Nutr* 129:779–782.

10. Kutzbach C, Stokstad E (1971) Mammalian methylenetetrahydrofolate reductase. Partial purification, properties, and inhibition by S-adenosylmethionine. *Biochim Biophys Acta* 250(3):459–477.

11. Metz J, Kelly A, Swett V, Waxman S, Herbert V (1968) Deranged DNA synthesis by bone marrow from vitamin B12-deficient humans. *Br J Haematol* 14(6):575–592.

12. Herbert V, Zalusky R (1962) Interrelations of vitamin B12 and folic acid metabolism: folic acid clearance studies. *J Clin Invest* 41(6):1263–76.

13. Scott JM, Weir DG (1981) The methyl folate trap. *Lancet* 318(8242):337–340.

14. Anderson DD, Woeller CF, Chiang EP, Shane B, Stover PJ (2012) Serine hydroxymethyltransferase anchors de novo thymidylate synthesis pathway to nuclear lamina for DNA synthesis. *J Biol Chem* 287(10):7051–7062.

15. Anderson DD, Stover PJ (2009) SHMT1 and SHMT2 are functionally redundant in nuclear de novo thymidylate biosynthesis. *PLoS One* 4(6):e5839.

16. Anderson DD, Woeller CF, Stover PJ (2007) Small ubiquitin-like modifier-1 (SUMO-1) modification of thymidylate synthase and dihydrofolate reductase. *Clin Chem Lab Med* 45(12):1760–1763.

17. Fox JT, Shin WK, Caudill MA, Stover PJ (2009) A UV-responsive internal ribosome entry site enhances serine hydroxymethyltransferase 1 expression for DNA damage repair. *J Biol Chem* 284(45):31097–108.

18. Herbig K, et al. (2002) Cytoplasmic serine hydroxymethyltransferase mediates competition between folate-dependent deoxyribonucleotide and S-adenosylmethionine biosyntheses. *J Biol Chem* 277(41):38381–38389.

19. MacFarlane AJ, et al. (2011) Nuclear localization of de novo thymidylate biosynthesis pathway is required to prevent uracil accumulation in DNA. *J Biol Chem* 286(51):44015–44022.

20. Blount B, et al. (1997) Folate deficiency causes uracil misincorporations into human DNA and chromosome breakage: implications for cancer and neuronal damage. *Proc Natl Acad Sci U S A* 94(7):3290–5.

21. Jensen MK (1977) Cytogenetic findings in pernicious anaemia. Comparison between results obtained with chromosome studies and the micronucleus test. *Mutat Res Mol Mech Mutagen* 45(2):249–252.

22. Rana S, Colman N, Goh KO, Herbert V, Klemperer M (1983) Transcobalamin II deficiency associated with unusual bone marrow findings and chromosomal abnormalities. *Am J Hematol* 14(1):89–96.

23. Minnet C, Koc A, Aycicek A, Kocyigit A (2011) Vitamin B12 treatment reduces mononuclear DNA damage. *Pediatr Int* 53(6):1023–7.

24. Wickramasinghe SN, Fida S (1994) Bone marrow cells from vitamin B12- and folate-deficient patients misincorporate uracil into DNA. *Blood* 83(6):1656–61.

25. Kapiszewska M, Kalemba M, Wojciech U, Milewicz T (2005) Uracil misincorporation into DNA of leukocytes of young women with positive folate balance depends on plasma vitamin B12 concentrations and methylenetetrahydrofolate reductase polymorphisms. A pilot study. *J Nutr Biochem* 16(8):467–78.

26. Field MS, et al. (2014) Nuclear enrichment of folate cofactors and methylenetetrahydrofolate dehydrogenase 1 (MTHFD1) protect de novo thymidylate biosynthesis during folate deficiency. *J Biol Chem* 289(43):29642–29650.

27. Wilson A, et al. (1998) Functionally null mutations in patients with the cblG-variant form of methionine synthase deficiency. *Am J Hum Genet* 63(2):409–414.

28. Stover P, Schirch V (1991) 5-formyltetrahydrofolate polyglutamates are slow tight binding inhibitors of serine hydroxymethyltransferase. *J Biol Chem* 266(3):1543–1550.

29. Woeller CF, Anderson DD, Szebenyi DME, Stover PJ (2007) Evidence for small ubiquitin-like modifier-dependent nuclear import of the thymidylate biosynthesis pathway. *J Biol Chem* 282(24):17623–17631.

30. MacFarlane AJ, et al. (2008) Cytoplasmic serine hydroxymethyltransferase regulates the metabolic partitioning of methylenetetrahydrofolate but is not essential in mice. *J Biol Chem* 283(38):25846–25853.

31. Lamm N, et al. (2015) Folate levels modulate oncogene-induced replication stress and tumorigenicity. *EMBO Mol Med* 7(9):e201404824.

32. Hagen L, et al. (2008) Cell cycle-specific UNG2 phosphorylations regulate protein turnover, activity and association with RPA. *EMBO J* 27(1):51–61.

33. Wickremasinghe R, Hoffbrand A (1980) Reduced rate of DNA-replication fork movement in megaloblastic-anemia. *J Clin Invest* 65(1):26–36.

34. Stover P, Schirch V (1993) The metabolic role of leucovorin. *Trends Biochem Sci* 18(3):102–106.

35. Field MS, Szebenyi DME, Stover PJ (2006) Regulation of de novo purine biosynthesis by methenyltetrahydrofolate synthetase in neuroblastoma. *J Biol Chem* 281(7):4215–4221.

36. Kirke PN, Daly LE, Burke H, Weir DC (1993) Maternal plasma folate and vitamin B12 are independent risk factors for neural tube defects. *Q J Med* 86:703–708.

37. Molloy AM, et al. (2009) Maternal vitamin B12 status and risk of neural tube defects in a population with high neural tube defect prevalence and no folic Acid fortification. *Pediatrics* 123(3):917–23.

38. Ray JG, et al. (2007) Vitamin B12 and the risk of neural tube defects in a folic-acid-fortified population. *Epidemiology* 18(3):362–366.

39. Czeizel A, Dudas I (1992) Prevention of the first occurrence of neural tube defects by periconceptional vitamin supplementation. *N Engl J Med* 327(26):1832–5.

40. Group MVSR (1991) Prevention of neural tube defects: Results of the Medical Research Council Vitamin Study. *Lancet* 338(8760):131–137.

41. Martiniova L, Field MS, Finkelstein JL, Perry CA, Stover PJ (2015) Maternal dietary uridine causes, and deoxyuridine prevents, neural tube closure defects in a mouse model of folate-responsive neural tube defects. *Am J Clin Nutr* 101(4):860–9.

42. Dunlevy LPE, et al. (2007) Abnormal folate metabolism in foetuses affected by neural tube defects. *Brain* 130:1043–1049.

43. Beaudin AE, et al. (2011) Shmt1 and de novo thymidylate biosynthesis underlie folate-responsive neural tube defects in mice. *Am J Clin Nutr* 93(4):789–98.

44. Girgis S, Suh JR, Jolivet J, Stover PJ (1997) 5-formyltetrahydrofolate regulates homocysteine remethylation in human neuroblastoma. *J Biol Chem* 272(8):4729–4734.

45. Anguera MC, et al. (2003) Methenyltetrahydrofolate synthetase regulates folate turnover and accumulation. *J Biol Chem* 278(32):29856–29862.

46. Suzuki K, Bose P, Leong-Quong RY, Fujita DJ, Riabowol K (2010) REAP: A two minute cell fractionation method. *BMC Res Notes* 3(1):294.

47. Field MS, Kamynina E, Watkins D, Rosenblatt DS, Stover PJ (2014) Human mutations in methylenetetrahydrofolate dehydrogenase 1 impair nuclear de novo thymidylate biosynthesis. *Proc Natl Acad Sci U S A* 112(2):1–6.

48. Muslimovic A, Ismail IH, Gao Y, Hammarsten O (2008) An optimized method for measurement of gamma-H2AX in blood mononuclear and cultured cells. *Nat Protoc* 3(7):1187–1193.

49. Molloy AM, Scott JM (1997) Microbiological assay for serum, plasma, and red cell folate using cryopreserved, microtiter plate method. *Methods Enzymol* 281:43–53.

SUMMARY

The overarching purpose of this work was to test for a metabolic link between cytosolic vitamin B_{12} deficiency and nuclear one-carbon metabolism, a goal motivated by the recent findings demonstrating compartmentalization between the folate-dependent *de novo* dTMP biosynthesis and homocysteine remethylation pathways. These findings called into question those previous studies that have characterized the impact of the 5-methylTHF trap that occurs in vitamin B_{12}-associated pathologies, including megaloblastic anemia, as depleting cytosolic folate cofactors for dTMP synthesis. This work additionally aimed to explore the vitamin B_{12}-folate interrelationship in *de novo* dTMP biosynthesis, given the conflicting evidence with respect to elevated folate intakes in vitamin B_{12} deficiency and related worsening or improvement of clinical outcomes. These gaps in the literature called for a systematic investigation of these relationships with respect to genome stability and disease pathogenesis. A conceptual figure summarizing the findings from this work is included at the end of this section.

The first aim of this work investigated the impact of maternal vitamin B_{12} deficiency on NTD pathogenesis in embryos with impairments in *de novo* dTMP biosynthesis under conditions of folate-repletion and deficiency. Maternal vitamin B_{12} deficiency caused vitamin B_{12}-responsive NTDs in *Shmt1*$^{-/-}$ and *Shmt1*$^{-/+}$ embryos but did not impair homocysteine remethylation or embryonic growth. Supplemental folate did not rescue rates of NTDs in vitamin B_{12} deficiency, suggesting that the neuroepithelium may not be rescued with folate in vitamin B_{12} deficiency, similar to what has been observed in the case of vitamin B_{12}-associated neuropathies. The non-significant rates of NTDs between the vitamin B_{12}-deficient groups suggest that

elevated folate intakes do not exacerbate NTD incidence. Taken together, these findings indicate that neural tube closure is more sensitive than cytosolic homocysteine remethylation or embryonic growth.

The second aim of this work sought to determine a mechanism by which cytosollc vitamin B_{12} depletion impairs nuclear *de novo* dTMP biosynthesis. We investigated this aim in two cell models of vitamin B_{12} deficiency, namely, MTR loss-of-function human fibroblasts and nitrous oxide-treated HeLa cells. Both cell types exhibited increased intracellular 5-methylTHF compared to vitamin B_{12}-replete HeLa cells or control fibroblasts. In contrast, the nucleus exhibited a marked increase in 5-methylTHF accumulation compared to total cellular 5-methylTHF concentrations in vitamin B_{12}-depleted HeLa cells, indicating that this compartment is the most sensitive to 5-methylTHF accumulation. Technical challenges prevented the quantification of nuclear one-carbon forms in human fibroblast lines.

Vitamin B_{12} depletion depressed rates of *de novo* dTMP biosynthesis in both cell types. In vitamin B12-depleted HeLa cells, rates of *de novo* dTMP biosynthesis were further exacerbated by folate depletion. Vitamin B_{12} depletion in HeLa cells increased DNA damage under folate-replete conditions as quantified by phosphorylated histone H2AX (γH2AX), and this damage was exacerbated by folate depletion. When stratified by cell cycle phase, γH2AX increased the most in the G2/M phase of the cell cycle within treatment condition; however, substantial damage was observed in both the S- and G2/M cell cycle phases. This observed increase in DSBs may arise as a consequence of replication stress in S-phase, including reduced replication fork stability, which may be unresolved in G2/M. Furthermore, the removal of genomic uracil incorporated into DNA during replication by repair enzymes may

result the formation of DSBs, especially within fragile sites. In human fibroblasts, folate depletion increased DNA damage, but MTR loss-of-function did not. This observation may be explained by the fact that specific tissues exhibit varying degrees of responsiveness to vitamin B_{12} deficiency. *De novo* purine biosynthesis was not affected in fibroblasts, suggesting that the nucleus may be more sensitive to vitamin B_{12} depletion. An unexpected finding from this work revealed a striking increase in nuclear 5-formylTHF concentrations in HeLa cells. This observation is likely explained by the fact that 5-formylTHF is a tight-binding inhibitor of SHMT, and corroborates those previous findings indicating that SHMT does not provide the majority of one-carbon units in dTMP, thereby suggesting a new role for 5-formylTHF in one-carbon metabolism.

In summary, the findings from this work advance our understanding of the role of vitamin B_{12} in nuclear *de novo* dTMP biosynthesis, and provide a mechanism linking cytosolic vitamin B_{12} depletion to nuclear 5-methylTHF accumulation, depressed rates of *de novo* dTMP biosynthesis, and increased genome instability. Additionally, the findings presented here challenge our fundamental understanding of the 5-methylTHF trap and its role in genome instability and disease pathogenesis, as elevated folate did not exacerbate genome instability (γH2AX) or rates of NTDs under conditions of vitamin B_{12} deficiency. Furthermore, maternal vitamin B_{12} deficiency increased NTD incidence in mice with reductions in *Shmt1* expression, but did not impair rates of fetal growth or maternal plasma homocysteine, suggesting that the nuclear compartment may be more sensitive to vitamin B_{12} deficiency than the cytosol.

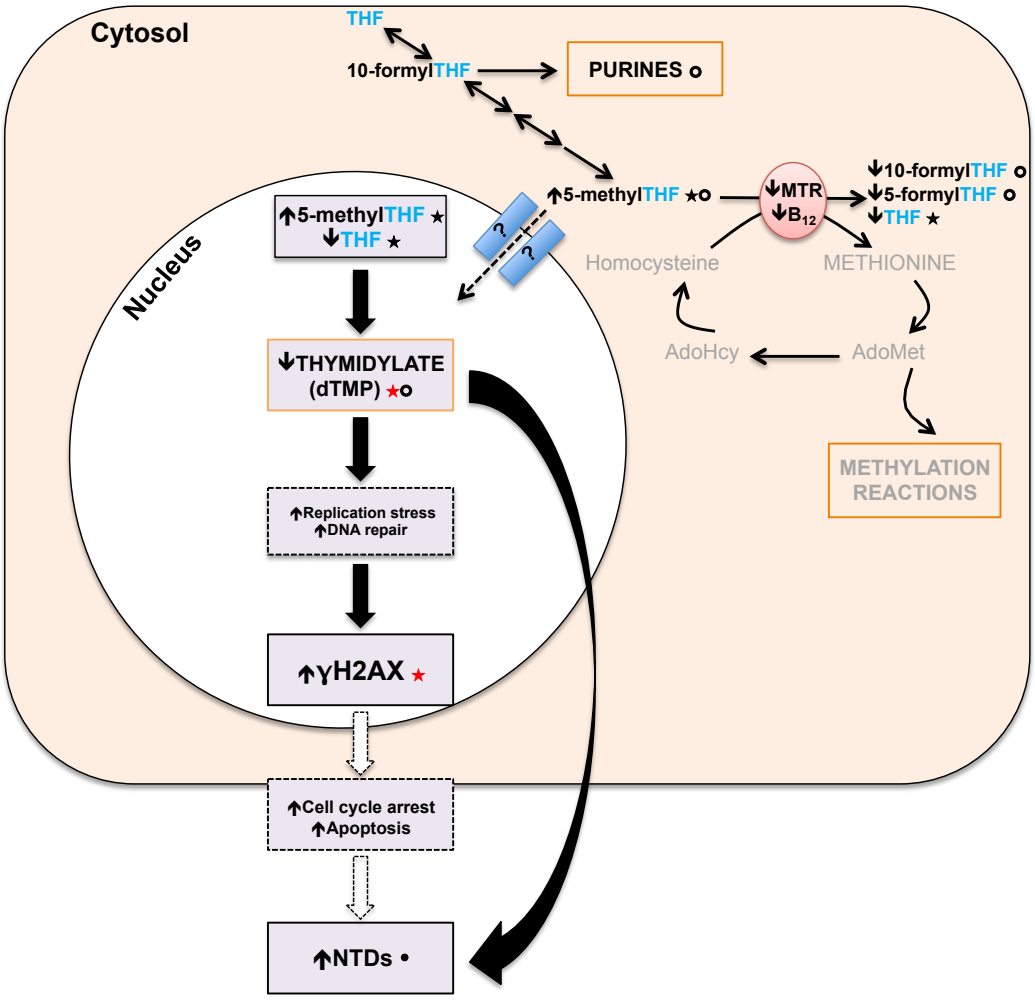

Figure 4.1. Conceptual figure delineating the role of vitamin B_{12} deficiency in genome stability and disease pathogenesis. Vitamin B_{12} depletion, either by N_2O treatment or MTR loss-of-function, traps intracellular folate as 5-methylTHF. In vitamin B_{12}-depleted HeLa cells, a nuclear trapping of 5-methylTHF occurs at the expense of THF, which leads to depressed rates of *de novo* dTMP biosynthesis and increased DNA damage (γH2AX). Both of the aforementioned outcomes are exacerbated by folate depletion. MTR loss-of-function fibroblasts exhibit decreased *de novo* dTMP biosynthesis capacity, but no impairments in *de novo* purine biosynthesis or increased γH2AX. Vitamin B_{12} deficiency causes NTDs in mouse embryos with reductions in *Shmt1* expression independently of folate status. Gray text designates intracellular metabolites not directly measured. The blue transporters with a dashed arrow indicate the lack of mechanism for folate transport between the cytosol and nuclear compartments. Dashed arrows indicate the proposed sequence of events linking genome instability and NTD pathogenesis. Dashed boxes designate proposed events in the causal pathways underlying vitamin B_{12} depletion. Stars correspond to observations in vitamin B_{12}-depleted HeLa cells; red stars indicate outcomes exacerbated by folate depletion. Black circles with open holes correspond to observations in MTR-loss-of-function fibroblasts. Closed black circles indicate vitamin B_{12}-responsive outcomes that are not affected by folate status.

FUTURE WORK

There are several findings raised by the results of this work that warrant further investigation and attention.

The findings from Chapters 2 & 3 suggest that specific cell types exhibit increased sensitivity to vitamin B_{12} depletion. MTR-null fibroblasts exhibited impaired nuclear *de novo* dTMP biosynthesis and elevated intracellular 5-methylTHF, but did not demonstrate increased DNA damage in contrast to vitamin B_{12}-depleted HeLa cells. Furthermore, neural tube closure was sensitive to maternal vitamin B_{12} deficiency, which could not be rescued with folate. It remains to be determined why some cell types are more responsive to vitamin B_{12} deficiency than others. To further investigate this unresolved issue, it may be useful to develop specialized cell models of vitamin B_{12}-responsive cell types that would enable more detailed analysis of the relationship between cellular vitamin B_{12} deficiency, nuclear 5-methylTHF accumulation, and other cellular processes.

Additional findings from this work underscore a need to improve the development of functional biomarkers that link diet and nutrition to disease pathogenesis. The findings from both Chapters 2 & 3 indicate that the nucleus may be more sensitive to vitamin B_{12} deficiency than the cytosol. Several of the current biomarkers used to measure vitamin B_{12} status and function have limited sensitivity or account for activities in the cytosol, but do not adequately reflect functional consequences of deficiency in the nucleus. Two examples of such biomarkers that are commonly used include total serum vitamin B_{12} and homocysteine. Therefore, it may be a worthwhile endeavor to develop a new biomarker (or a set of biomarkers) used to assess genome stability. γH2AX is a biomarker with the potential to fulfill this

requirement, as it may be easily quantified in peripheral lymphocytes using a high-throughput approach such as FACS. This approach would ideally be used in conjunction with more traditional measures of nutrient status. The development of functional biomarkers holds potential for significant implications when applied to a given population, as individuals have specific nutrient requirements that are modified by such factors as genetic variability, disease process, and medication intake, among others.